Universidade de Aveiro Departamento de Biologia
Ano 2011

NADINE CASTELHANO SANTOS

SARP2 as molecular marker of human sperm morphology

SARP2 como marcador molecular de morfologia de espermatozóides humanos

Universidade de Aveiro Departamento de Biologia
Ano 2011

NADINE CASTELHANO SANTOS

SARP2 como marcador molecular de morfologia de espermatozóides humanos

SARP2 as molecular marker of human sperm morphology

Dissertação apresentada à Universidade de Aveiro para cumprimento dos requisitos necessários à obtenção do grau de Mestre em Biologia Aplicada ramo Biologia Molecular e Celular, realizada sob a orientação científica da Professora Doutora Margarida Sâncio da Cruz Fardilha, Professora Auxiliar Convidada da Secção Autónoma de Ciências da Saúde da Universidade de Aveiro.

o júri

presidente	Professora Doutora Maria de Lourdes Gomes Pereira Professora associada com agregação, Departamento de Biologia da Universidade de Aveiro
orientador	Professora Doutora Margarida Sâncio da Cruz Fardilha Professora auxiliar convidada, Secção Autónoma de Ciências da Saúde da Universidade de Aveiro
arguente	Professora Doutora Odete A B da Cruz e Silva Professora associada com agregação, Secção Autónoma de Ciências da Saúde, Universidade de Aveiro

agradecimentos

À minha orientadora Professora Margarida Fardilha por todas as ideias novas que fomentou em mim e por toda a dedicação.

A todas as pessoas que constituem e que passaram pelo Laboratório de Transdução de Sinais, em especial à Mónica Ferreira por todos os ensinamentos e atenção que me dispensou.

A todas as pessoas do Laboratório de Neurociências pela disponibilidade que me dispensaram sempre que necessitei de ajuda, em especial à Sandra Rebelo por me ter ajudado na obtenção de imagens no microscópio confocal.

A todas as pessoas do Laboratório coordenado pelo Dr. Michael Schrader por toda a simpatia e a alegria contagiante. Por toda a ajuda que me puderam prestar em coisas simples e também na utilização do microscópio de fluorescência.

A todos os meus amigos, e a alguns em especial que de algum modo me ajudaram a fazer esta tese. Por me ajudarem a superar e celebrar todas as dificuldades e alegrias que encontrei.

Ao meu namorado, Miguel Sarabando, por todo o apoio e ajuda que me deu a realizar esta tese, levando-me sempre a pensar positivo. Por todas as vezes em que algo necessitava de ser melhorado e ele estava sempre predisposto a ajudar-me e por ser sempre o meu melhor ouvinte.

Aos meus pais e irmãos por todo o apoio e por me terem deixado chegar até aqui, acreditando sempre em mim, no meu potencial nunca me deixando desanimar nas barreiras que fui encontrando. Aos meus pais agradeço por ter feito de mim a pessoa que sou hoje, por se orgulharem de mim e me deixarem ser quem sou.

palavras-chave

Fosforilação, PP1, PP1γ2, espermatozóides, SARP2, infertilidade masculina, marcador molecular.

resumo

A fosforilação proteica resulta de um equilíbrio entre fosfatases e quinases constituindo o principal regulador da maioria dos mecanismos existentes nos sistemas biológicos. Muitas doenças (cancro, diabetes, doenças neurodegenerativas, infertilidade, etc.) estão associadas à disrupção deste equilíbrio levando a mudanças nas actividades enzimáticas das proteínas fostatase e quinase. A proteína fosfatase 1 (PP1) é a principal fosfatase serina/treonina sendo ubíqua e altamente conservada nos eucariotas. A PP1 controla várias funções, tais como, a divisão celular, a transcrição, a neurotransmissão, a mobilidade dos espermatozóides, entre outras. A fosforilação proteica é uma das formas de os espermatozóides adquirirem funcionalidade, sendo a proteína PP1γ2 a isoforma mais fortemente enriquecida. Assim, no interior do espermatozóide podemos encontrar a PP1γ2 associada ao comprimento total da cauda e à região equatorial da cabeça, sugerindo uma possível função na mobilidade e reacção acrossómica, respectivamente. Existem inúmeras proteínas que interagem com a PP1γ2 que têm vindo a contribuir para a compreensão do seu papel nas funções fisiológicas do espermatozóide. Apesar de existirem outros, nesta tese, o complexo que serviu de ponto de partida foi o complexo SARP2/PP1γ2. Este complexo inclui uma nova proteína derivada de *splicing*, primeiramente descrita por Browne e os seus colaboradores em 2007, contendo três isoformas. Nesta tese foi usada a isoforma SARP2. O complexo foi encontrado fortemente enriquecido em espermatozóides e esta descoberta levou a estudos futuros com vista a descobrir a sua função fisiológica no espermatozóide. Usando a proteína SARP2 como um possível marcador molecular procurou-se verificar se era possível distinguir os espermatozóides em normais ou anormais. Considerando a actual necessidade em desenvolver novas técnicas de diagnóstico da infertilidade masculina, a descoberta de biomarcadores pode apresentar uma possível via, especialmente devido à perda de valor da avaliação dos parâmetros de um espermograma. No presente trabalho descobriu-se uma localização sub-celular no espermatozóide diferente da descrita anteriormente. O padrão de expressão da SARP2 é muito variável existindo catorze padrões diferentes do padrão normal encontrado. Contudo não foi possível confirmar com total certeza de que tínhamos um putativo marcador molecular. O presente trabalho fornece dados suficientes para que no futuro se possa realizar um plano experimental optimizado, com mais voluntários, representativo da população Portuguesa. Por fim, é necessário complementar o estudo com testes paralelos (fragmentação do DNA, ROS, etc.) que permitam avaliar a normalidade ou não de um espermatozóide em contraponto com a observada no estudo.

keywords

Phosphorylation, PP1, PP1γ2, spermatozoa, SARP2, men infertility, molecular marker.

abstract

Protein phosphorylation, is the result of a balance between phosphatases and kinases being the key regulator for the major mechanisms in biological systems. Many diseases (cancer, diabetes, neurodegenerative conditions, infertility, etc.) are associated to the disruption of this balance leading to changes in the activities of both kinases and phosphatases enzymes. Protein phosphatase 1 (PP1) is a major serine/threonine phosphatase, ubiquitous and conserved in eukaryotes. PP1 controls a variety of functions, such as, cell division, transcription, neurotransmission, sperm motility, among others. Protein phosphorylation is one of the ways by which spermatozoa acquire functionality; being PP1γ2 a sperm enriched protein. Moreover, within spermatozoa PP1γ2 is present along the entire length of the tail and equatorial region of the head, suggesting a role in sperm motility and acrossome reaction, respectively. There are several interacting proteins of PP1γ2 which are leading to a revelation of its role in sperm functions. Although there are others, in this thesis, the complex that was the leading point of the study was the new complex SARP2/PP1γ2. This complex includes a new spliced protein firstly described by Browne and co-workers in 2007, which has three different isoforms. In this thesis SARP2 was the isoform used. The complex was found to be enriched in sperm, and this discovery lead to further studies on the possible role of this complex in sperm functions. The relevance of using SARP2 as a putative molecular marker to distinguish normal and abnormal spermatozoa was studied. Since nowadays there is a urgent need to change the way in which men infertility is being diagnosed, especially by the use of the traditional semen parameters evaluated in a spermogram, the biomarker discovery could be a way. In this thesis it was discovered a subcellular localization within human spermatozoa different from the one described before. The expression pattern of SARP2 is very variable; there are fourteen other patterns besides the normal one. Although, it was not possible to confirm with certain that we had a putative molecular marker. The present study gave enough data to proceed in the future, with the elaboration of an optimized experimental plan using more volunteers, to get a representative sample of the Portuguese population. Finally, it is necessary to complement this study with parallel tests (DNA fragmentation, ROS, etc) to ascertain if having a spermatozoon classified as normal, according to our study, is always synonymous of having a normal spermatozoon.

Index

Abbreviations

AC	Adenyl cyclase
ADP	Adenosine diphosphate
AKAPs	A-kinase-anchoring-proteins
ART	Assisted Reproduction Techniques
ATP	Adenosine triphosphate
BSA	Bovine Serum Albumin
DAPI	4',6-diamidino-2-phenylindole
DNA	Deoxyribonucleic acid
GSK-3	Glycogen synthase kinase-3
HE	Hematoxylin – Eosin staining
HGG Y gene	Hemochromatosis candidate gene V
I-1	Inhibitor 1
I-2	Inhibitor 2
I-3	Inhibitor 3
IM	Immotile spermatozoa
mRNA	messenger RNA
MYPT1	Myosin phosphatase target subunit 1
NCB	Non-capacitating buffer
NP	Non-progressive spermatozoa
PBS	Phosphatase Buffered Saline
PH	Phase contrast

PI3-kinase	Phosphatidyl inositol kinase-3
PIPs	PP1 interactors
PKA	Protein kinase A
PKB	Protein kinase B
PP1	Protein Phosphatase 1
PP1c	PP1 catalytic subunit
PP1α	Protein Phosphatase 1alpha
PP1β	Protein Phosphatase 1beta
PP1γ1	Protein Phosphatase 1gamma 1
PP1γ2	Protein Phosphatase 1gamma 2
PP1δ	Protein Phosphatase 1delta
PP2	Protein Phosphatase 2
PP2A	Protein Phosphatase 2A
PP2B	Protein Phosphatase 2B (calcineurin)
PP2C	Protein Phosphatase 2C
PP4	Protein Phosphatase 4
PP5	Protein Phosphatase 5
PP6	Protein Phosphatase 6
PP7	Protein Phosphatase 7
PPM	Metal ion dependent protein phosphatase
PPP	Phosphoprotein Phosphatase
PPP1R11	Phosphoprotein Phosphatase 1 Regulatory Subunit 11
PPP1R7	Phosphoprotein Phosphatase 1 Regulatory Subunit 7

PPs	Protein Phosphatases
PR	Progressive motile spermatozoa
RNA	Ribonucleic acid
ROS	Reactive oxygen species
RT	Room Temperature
SARP	Several Ankyrin Repeat Protein
SARP1	Several Ankyrin Repeat Protein 1
SARP2	Several Ankyrin Repeat Protein 2
SARP3	Several Ankyrin Repeat Protein 3
SCPs	Small C-terminal domain Phosphatase
SDS-PAGE	Sodium Dodecyl Sulfate Polyacrylamide Gel Electrophoresis
SEARP	Six to Eight Ankyrin Repeat Protein
SPSS	Statistical Package for Social Sciences
STPPs	Serine/Threonine protein Phosphatases
WHO	World Health Organization
YTH	Yeast Two-Hybrid

1: Introduction

1.1 Protein phosphorylation - a balance between phosphatases and kinases

The delicate balance between protein kinase and phosphatase activities in eukaryotic cells is responsible for controlling levels of protein phosphorylation, and is thought to be the major regulatory mechanism in biological systems (Fardilha, *et al.*, 2010; Meiselbach, *et al.*, 2006; da Cruz e Silva, *et al.*, 1995). Phosphorylation is a post-translation modification that is involved in almost all cellular functions, from metabolism to signal transduction, cell division and memory (Fardilha, *et al.*, 2010; Han, *et al.*, 2007). The mechanism of reversible protein phosphorylation is the most common mechanism in eukaryotic cells, which is mediated through the addition and/or removal of phosphate groups from serine, threonine or tyrosine residues of proteins. This can induce allosteric modifications resulting in conformational changes in proteins leading to their activation or inactivation (Figure 1). This process is mainly regulated by protein kinases and phosphatases. Protein kinases add a phosphate group to the hydroxyl group of serine, threonine or tyrosine residues whereas phosphatases remove it (Figure 1) (Cohen, 1992).

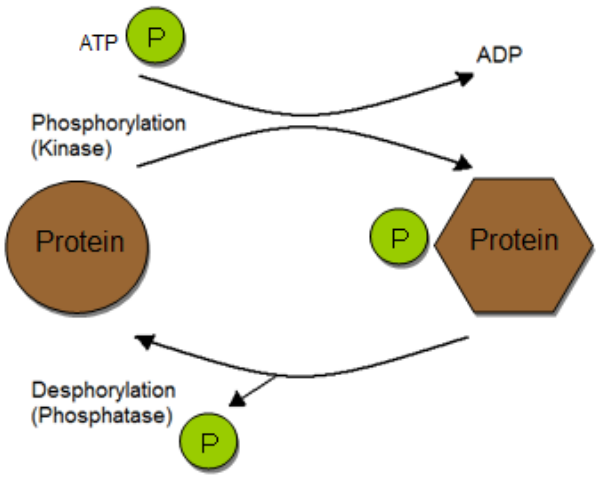

Figure 1: The balance between phosphatases and kinases. Protein kinase moves a phosphate group from ATP to a target protein (protein phosphorylation). Protein

phosphatase removes the phosphate group from the target protein (protein desphosphorylation).

About one-third of all eukaryotic proteins are controlled by reversible phosphorylation. Several thousands of human proteins have already been found to be phosphorylated *in vivo* mostly on serines or threonines (Hendrickx, *et al*., 2009; Ceulemans and Bollen, 2004). Consequently, is not surprising that 2-3% of all eukaryotic genes encode protein kinases or protein phosphatases. The number of protein tyrosine phosphatases approximates to the number of protein tyrosine kinases (~100 each). In contrast, the protein serine/threonine kinases tend to overcome the number of protein serine/threonine phosphatases (Bollen, *et al*., 2010; Ceulemans, *et al*., 2002).

The human genome, encodes more than 400 genes for protein serine/threonine kinases and only about 40 genes for protein serine/threonine phosphatases. This imbalance in gene number could be explained by distinct diversification strategies during evolution. Indeed, protein serine/threonine kinases have mainly diversified by gene duplication and subsequently specification, whereas protein serine/threonine phosphatases increase their diversity by the acquisition of a variety of binding partners (regulatory subunits), thereby forming a large number of holoenzymes. Nevertheless, both protein serine/threonine kinases and protein serine/threonine phosphatases are equally diverse and restricted substrate specific at the holoenzyme level (Hendrickx, *et al*., 2009; Meiselbach, *et al*., 2006).

Alterations in the phosphorylation state can result in changes in the activities of both kinases and phosphatases enzymes (Ceulemans and Bollen, 2004). In fact, cellular homeostasis is strictly dependent on the fine equilibrium of protein phosphorylation systems and therefore, many diseases and dysfunctional states are associated with abnormal phosphorylation of key proteins (e.g. cancer, diabetes, neurodegenerative conditions, infertility, etc.). In neurodegenerative diseases, such as the Alzheimer's disease, an abnormal regulation of protein kinases was identified. Parkinson's and Huntington's are two other neurodegenerative diseases that have shown evidence of abnormal phosphorylation processes. In cancer, several protein kinases appear to be deregulated during the cell cycle and altered phospholylation has also been

implicated in heart failure and in Diabetes. Currently, protein phosphorylation systems represent attractive targets for diagnostic and therapeutic strategies of several neurodegenerative and non-neurodegenerative diseases such as infertility (Fardilha, et al., 2011; Fardilha, *et al*., 2010).

1.2 Protein phosphatases

The pioneering system of categorization of the known PPs (protein phosphatases) was based on: biochemical characteristics, sensitivity to endogenous inhibitor proteins, and a limited amount of substrate specificity, which can be demonstrated *in vitro*. This work was first done by Ingebritsen and Cohen (1983) (Ingebritsen and Cohen, 1983). Thus, STPPs (Serine/Threonine Protein Phosphatases) were initially divided into two major subtypes. The type 1 PPs (PP1) that essentially dephosphorylates the β-subunit of phosphorylase kinase, and are inhibited by two heat-stable proteins, inhibitor-1 (I-1) and inhibitor-2 (I-2). The type 2 PPs (PP2) dephosphorylates principally the α-subunit of phosphorylase kinase and are insensitive to heat-stable inhibitors (Fardilha, *et al*., 2010; Honkanen and Golden, 2002).

The type-2 PPs were further subdivided into cation independent (PP2A), Ca^{2+}-dependent (PP2B - calcineurin) and Mg^{2+}-dependent (PP2C) classes (Fardilha, *et al*., 2010). The studies of the primary amino acid sequence of PP1, PP2A and PP2B have revealed similarities, while PP2C is structurally distinct and belongs to a different gene family (Honkanen and Golden, 2002). Therefore, STPPS comprises three different gene families, the PPM (Metal ion Protein Phosphatase), the FCP and the PPP (Figure 2) (Fardilha, *et al.*, 2010; Ceulemans and Bollen, 2004).

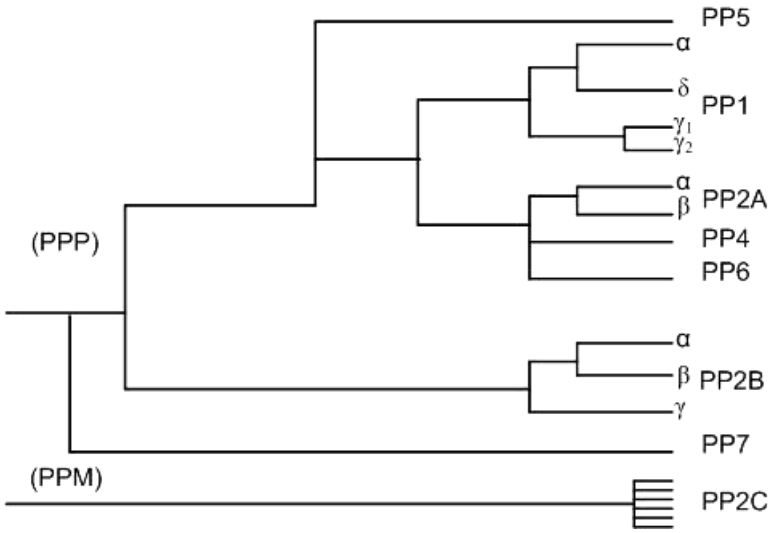

Figure 2: A phylogenetic tree depicting the similarity between the known PPases based on their primary amino acid sequence (adapted from Honkanen and Golden, 2002).

The PPM family (Figure 2) incorporates the Mg^{2+}-dependent PPs, like pyruvate dehydrogenase, PP2C, and relatives. The FCP family incorporates the new FCP1 and SCPs (Small C-terminal domain Phosphatase) 1-3 PPs that have specificity for the substrate RNA polymerase II. The PPP family (Figure 2) comprises PP1, PP2A/PP4/PP6, PP2B, PP5 and PP7 gene subfamilies that share high homology in the catalytic domains but differ in the N- and C-terminal domains (Fardilha, *et al*., 2010). A key-defining characteristic of this family is that they are multimeric enzymes. In fact, while only 13 human genes encode PP catalytic subunits, these are associated with numerous PPP regulatory subunits that are still being discovered (Virshup and Shenolikar, 2009).

1.3 Protein phosphatase 1 (PP1)

Protein phosphatase 1 (PP1) is a major serine/threonine phosphatase, a ubiquitous and conserved eukaryotic enzyme that is estimated to catalyze about one third of all protein desphosphorylations (Hendrickx, *et al.*, 2009, Meiselbach, *et al.*, 2006; Ceulemans and Bollen, 2004). It controls a variety of cellular activities, such as cell division, transcription, translation, RNA splicing, muscle contraction, glycogen and lipid metabolism, neurotransmission, synaptic plasticity and memory, apoptosis and sperm motility (and other sperm functions)

(Fardilha, *et al*., 2011; Chakrabarti, *et al.*, 2007; Meiselbach, *et al.*, 2006; Egloff *et al.*, 1997). This multifunctionality of PP1 is correlated with dozens of different substrates that appear to be mediated via binding to specific proteins, which play critical regulatory and targeting roles (Browne *et al.*, 2007; Ceulemans and Bollen, 2004). Those PP1 interactors (PIPS) exist tightly connected with mammalian PP1 isoforms function such as: activity regulators, substrate-targeting proteins, substrate specifiers, and/or substrates. These types of associations determine when and where a specific phosphatase acts (Hendrickx, *et al.*, 2009).

1.3.1 PP1 catalytic and regulatory subunits

The PP1 catalytic subunit (PP1c) is a member of PPP family of protein serine/threonine phosphatases that in humans includes, PP1, PP2A, PP4, PP6, PP2B, PP5 and PP7. There are multiple genes that encode PP1c isoforms in most eukaryotes, being the only exception *Saccharomyces cerevisiae*, which possesses only one gene (*Glc7*) encoding PP1c (Cohen, 2002). Mammalian PP1c have three different PP1 genes, encoding the isoforms PP1α, PP1β (also termed PP1δ), PP1γ1 and PP1γ2, the latter two arising through alternative splicing (Cohen, 2002; Ceulemans and Bollen, 2004) of the same primary transcript that gives rise to two proteins that only differ at their C-terminal ends. PP1γ1 is ubiquitously expressed in most tissues, whereas PP1γ2 is testis/sperm enriched (Fardilha, *et al*., 2011; Han, *et al.*, 2007; Smith, *et al.*, 1996). Mammalian PP1c isoforms (35-38 kDa) are about 90% identical varying in their extremities and also in tissue distributions and subcellular localizations (Wakula, *et al.*, 2003; Cohen, 2002). The sequence of the catalytic core of PP1c is almost identical for all isoforms, and shows a high degree of similarity (40%) with all members of PPP family that share the same three-dimensional structure and catalytic mechanism (Bollen, *et al.*, 2010; Bollen, 2001; Ceulemans, *et al.*, 2002). The difference between the PPP family enzymes reside mainly in the solvent-exposed loops that determine the shape and charge of the surface, and so the affinity for ligands (Bollen *et al.*, 2010). According to crystallographic

studies, the crystal structure of PP1c shows a compact fold with a central β-sandwich that excludes only the COOH terminus and the extreme NH_2 terminus (Figure 3). The active site is located at the bifurcation point of an extended Y-shaped surface depression. The arms of this depression are designated as the COOH-terminal groove, the acidic groove, and the hydrophobic groove (Ceulemans and Bollen, 2004) (Figure 3).

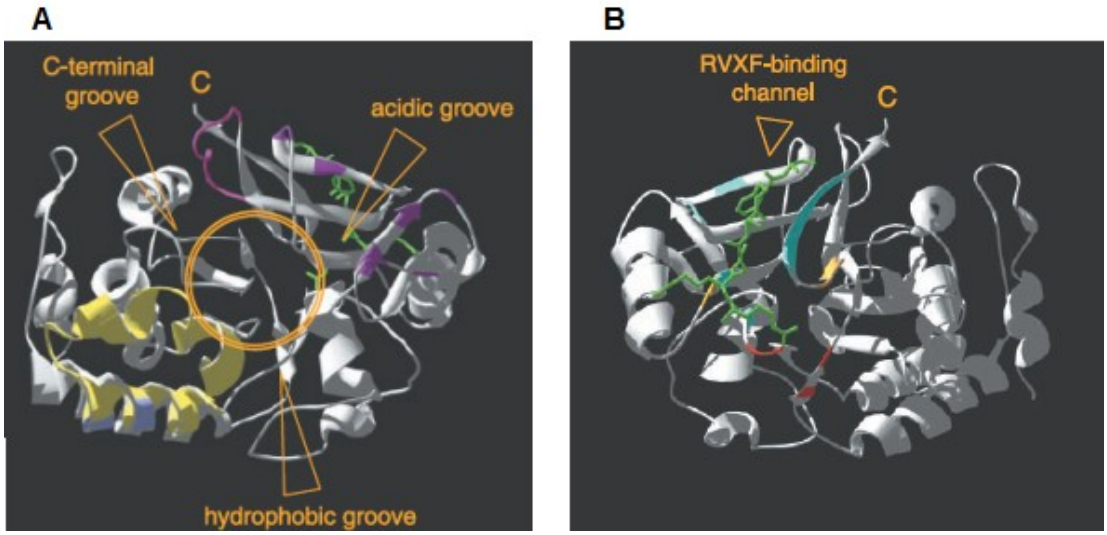

Figure 3: A: Frontal view of PP1 with the catalytic site (encircled) and the three grooves that emanate from the catalytic site. B: The RvXF-containing peptide is rendered as a green sticks representation (adapted from Ceulemans and Bollen, 2004).

PP1s do not exist freely in the cell but are tightly associated with a large variety of polypeptides that determine when and where PP1 acts. These PIPs (regulatory subunits) based on their effect on PP1c can be categorized in three groups. The first group comprises the activity-modulating proteins, including true inhibitors such as inhibitor-1 and CPI-17 that, in their phosphorylated form, block the activity of PP1c against all substrates. There are other members of this group that, instead, act as substrate-specifiers of PP1c. The second group includes the targeting proteins that bind both PP1c as well as specific substrates such as myosin. However, other targeting proteins do not bind the substrate directly but instead associates with a subcellular structure that contains the substrate, like G subunits that target PP1 to glycogen particles, which also bind the substrate glycogen synthesis. The targeting proteins also include proteins called scaffolding proteins, which mediate the formation of protein complexes. An example of the latest protein is A-kinase-anchoring-

proteins (AKAPs) and MYPT1. The third group of proteins are directly and tightly associated with PP1c defining a subset of its substrates. Surprisingly, some of these substrates also function as targeting proteins (Nek2). In addiction, hormones, growth factors and metabolites control the function of the PP1 holoenzymes mainly by modulating the interaction of the subunits (Han, *et al*., 2007; Bollen, 2001).

The surface of the catalytic core is too small to harbour specific binding sites for each of all known mammalian interactors. Thus, some evidences rather suggest that PIPs compete for a limited number of common or over-lapping binding sites. The binding to these sites is mainly mediated by short (4-6 residues) degenerate motifs, and this accounts for the lack of structural similarity between PIPs (Wakula *et al.*, 2003). The majority of the known PIPs, although being quite different, contain a variant of a motif that is currently referred as “RVxF motif”. Crystallographic studies revealed that this motif binds tightly as an extended β strand to a hydrophobic groove of PP1 that is remote from the catalytic site (Figure 3) (Hendrickx *et al.*, 2009). This RVxF motif is often preceded by one or more basic residues and followed by one or more C-terminal acidic residues (Wakula *et al*., 2003). Surprisingly, The RVxF motif *per se* does not have effect on the conformation of PP1c, but increases the local concentration of the interactor. And, thus promotes secondary interactions that can affect the activity or substrate specificity of the phosphatase. RVxF is a degenerated motif mainly defined as a five-residue motif with the consensus sequence [RK]-X(0,1)-[VI]-{P}-[FW], where X is any residue and {P} any residue but proline (Hendrickx *et al.*, 2009). Additionally, it has been demonstrated for various PIPs that a mutation of the hydrophobic (V/I/L) and/or aromatic (F/W/Y) residue in this motif is sufficient to disrupt or weaken their interaction with PP1c. Even synthetic peptides containing the RVxF motif (or naturally occurring variants) can competitively disrupt or weaken the binding of various PIPs to PP1c (Bollen *et al*., 2010). Although the previous definition is sensitive because it covers about 90% of all known PP1-binding RVxF variants lacks specificity, because it occurs randomly in about one quarter of all proteins (Hendrickx *et al.*, 2009). Meiselbach and co-workers (2006) introduced a less sensitive but more sensitive definition and tested a different consensus sequence experimentally:

[HKR][ACHKMNQRSTV][V][CHKNQRST][FW] (Fardilha, *et al*., 2010, Meiselbach *et al*., 2006). This motif favors basic residues at positions +1 and +2, valine at position +3, polar amino acids, with amino or hydroxyl groups that are able to accept or donate protons, at position +4, and hydrophobic aromatic residues at position +5 (Meiselbach *et al*., 2006). More recently, the work from Bollen and co-workers allowed the redefinition of the RVxF motif and its flanking residues based on the sequences of 143 PIPs – [KRL]-[KRSTAMVHNQ]-[VI]-{FIMYDP}-[FW]. Moreover, other PP1 binding motifs have been described: the SILK motif present in I-2 and SIPP-1; G/S I L R/K, that also appears to exist in several PP1 interactors; and the MyPhoNE motif (RxxQ[VIL][KR]x[YW]) present in MYPT-1 (Bollen, *et al*., 2010; Fardilha, *et al*., 2010).

Surprisingly, the presence of an RVxF motif in itself is not sufficient to classify a protein as a putative PIP. Additional information regarding the function of an RVxF motif could come from the use of competing RVxF-containing peptides or from RVxF mutants (Wakula, *et al*., 2003). PIPs have been identified by the Yeast Two Hybrid (YTH) system, bioinformatics approaches based on genome scanning for proteins possessing the PP1 binding motifs and by affinity purification coupled to mass spectrometry identification. Furthermore, classical biochemical approaches and YTH screens identified the majority of the PIPs. Thus, the diverse approaches need to be complemented by independent methodologies to validate the novel PIPs and to determine their physiological relevance (Fardilha, *et al*., 2010). A more selective approach could be applied using the recently acquired structural insights, involving the functional disruption of subsets of PP1 holoenzymes with small-molecule compounds that bind to PIP interaction sites on PP1, such as the hydrophobic binding grooves for the RVxF, SILK and MyPhoNE sequences (Bollen, *et al*., 2010). The structural information reported should simplify the rational design of peptide inhibitors that could target the binding site, which leads to the possibility of selective interfere with PP1 functions (Fardilha, *et al*., 2010; Zhao and Lee, 1997).

1.3.2 PP1 in testes and sperm

Mammalian sperm is formed by a well-defined sequence of mitotic and meiotic divisions, which are followed by a long period of complex morphogenetic differentiation, leading to the production of mature spermatozoa. Mammalian sperm development takes place in the seminiferous tubules of the testes and, can be divided into three distinct stages: proliferative, meiotic (spermatogenesis), and spermiogenic (post-meiotic differentiation and morphogenesis) (Chakrabarti, *et al.*, 2007).

Spermatogenesis is comprised of a series of developmental changes, which starts at puberty and continues throughout adult life, leading to the transformation of a precursor germ cell into a highly specialized spermatozoon (Wang and Sperry, 2008; Küpker *et al.*, 1998). The final stage of this process, called spermiogenesis, involves morphological changes including formation of the acrossome, elongation and condensation of the nucleus, formation of the flagella, and disposal of unnecessary cytoplasm (Wang and Sperry, 2008).

Immotile mammalian spermatozoa acquire the capacity for motility and fertilization during their passage through the epididymis. The human epididymis presents a difuse pattern of clear-cut divisions into head (caput), body (corpus) and tail (cauda) contrary to other species (De Jonge, *et al*., 2006). Thus, spermatozoa isolated from the caput region of the epididymis are morphologically mature but immotile, in contrary sperm from caudal region of the epididymis presents vigorous motility, forward progression and the ability to bind and fertilize the egg. Nevertheless, the capacity of motility already exists in immotile testicular and epididymal sperm because motility can be induced in demembranated immotile spermatozoa (Chakrabarti, *et al.*, a2007). During the epididymal maturation, sperm undergo changes under control of different factors, such as cyclic AMP, pH, calcium and phosphorylation of sperm proteins (Han, *et al*., 2007). However, little is known about how the levels of these factors are regulated and how they function within spermatozoa. The process is regulated by reversible phosphorylation. Sperm protein phosphorylation is

tightly connected to motility, which is increased by agents that elevate sperm cAMP levels (Vijayaraghavan, *et al*., 1996).

Nowadays, it is widely accepted that protein phosphorylation is an important mean by which spermatozoa can acquire functionality. PP1α, PP1β/δ, PP1γ1 and PP1γ2 are all expressed in testis whereas PP1γ2 is a sperm enriched isoform (Fardilha, *et al*., 2011; Han, *et al*., 2007). PP1γ2 differentiates from the other PP1 isoforms because of its unique, almost conserved 21-amino acid carboxyl terminus extension, present in all mammalian spermatozoa that have been tested so far: mouse, rat, hamster, bull, non-human primate, and human (Cheng, *et al*., 2009; Huang and Vijayaraghavan, 2004).

In testis, PP1γ2 is present in abundance in the cytoplasm of secondary spermatocytes, round spermatids, elongating spermatids and testicular and epididymal spermatozoa, whereas PP1γ1 and PP1α expressions are observed in spermatogonia, pachytene spermatocytes, and interstitial cells (Chakrabarti, *et al.*, 2007). In sperm, PP1γ2 is present along the entire tail including the middle piece, consistent with a role in sperm motility, and is also found in the equatorial region of the head, suggesting a role in the acrossome reaction (Figure 4) (Fardilha, *et al*., 2011a; Huang, *et al*., 2002).

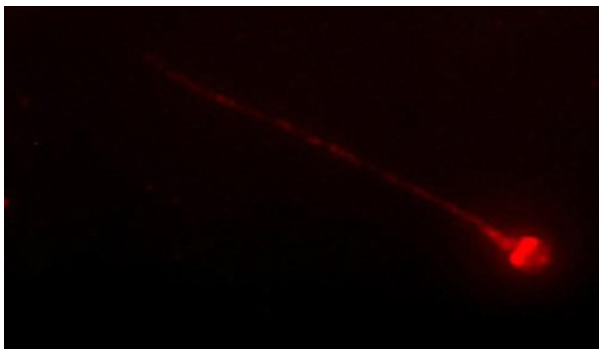

Figure 4: Subcellular localization of PP1γ2 spermatozoa. The figure shows that PP1γ2 localizes to the entire tail and at the equatorial region of the head (adapted from Fardilha, *et al*., 2011a).

High catalytic activity of sperm PP1γ2 is correlated with low sperm motility or lack of motility in immature caput epididymal spermatozoa, whereas low catalytic activity is correlated with vigorous motility in caudal epididymal spermatozoa (Chakrabarti, *et al.*, a2007). Indeed, inhibition of protein

phosphatase activity by okadaic acid and calyculin A initiates motility in caput epididymal sperm similar to mature sperm and without requirement for a change in cAMP levels (Smith, *et al*., 1996; Vijayaraghavan, *et al*., 1996). Indeed, inhibition of PP1γ2 causes motility stimulation and changes in flagella beat in mature spermatozoa (Chakrabarti, *et al.*, 2007).

Targeted disruption of *Ppp1 cc*-null gene, resulting in the loss of PP1γ1 and PP1γ2, resulted in male mice infertility due to impaired spermiogenesis, leading to the absence of epididymal spermatozoa. In contrast to *Ppp1 cc*-null females that were fertile, males were infertile, due to spermiation failure, resulting in the release of mature sperm from the seminiferous epithelium into the lumen (Chakrabarti, *et al.*, 2007; Varmuza, *et al*., 1999). Furthermore, Chakrabarti and co-workers (2007) observed numerous structural defects in elongating spermatids and testicular spermatozoa, including some abnormal head shapes, poorly developed or missing mitochondrial sheaths and supernumerary, disorganized outer dense fibber florets throughout sperm tails. They also detected frequent degeneration of condensing spermatids, indicated by the fragmentation of tail structures and the presence of numerous vacuoles in the cytoplasm of elongating spermatids. In fact, this partially explained the complete absence of spermatozoa in the epididymis. Although PP1α expression was increased and its localization altered, it could not substitute for PP1γ1, suggesting a specific role for PP1γ2 in sperm differentiation and morphogenesis (Chakrabarti, *et al.*, 2007).

1.4 PP1 Interacting Proteins – PIPs – in male germinative tissues

To unreveal the role of PP1γ2 in sperm motility and morphogenesis, several studies were carried out during the last decades to identify the interacting proteins of PP1γ2 in testis and spermatozoa (see the review of Fardilha, *et al*. 2011.)

1.4.1 The complex PP1γ2/I2-L/GSK-3

PP1 is inhibited by the endogenous heat-stable inhibitors, Inhibitor-1(I-1) and Inhibitor-2 (I-2). I-1 and I-2 are distinguishable by their response to

phosphorylation, I-1 is stimulated by PKA phosphorylation and I-2 is PKA-independent. In contrast to somatic cells, in human and monkey sperm extracts, only I-2 like activity was found (Smith, *et al.*, 1996). I-2 binds to the catalytic subunit of PP1 to form an inactive stable complex PP1-I-2 that can be converted to the active form by glycogen synthase kinase-3 (GSK-3) which phosphorylates I-2, relieving the inhibition and producing active PP1 (Vijayaraghavan, *et al.*, 1996; Smith, *et al.*, 1996). Immotile bovine caput epididymal sperm contain levels of protein phosphatase activity (PP1γ2) twofold higher than do mature motile caudal sperm. This is probably due to six fold higher GSK-3 activity that is suggested to be responsible to hold their motility in check (Vijayaraghavan, *et al.*, 1996). Another study conducted in monkey sperm extracts showed, that caput epididymal sperm contain more PP1 and GSK-3 activity than caudal sperm does (Smith, *et al.*, 1999). The decrease of GSK-3 and PP1γ2 activities in sperm is probably the key event in motility development in the epididymis (Vijayaraghavan, *et al.*, 2000). GSK-3 was first identified as a protein kinase involved in regulating the activity of glycogen synthase, but many other important functions were found afterwards. Surprisingly, mammalian sperm do not contain glycogen or enzymes responsible for glycogen metabolism using other exogenous energy sources like glucose and fructose for example (Embi, *et al.*, 1980). One of the functions of GSK-3 is activation of PP1γ2 that is accomplished through phosphorylation of I-2 on a threonine residue resulting in the dissociation of the PP1γ2-I-2 complex. Activity of GSK-3 is regulated by tyrosine and serine/threonine phosphorylation, tyrosine phosphorylation increases GSK-3 catalytic activity. Alternatively, serine/threonine phosphorylation is mediated by phosphatidyl inositol kinase-3 (PI3-kinase) that activates PKB (also known as cAkt) resulting in phosphorylation and inactivation of GSK-3. Immunocytochemistry using the GSK-3α antibody showed that GSK-3 is located at the equatorial, in the post-acrosomal region of the head, and in the principal piece of the tail in both caudal and caput spermatozoa (Somanath, *et al.*, 2004; Vijayaraghavan, *et al.*, 2000).

1.4.2 The complex PP1γ2/I3 (PPP1R11)

Inhibitor 3 (I-3) is a potent heat-stable PP1 inhibitor, PPP1R11 (phosphoprotein phosphatase 1 regulatory subunit 11), was first identified in yeast (Ypi1), and latter in human brain through YTH screening where HCG V gene (Hemochromatosis candidate gene V) was found to be a novel PP1 binding inhibitor and named I-3 (Lesage, *et al*., 2007, Zhang, *et al*., 1998; Giffon, *et al*., 1996). I-3 has some general similarities with the other two well-characterized heat-stable inhibitors of PP1, I-1 and I-2. All of them are highly hydrophilic proteins, which behave anomalously on SDS-PAGE, and are specific for the inhibition of PP1 (Lesage, *et al*., 2007). I-3 was subsequently identified as the orthologue of the mouse *t complex testis expressed* (*tctex*) genes (localized in the proximal half of chromosome 17), and defined as *t-complex-testis-expressed 5* (Tctex5), which might be a candidate gene to male sterility or Transmission Ration Distortion (TRD) in mouse (Han, *et al*, 2007a). Tctex5 is genetically linked to the male sterility phenotypes of male *t* halotypes that are naturally occurring structure/function variants of the *t complex*, associated to homozygotic males that are completely sterile. This type of variant from chromosome 17 has evolved because of the ability to propagate through natural populations by the phenomenon of TRD, in which heterozygous +/t males transmit their carrying chromosome to 95% or more of their offspring. The sterility of male *t* homozygotes is the consequence of altered sperm differentiation, resulting in abnormal sperm motility, zona pellucida binding, and penetration of the oolemma (Han, *et al*., 2007a; Hui, *et al*., 2006; Pilder, *et al*., 1993; Pilder, *et al*., 1991; Cebra-Thomas, *et al*., 1991). Tsga2 and Tctex5 genes act synergistically in the expression of the “curlicue”, which is a phenotypic signature of *t*-males, characterized by a $^{+2}$Ca-sensitive sperm tail curvature abnormality, and also by the “stop” phenotype in which prevents sperm-egg interaction (Pilder, *et al*., 2007; Hui, *et al*., 2006). Like I-3 Tctex5 is also shown to be bind to PP1γ2 in mouse spermatozoa *in vitro.* Han and co-workers (2007) have studied the expression of protein Tctex5 in testis, epididymis, and epididymal spermatozoa. Tctex5 was shown to be present in the nuclei of spermatogonia, pachytene spermatocytes, and round spermatids but not in elongated spermatozoa in the testis. Tctex5 was also localized in the spermatozoa head and principal piece of the tail, which was previous described

for subcellular localization of PP1γ2 (Han, et al., 2007a; Huang, *et al.*, 2002). Lesage and co-workers (2007) described for the first time a novel mammalian heterotrimeric complex PP1 holoenzyme that contains the ancient PP1 interactors sds22 and I-3, which is catalytic inactive *in vivo*. They speculated that the activation of this complex might be regulated through phosphorylation of sds22 or I-3. Physiologically I-3 may function as an inhibitor of PP1 and act like a nuclear targeting until being transferred for its final destination, (Lesage, *et al*., 2007). The conserved presence of I-3 and sds22 in a broad range of eukaryotic organisms and tissues, including the mammalian testis, suggest that both may be vital regulators of PP1 activity in the male gonad. Recently Cheng and co-workes (2009) demonstrated the formation of a complex, in testicular germ cells and sperm, between PP1γ2-I3-sds22, which is also inactive, but surprisingly, contains actin. They also showed that there is a reciprocal relationship between the level of PP1γ2 and the steady state level of I-3 (Cheng, *et al*., 2009).

1.4.3 The complex PP1γ2/sds22 (PPP1R7)

The yeast protein sds22 is a prototypical member of a family of proteins containing repeats of a leucine-rich an amino acid sequence motif. Human sds22 (PPP1R7) contains 11 repeats of leucine-rich 22 amino acid segment. The leucine–rich repeat is a structural motif used in several molecular functions as; signal transduction, cell adhesion, cell development and RNA processing. This protein contains consensus sites for protein kinase A, calmodulin-dependent kinase, and glycogen synthase kinase 3, which are all present in spermatozoa (Mishra, *et al*., 2003; Huang, *et al*., 2002). Sds22 was found to be present in an inactive heterodimer with PP1γ2 in motile caudal epididymal spermatozoa, thus sds22 is a PP1γ2 inhibitor. In immotile caput spermatozoa, sds22 is not bound to PP1γ2 but is either free or bound to a 17-kDa protein (p17). In fact, a portion of caput sperm PP1γ2 is catalytically active and in a free form. The inability of sds22 to bind to PP1γ2 is probably not due to a modification in PP1γ2 but to the complex formed between sds22 and p17, which prevents the formation of PP1γ2-sds22 complex. The dissociation of the complex sds22-p17 and subsequently association of PP1γ2-sds22 is probably

caused by phosphorylation of sds22 or p17, which may even proteolyzed during the epididymal sperm maturation. Therefore, it is possible that sds22 phosphorylation may be necessary for its binding to PP1γ2 leading to a scenario where sds22 may be phosphorylated in caudal but not in caput spermatozoa. Nevertheless, is probable that all of the reasons mentioned before contribute for the higher PP1γ2 activity in caput, compared with caudal spermatozoa, so the inability of sds22 to bind and inactivate PP1γ2 could be the main reason. Mishra and co-workers (2003) hypothesize that the change in binding partners of sds22 from p17 to PP1γ2 and the development of the binding capacity of sds22 for PP1γ2 are key events responsible for the decline of protein phosphatase activity during epididymal sperm maturation and motility initiation (Mishra, *et al*. 2003). The immunolocalization of sds22 and PP1γ2 within spermatozoa revealed that both proteins are present in the tail although sds22 staining at the head is different from PP1γ2 (Huang, *et al*., 2002).

1.4.4 The complex PP1γ2/14-3-3

14-3-3 comprises a family of abundant, small acidic proteins (~30 kDa) expressed in all eukaryotic cells and its amino acid sequence is highly conserved in species ranging from yeast to mammals. In mammals, despite their highest expression in the central nervous system, these proteins are ubiquitous in almost all other tissues, especially in the intestines and testis. These proteins comprise seven isoforms (β, γ, ε, ζ, η, θ, σ) in mammals that are highly conserved and share about 50% amino acid identity and, consequently, highly similar protein conformations to form either homodimers or heterodimers. More than 200 binding partners of 14-3-3 have been reported, these are involved in a ranging of cellular activities such as cell cycle progression, the DNA damage response, apoptosis, protein trafficking, signal transduction, cytoskeletal rearrangements, metabolism and transcriptional regulation of gene expression. This type of promiscuous behavior remains completely unresolved (Sun, *et al*., 2009; Gardino, *et al*., 2006). The regulation of 14-3-3 activity can occur either on the binding partners or on the 14-3-3 *per se*, both forms of regulation are carried out through phosphorylation, at least for a subset of 14-3-3 proteins (Sun, *et al*., 2009; Gardino, *et al*., 2006). 14-3-3 is conferring protein-

protein interactions in different cells, and it is found abundantly in testis playing a crucial role in Sertoli-Sertoli and/or Sertoli-germ cell interactions during spermiogenesis (Sun, *et al*., 2009). Nevertheless, while protein 14-3-3 isoforms have been detected in testis and developing spermatocytes, their presence in mature epididymal spermatozoa was only first documented by Huang and co-workers (2004a). In this study they demonstrated that 14-3-3 ζ was present in spermatozoa not only from bovine caudal epididymal spermatozoa, but also from bull, hamster, horshoe crab, monkey, rat, turkey, and *Xenopus*. PP1γ2 is one of the many binding partners of 14-3-3 (Puri, *et al*., 2008; Huang, *et al*., 2004a). Sperm PP1γ2 contains a similar sequence, RXXT(p)XP, where T(p) refers to phosphorylated threonine, which may be the site for protein 14-3-3 binding. Since, protein 14-3-3 binds to phosphorylated domains (Gardino, *et al*., 2006) it would be expectable that PP1γ2 bound to protein 14-3-3 in sperm extracts to be phosphorylated. However, it does not prove that phosphorylation is essential for 14-3-3 binding. PP1γ2 is not the only binding partner of 14-3-3 in spermatozoa, p114 and p51 are also present in sperm extracts bind to 14-3-3. Huang and co-workers (2004a) proposed that the action of protein 14-3-3 does not appear to inhibit PP1γ2 but rather regulates PP1γ2 by altering is ability to interact with other proteins. One possible explanation is that 14-3-3 acts as a bridge or an adaptor (Gardino, *et al*., 2006) between PP1γ2 and other sperm proteins involved in the regulation of sperm maturation and motility initiation, or alternately 14-3-3 may protect PP1γ2 from degeneration or desphosphorylation. This latter hypothesis could be linked to the fact that, inhibition of protein phosphatases stimulates motility, and so 14-3-3 may protect PP1γ2 phosphorylation and thus maintain the low PP1γ2 catalytic activity required for motility. The immunocytochemistry analysis results revealed phospho-PP1γ2 and protein 14-3-3 both located in the post-acrosomal region of the head and principal piece of the tail spermatozoa. Therefore, confirming the interaction between PP1γ2 and 14-3-3 (Huang, *et al*., 2004a). Other study from Puri and co-workers (2008) confirmed that, GSK-3 was found to bind to 14-3-3 establishing a complex with PP1γ2. These results suggest that 14-3-3 may have an important regulatory role in male germ cell maturation in the testis (Puri, *et al*., 2008).

1.5 SARP a new alternatively spliced PIP

Browne and co-workers (2007) were the first to describe a novel protein possessing several ankyrin repeats termed initially by Fardilha (2004) as SEARP (six to eight ankyrin repeat protein) and nowadays by SARP (several ankyrin repeat protein). Initially, in order to identify proteins capable of interacting with PP1, PP1γ1 was used as bait in an YTH approach to screen two different libraries, human B-lymphocyte and human testis cDNA. As a result were identified and isolated, one of ten positive clones (H2) from the first library and one of 120 positive clones (40Q3) (Fardilha, 2004) from the second. These clones encoded the novel protein SARP in which H2 comprise an open reading frame of 1779nt that encoded 593 amino acids followed by a stop codon and a short 3´-untranslated region, while 40Q3 comprise an open reading frame of 2346nt that encoded 782 amino acids followed by a stop codon and a different 3´-untranslated region. Furthermore, these clones were termed as SARP1(H2) which contains eight ankyrin repeats preceded by a potential PP1-binding motif and SARP2(40Q3) which also contains eight ankyrin repeats but represents a splice variant differing in its C-terminal sequence (Browne, *et al.*, 2007; Fardilha, 2004) (Figure 5). Additionally, a new screening using the human universal cDNA library and 300bp fragment from 5´end of H2 as bait, resulted in the discovery of a new clone 1G07 with overlapping sequence but different 3´end. This new clone was termed as SARP3 and comprises an open reading frame encoding 591 amino acids and just six ankyrin repeats (Figure 5) (Browne, *et al*., 2007).

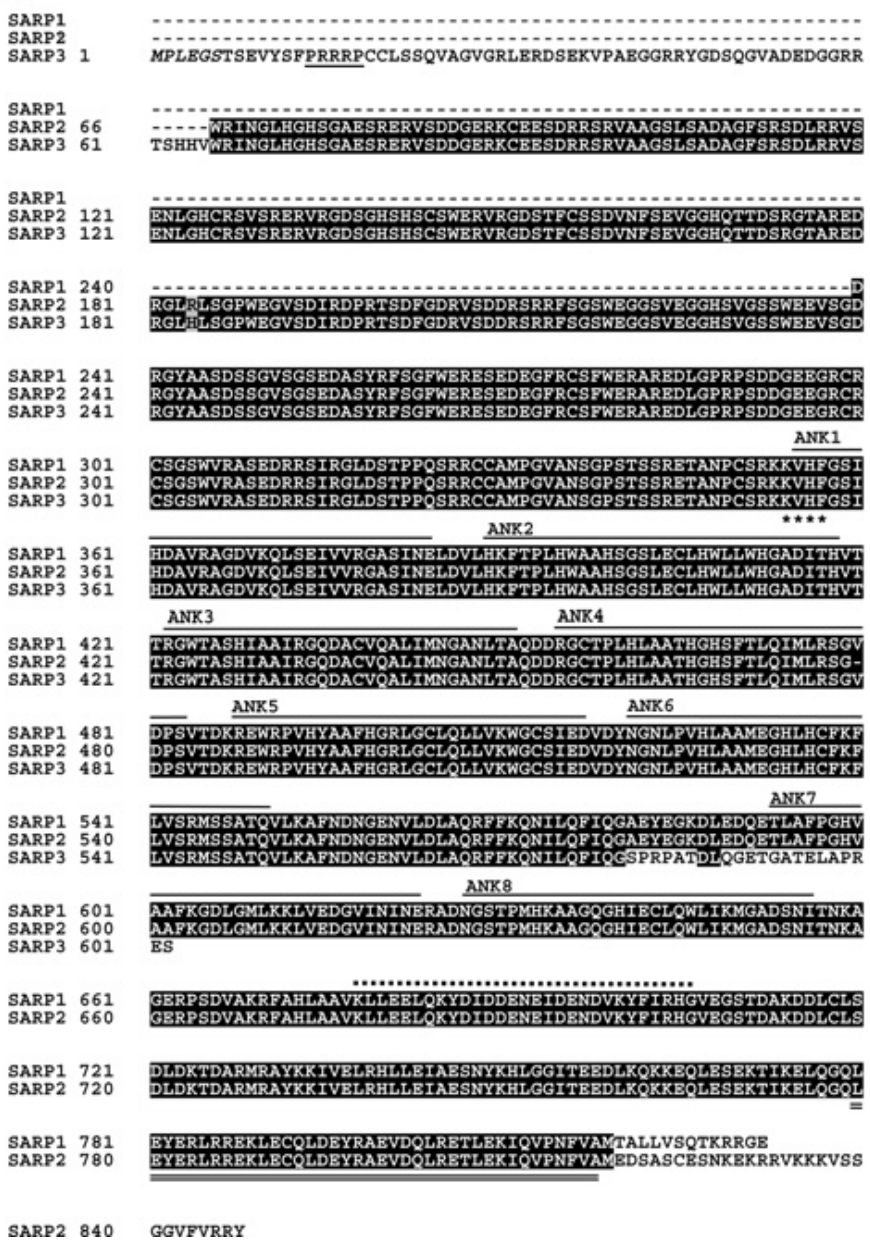

Figure 5: Comparison of the SARP1, SARP2 and SARP3 amino acid sequences. The PP1-binding motif is underlined with asterisks. The eight ankyrin repeats (ANK1-ANK8) are indicated by a single line above the sequences. The dotted line above the sequences indicates putative EF hand in SARP1 and SARP2. A double underline indicates a putative leucine-zipper domain present in SARP1 and SARP2 (adapted from Browne, *et al.*, 2007).

The three isoforms of SARP had derived by alternative splicing from a single gene of at least 65kb and 14 exons on the chromosome 11. According to the amino acid sequence (Figure 5) of the three different isoforms the molecular masses were calculated being 66kDa for SARP3, and for SARP1/2, assuming the same N-terminal section, 92,5kDa and 94,3 kDa respectively. Bioinformatics analysis of the encoded protein SARP revealed several interesting features of

its domain structures, like the number of ankyrin repeats present in the different isoforms. Six ankyrin repeats were identified in SARP3, while SARP1 and SARP2, also possess a putative Ca^{2+}-binding EF hand and a putative leucine zipper domain besides eight ankyrin repeats (Figure 6). Additionally to these structures also a possible nuclear localization sequence was predicted at amino acids 14-18 in the N-terminus of SARP (Figure 6) (Browne, *et al.*, 2007; Fardilha, 2004).

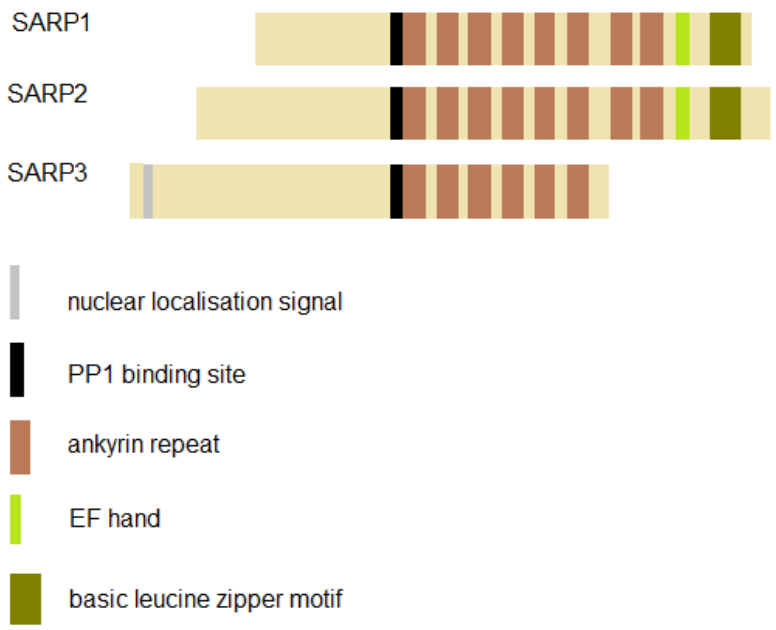

Figure 6: Schematic comparison of the protein domain structures of SARP1, SARP2 and SARP3 (adapted from Browne, *et al.*, 2007).

The interaction of SARP with PP1 was confirmed both *in vitro* and *in vivo*, by several techniques such as YTH screening, bacterially expressed SARP experiments confirmed by immunoadsorption and blot overlay and also by immunodetection of endogenous SARP forming different immune complexes. Additionally, it was found that bacterially expressed SARP bind bacterially expressed PP1γ1 and PP1γ2 by immunoadsorption and blot overlay respectively. Regarding endogenous SARP, it was found to be forming immune complexes with PP1α and PP1β in tissues (brain cortex) or cell lines (HEK-293-human embryonic kidney 293) where these PP1 isoforms were more abundant (Browne, *et al.*, 2007). At the same time in immunoblotting lysates from rodent and human tissues it revealed that both SARP1 and SARP2 were present in all

mouse tissues with higher levels in testis, liver, spleen, lung and ovary in a descending order of magnitude. According to densiometric analysis of SARP mRNA band, the amount of SARP mRNA in testis was more abundant than in all other tissues analysed. SARP 1 and SARP2 appeared to be extremely abundant in human sperm comparing to human testis (Figure 7) (Browne, *et al*., 2007, Fardilha, 2004). An analogous experiment was done for SARP3 and the highest levels were found in mouse brain. Immunocytological localization of SARP revealed that endogenous SARP isoforms appeared to be highly enriched in the nucleus of COS-7 cells but also at lower levels in the cytoplasm. This nuclear localization is consistent with a putative nuclear localization signal at the N-terminus like the one found in SARP3 (Figure 6). SARP is associated with and modulates the phosphatase activity of PP1. This was corroborated by an experiment with phosphorylase *a* as substrate in which, the highest phosphatase activity was found in rat testis and brain. When phosphorylase was used, SARP inhibited the bound PP1 catalytic activity but Browne and co-workers (2007) hypothesized that PP1 might be less inhibited or even activated towards an *in vivo* substrate the PP1-SARP complex. The putative PP1 binding motif of SARP, $K^{354}VHF^{357}$, was identified by sequence comparison with the consensus PP1-interaction motif. In order to verify if the $K^{354}VHF^{357}$ motif was uniquely responsible for the maintenance of SARP-PP1 binding a few studies were conducted, revealing that neither the mutation of Phe^{357} to alanine within the $K^{354}VHF^{357}$ motif nor the addition of a peptide covering this region resulted in a complete disruption of the binding of SARP-PP1 (Browne, *et al*., 2007). Indeed, this indicates the existence of one or more SARP interactions sites with PP1, such as the ankyrin repeats that in MYPT1 crystal structure (Terrak, *et al*., 2004) appear to form secondary interactions with PP1. There are other regulatory subunits of PP1 that also share with SARP the coupling of a canonical PP1-binding motif and an ankyrin repeat domain, like for example 53BP2, TIMAP and MYPT1. The first two proteins have four ankyrin repeats and the last one has seven ankyrin repeats domains and the PP1 binding motif immediately precedes the start of the first ankyrin repeat. Although, in SARP the $K^{354}VHF^{357}$ motif lies partially within the first ankyrin repeat, which is a novelty, suggest that the ankyrin repeat appears to be flexible and fold favourably to present and exposed RVxF motif independently from its position. Moreover, the

localization of the canonical PP1 binding motif partially within the first ankyrin repeat may aid stabilization of the SARP-PP1 complex (Browne, *et al*., 2007).

SARP is highly abundant in the nucleus and interacts with DNA more specifically mammalian DNA. SARP2 binds especially to mammalian DNA suggesting a role in the regulation of transcription, which has been identified before in several studies where it was observed that PP1 could interact with proteins that modulate transcription (Hox11, HCF, etc.). Furthermore, the existence of a leucine- zipper motif nears to the C-terminus of both SARP1 and SARP2 (Figure 6) support the hypothesis that these isoforms may function as transcription factors or cofactors. The shorter isoform SARP3, which ends before the leucine-zipper motif and has totally different tissue localization, is expected to have a different function, when compared with SARP1 and SARP2 (Browne, *et al*., 2007).

1.5.2 The complex SARP2-PP1γ2

The discoveries on this novel protein SARP, and particularly in SARP2, encouraged further studies on the possible function in human testis and sperm motility. The analysis of an immnunoblot with SARP2 and PP1γ2 in rat tissues, human testis and human sperm, revealed that SARP is expressed more abundantly in testis, sperm, ovary, lung and liver. The highest levels of PP1γ2 were detected in testis, ovary and lung in a descending order of magnitude. Furthermore, both SARP2 and PP1γ2 appeared to be enriched in sperm, in contrast to PP1α, which is equally expressed in human testis and human sperm (Fardilha, 2004) (Figure 7).

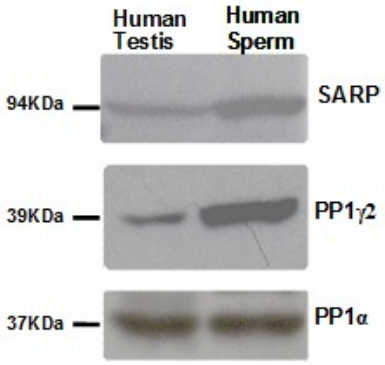

Figure 7: Immunoblot analysis of SARP, PP1γ2 and PP1α expression in human testis and human sperm (50µg) (adapted from Fardilha, 2004).

In order to confirm the interaction of the SARP2-PP1γ2 complex two different approaches were used. These experiments revealed that SARP2 interacts with PP1γ1 and PP1γ2 but not with the unique C-terminus of PP1γ2, and that the interaction seems stronger with PP1γ2 than with PP1γ1. Immunohistochemistry studies on rat testis sections revealed that there is a relationship between SARP2, PP1γ2 and PP1γ1, which are found in the spermatozoa tails and possibly in the acrossome region of the head and in other surrounding cells. Therefore, it is possible to speculate that all of the three proteins are present in a variety of cells throughout spermatogenesis and spermiogenesis (Fardilha, 2004).

Immunofluorescence analysis was also used to further support the presence of SARP in human sperm and to localize PP1γ2 and SARP within human spermatozoa. SARP immunoreactivity was detected in the principal piece of the tail and the connecting piece, an also in the middle piece although with a relatively weak staining. In the head region, immunoreactivity was also observed in the equatorial area (Figure 8). Therefore, there are regions within human spermatozoa where PP1γ2 and SARP co-localize (Figure 9) (Fardilha, 2004).

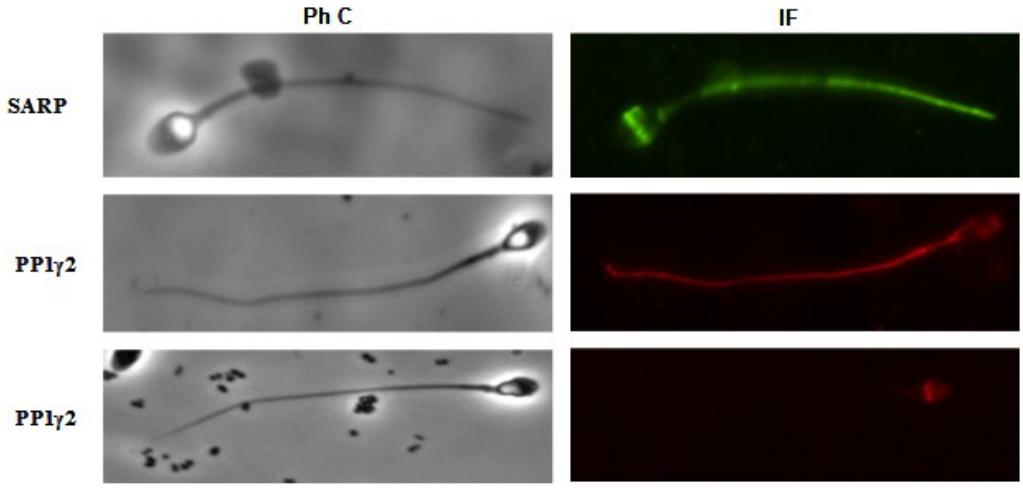

Figure 8: Immulocalization of PP1γ2 and SARP in human spermatozoa. PH, phase contrast; IF, immunofluorescence (60X magnification) (adapted from Fardilha, 2004).

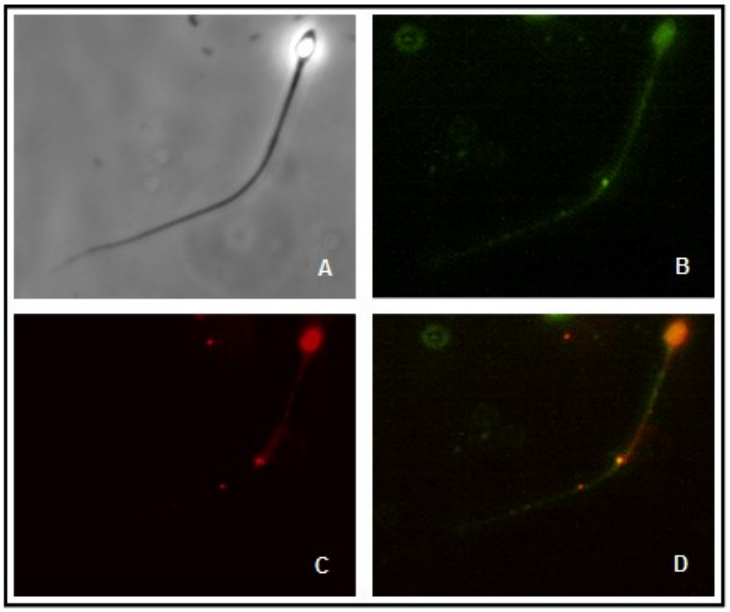

Figure 9: Co-localization of PP1γ2 and SARP in human spermatozoa. A: phase contrast; B: immunolocalization of SARP; C: immunolocalization of PP1γ2; D: merge of PP1γ2 and SARP immunoreactivity (adapted from Fardilha, 2004).

The data suggested two possible SARP functions related to sperm function. First, associated with PP1γ2 in the sperm tail, it might suggest a possible role in sperm motility. Secondly, SARP could also be essential for the acrossome reaction, and after sperm-egg interaction it might be able to

translocate to the nucleus where it might alter gene expression. This later hypothesis is further supported by the presence of the leucine zipper motif on the C-terminal domain of SARP, and finally SARP could also act as an intermediary between calcium signalling and PP1γ2 regulation in sperm motility because of its putative Ca^{2+}-binding EF hand (Figure 6) (Fardilha, 2004).

1.6 Biomarkers to address sperm defects or andrological related disorders

Epidemiological data suggest that approximately 15-20% of all couples that attempt to concieve face the problem of infertility (Deepinder, *et al*., 2007). Sperm dysfunction is the most common cause of infertility, yet there is no drug a man can take or add to his spermatozoa *in vitro* to improve fertility (Barratt, *et al*., 2011). The management of male-factor infertility is still a challenge and the lack of progress in this area is due to our limitations in the understanding of the cellular and molecular mechanisms underlying sperm functions. However, over the last few years there has been appreciable progress in addressing new methods to diagnose sperm dysfunction (Barratt, *et al*., 2011).

The recent fifth edition of WHO semen analysis manual is much more complete including now; step by step methods, constructive discussion of quality control and quality assurance and detailed description of the assessment of sperm morphology (Barratt, *et al*., 2011). Even though with all of these new improvements, the value of the traditional semen parameters (concentration, motility and morphology) as a clinical tool in diagnosis and prognosis of male infertility is still a polemic subject (Barratt, *et al*., 2011; Lefièvre, *et al*., 2007). Three particular aspects mainly caused this scenario. Firstly, technicians are not using the detailed laboratory methods correctly even when provided with comprehensive manuals. A shocking example, not only limited to UK, is that 69% of the laboratories counted ≤ 100 sperm for morphology assessments making the assay redundant. Secondly, training methods exist- but are they used/useful? A series of programs have been developed and proven to reduce variability that have been observed by external quality control programs

between analysts in the majority of the laboratories. Thirdly, the value of semen assessments is being consistently denigrated by scientists and clinicians who assume, wrongly, that are being currently performed in adequate manner. This type of assumptions leads to serious problems, such as the evidence of external quality control schemes, which demonstrates that a large number of couples are being exposed to inappropriate treatment, e.g., ICSI when they may not need ART (Assisted Reproduction Techniques) (Barratt, *et al*., 2011). The management of male-factor infertility is still a challenge, especially because of two factors: the lack of a rapid, non-invasive test to evaluate semen quality; and the inability to predict gamete quality and embryo viability (Deepinder, *et al*., 2007; Lefièvre, *et al*., 2007). There is an urgent need to improve the assays to determine quality, which, must be robust, cheap (cost effective), easy to use and clinically useful (Barratt, *et al*., 2011). To date, only three potential test of sperm function have sufficient data to support their routine use: penetration into cervical mucus, measurement of reactive oxygen species production/lipid peroxidation and estimation of sperm chromatin/DNA damage. Nowadays, new technology developments are emerging which promise to transform our diagnostic and treatment pathways; e.g., the biomarkers discovery and home-testing of male infertility (Lefièvre, *et al*., 2007).

The widespread and acceptance of these home-testing for male infertility need to pass through, test some functional capacity of the cell rather than numbers and also be robust, cheap and widely available (Barratt, *et al*., 2011). Björndahl and co-workers (2006) developed a home-testing based on assessing the concentration of progressively motile sperm, which is one of the most predictive parameters for estimating infertility, in which they mimicked penetration into human cervical mucus *in vitro* using hyaluronic acid, a known cervical mucus substitute for sperm studies. The presumption is that men who test positive (red line-thus > 10 million progressively motile sperm/ml semen) will not require a semen assessment unless specific and rare circumstances. Nonetheless, men who were negative (no red line) would urgently required a normal and traditional semen parameters evaluation according to WHO (2010) (Figure 10) (Björndahl, *et al*., 2006). However, it is likely that in the future new and more robust versions of this type of tests will become available.

Surprisingly, these tests may also be taken a step further-from diagnosis to treatment (Barratt, *et al*., 2011).

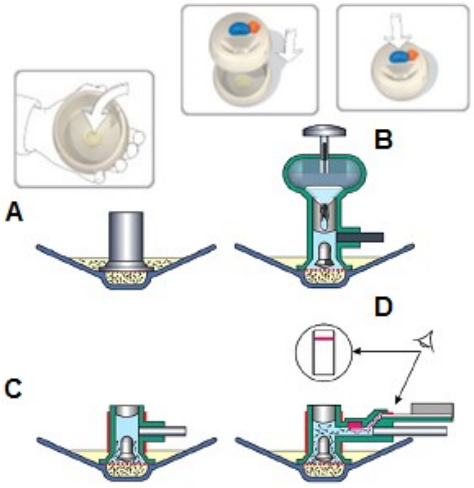

2

Figure 10: (A) Schematic drawing of the test device with 600 µl at the bottom sealed off by a swim-up chamber with mesh at the top of the semen volume. (B) The swim-up process is initiated by the depression of a button which releases a hyaluronate (hyaluronic acid) solution (blue) on top of the mesh at the semen surface. (C) During the half-hour swim.up phase, the swim-up chamber is heated with a heating collar (red line) to 37 °C. (D) After the swim-up phase, progressively motile sperm in the hyaluronic acid solution are released into capillary channel, labeled with anti-CD59 colloidal gold conjugated (red sperm) and trapped on the nitrocellulose strip, where a visible line is formed if sufficient numbers of progressively motile sperm have migrated into the hyaluronic acid solution (adapted from Björndahl, *et al*., 2006).

The biomarker discovery is linked to the new “omics” technologies, which have opened up exciting opportunities for screening and identifying putative biomarkers that may help define pathological states (Davis, *et al*., 2010). Presently, there is a deficiency of markers of human sperm function at molecular level (Barratt, *et al*., 2011). In order to get more detailed understanding at the molecular level of male infertility, it would be opportune to study the differences in gene expression between fertile and infertile men. There have been a number of studies suggesting that the mRNAs discovered in mature human sperm, could be used to trace differences in mRNA profiles, otherwise known as transcriptomes, and be used as diagnostic tool (Barratt, *et al*., 2011, Varghese, *et al*., 2007). Therefore, if the differences in mRNA profiles are uncovered, the potential could be tremendous being a great insight into

identifying potential biochemical markers for infertility, as well as clues to its indirect causes or direct triggers. The microarray technology has the potential to be used in clinical diagnosis of male infertility, in which is created an mRNA profile that can be compared with a physiologically normal gene expression profile for sperm (Varghese, *et al*., 2007). One variation between fertile and infertile men could reside in how the proteins are post-translationally modified as opposed to its mere presence or absence (Barratt, *et al*., 2011). Hence clinical proteomics is an emerging field that seeks to response to these questions through the search of biomarkers and the generation of profiles, which can help to predict, diagnose and monitor human pathologies (Varghese, *et al*., 2007). The availability of several databases of sperm proteins, catalogues of hundreds to thousands of proteins, are very valuable as they provide a list of proteins that make up the sperm. These databases are just the beginning of a new era that already provides an important reference for further research (Oliva, *et al*., 2009). There are already innumerous studies in the field of proteomics, for example Pixton and co-workers (2004) have found that infertile men have altered expression of at least 20 proteins regarding the fertile men (Pixton, *et al*., 2004). Barratt and co-workers 2011 have found a potential biomarker of sperm dysfunction the intra-acrosomal protein zonadhesin. Preliminary data suggest that like in mouse in which zonadhesin was only detectable at the sperm surface of live spermatozoa after incubation in capacitating conditions, the same is true for humans. Driven by the overwhelming clinical need to identify infertile men without the requirement for a semen parameters assessment, we may soon be able to obtain metabolomic profiling on blood samples which act as a surrogate for fertility (Barratt, *et al*. 2011). Metabolomics has been developed with the expectation that a body fluid (blood, urine, saliva, etc) can be optimized to create a low-cost, informative and medically relevant mean of measuring metabolic changes. The molecular markers of interest consist in small molecules, which are intermediates and products of metabolism that represent the functional phenotype in a cell tissue or organism (Davis, et al., 2010). Oxidative stress biomarkers have been found in both the male and female reproductive tracts and are known to affect sperm quality and function, oocyte quality and embryo viability. Recently, high levels of ROS (reactive

species of oxygen) were observed in 25-40% of semen samples from infertile men (Deepinder, *et al*., 2007).

A biomarker discovery always implies critical statistical validation methods, which evaluate the predictive power of a biomarker (Davis, *et al*., 2010, Hu, *et al*., 2008). Hence, it is challenging to translate candidate biomarkers from proteomic approaches or others into real-world diagnostic or prognostic applications. After all, the approval for using a biomarker or a set of biomarkers for a given clinical decision relies on the results of large-scale multicenter clinical trials and approval of the use of the detection technology for that purpose. Consequentely, the appropriate application of a biomarker in clinics can also be aided by novel diagnostic devices, such microfluidics-based chips for simple and high-throughput measurement of the biomarker (Hu, *et al*., 2008).

1.7 Aims of this thesis

The value of the traditional semen parameters (concentration, motility and morphology), evaluated according to WHO guidelines, have a limited degree of prognostic and diagnostic for the infertile couple. Indeed, those parameters are being applied wrongly to some couples who are “force” to get though an ART intervention, which is something extremely stressfull for the couple (Barratt, *et al*, 2011; Lefièvre, *et al*., 2007). However, over the last few years, there has been a considerable progress in our knowledge of the cellular and molecular workings of the mature spermatozoon (Barratt, *et al*, 2011). Therefore, future biomarkers of sperm dysfunction are being discovered and studied, through the transcriptomics, proteomics and metabolomics. In fact, some potential biomarkers have been already identified through proteomics, leading to a possible application on diagnostic or specific treatments (Oliva, *et al*., 2009). Unfortunately there is still a long way to go, currently there is a paucity of markers of human sperm function at molecular level that can lead us to distinguish between fertile and infertile man (Barratt, *et al*, 2011). This type of approach based on molecular markers could be an alternative to the traditional

semen parameters, which are full of flaws. In the future we could have a much more reliable way to evaluate sperm dysfunction. SARP2 could be one of these future potential molecular markers of sperm dysfunction, more specifically at the morphology level. At this thesis, the behavior of SARP2 within spermatozoa with different sperm morphologies was observed and analysed statistically. The main objectives of this thesis were:

1) Optimize the immunocytochemistry conditions for using antibody SARP-8C (custom-made antibody for SARP2),
2) Evaluate which was the best washing procedure, for immunocytochemistry analysis of SARP2 expression within human spermatozoa,
3) Assess SARP2 expression pattern within normal spermatozoa and abnormal spermatozoa, in terms of morphology,
4) Ascertain if SARP2 could be used as a molecular marker of sperm morphological defects through statistical validation.

2: Optimization of immunocytochemical conditions for using antibody SARP-8C

2.1 Introduction

SARP (several ankyrin repeat) is a protein which, was found through YTH screening, in which, three splice variants where found, SARP1, SARP2 and SARP3. SARP2 is enriched in human testis and sperm (Figure 7). In testis it binds to PP1γ1 and PP1γ2 whereas in sperm it only binds to PP1γ2 (Browne, *et al.,* 2007). In previous studies conducted by Fardilha (2004), SARP2 was showed to be present in spermatozoa (by immunocytochemistry) mainly in the principal piece of the tail, at the equatorial region of the head and also at the connecting piece (Figure 8) co-localizing with PP1γ2. (Figure 9) (Fardilha, 2004).

One of the initial challenges of this experiment was to ascertain if the antibody SARP-8C, produced commercially, could be used for immunocytochemistry. This antibody raised new possibilities for the subcellular localization of SARP within human spermatozoa, since with this antibody only SARP2 is detected in contrast to the antibody used by Fardilha (2004) that detected both SARP1 and SARP2. The primary antibody SARP-8C was obtained with an amino acid sequence of SARP2 (Figure 5) in rabbit commercially (Covalab, Cambridge, United Kingdom). The synthetic polypeptide with the amino acid sequence, DSACESNKEKRRVK, corresponding to part of the carboxy-terminus of SARP2 was used as antigen to obtain the antibody SARP-8C (Figure 11).

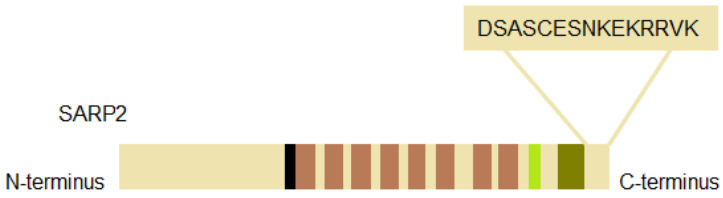

Figure 11: SARP-8C amino acid sequence: DSASCESNKEKRRVK, of the C-terminus of SARP2 used to raise the antibody SARP-8C (adapted from Browne, *et al*, 2007).

The first challenge, of this first experiment, was to optimize the conditions of the immunocytochemistry procedure, since the use of a new antibody always implies this type of analysis. The first thing to be optimized was the dilution of the antibodies used and the second was the type of washing procedure to apply. In order to evaluate the best washing procedure for the sperm preparation, in which the spermatozoa are separated from the seminal plasma, two different approaches were used. The first being used was the simple washing procedure with PBS, in which the great disadvantage is that all the spermatozoa, including the dead, moribund and abnormal ones, present in the original semen sample remain in the final sperm population. In fact, there are other cells present at the final preparation, as the cells from the germ line that were sloughed from the seminiferous epithelium and leucocytes of various types (personal communication, C. Barratt). The second approach used was a sperm preparation with a Density Gradient Centrifugation (Percoll®), in which, a series of layers of decreasing density are place one on top of the other and at the top is placed the semen sample. So, the layers create gradually changes in density that become clogged by cells or other materials, retarding or preventing the passage of more dense cells down the gradient. The major advantage of this approach is to be able to select a population of motile spermatozoa rejecting the immotile spermatozoa, the moribund and the dead ones (personal communication, C. Barratt).

2.2 Material and Methods

Human semen sample preparation

The analysis of the human semen samples was done according to the fifth edition of the manual from World Health Organization from 2010. The human semen samples were collected from healthy adult men by masturbation, in which an informed consent was signed.

During the first 5 min after collecting the semen, the sample was kept at an incubator at 37°C for liquefaction. After 30-60 min, the appearance of the ejaculated was analyzed for viscosity, pH and sample volume. Then, an aliquot of the sample was used to evaluate the general appearance under a phase-contrast microscope (400x), using a wet preparation. Sperm motility was assessed, as soon as possible, after liquefaction to limit the effects of dehydration, pH and changes in temperature. Therefore, the previously used, wet preparation was also used to assess motility, and at least 200 spermatozoa were evaluated per replicate (400 spermatozoa) in a total of at least five fields in each replicate. According to WHO (2010), the motility of each spermatozoon is graded in progressive (PR), non-progressive (NP) and immotile (IM) (Table 1).

Table 1: System of grading motility, according to WHO (2010) (adapted from WHO, 2010).

Motility categories	Definition
Progressive motility (PR)	Spermatozoa moving actively, either linearly or in a large circle, regardless of speed.
Non-progressive (NP)	All other patterns of motility with an absence of progression.
Immotility (IM)	No movement.

The average percentage for the motility grades (PR, NP, IM) was calculated. Using the same wet preparation for motility the sperm number was evaluated, and the appropriated dilution was assessed as follows (Table 2).

Table 2: Semen dilutions required, how to make them, which chambers to use and potential areas to assess. (adapted from WHO, 2010).

Spermatozoa per x400 field	Spermatozoa per x200 field	Dilution required	Semen (µ)	Fixative (µ)	Chamber	Area to be assessed
>101	>404	1:20 (1+19)	50	950	Improved Neubauer	Grids 5, 4, 6
16-100	64-400	1:5 (1+4)	50	200	Improved Neubauer	Grids 5, 4, 6
2-15	8-60	1:2 (1+1)	50	50	Improved Neubauer	Grids 5, 4, 6
<2	<8	1:2 (1+1)	50	50	Improved Neubauer or large-volume	All 9 grids or Entire slide

The number of spermatozoa was evaluated after having the correct dilution, which was fixated with 4% of formaldehyde, followed by a counting at a Neubauer Chamber after waiting 10 to 15 min for the spermatozoa to settle down. At the counting step at least 200 spermatozoa were counted per replicate, and the spermatozoa concentration was expressed in concentration of spermatozoa per ml in the total ejaculated volume, according to WHO specifications. The total sperm count was calculated using the sperm concentration multiplied by the volume of the ejaculated. To determinate the sperm morphology, a smear of semen on a slide was prepared followed by, air-drying, fixation and staining of the slide. The staining was done with haematoxylin eosin (HE) and the mounting of the slide and coverslip with Eukitt®. The slide was observed at phase-contrast microscope (1000x), where 200 spermatozoa were counted per each replicate (400 spermatozoa) with categorization in normal spermatozoa, abnormal spermatozoa with: head defects, neck and middle piece defects, tail defects, excess of residual cytoplasm (WHO, 2010).

The analysis of the human semen samples was only completed with the comparison of the reported values obtained with the standard reference values indicated by the WHO (2010) (Table 3). So the human semen samples were

then classified as normal or abnormal indicating if the volunteer was consider fertile or infertile.

Table 3: Standard reference values for each of the semen parameters evaluated according to WHO (2010).

WHO (2010) reference values	
Volume	1.5 ml or more
Sperm concentration	$15x10^6$ spermatozoa/ml or more
Total sperm count	$39x10^6$ spermatozoa/ejaculate or more
Total motility (PR+NP) Progressive motility	40% or more 32%or more
Morphology	4% or more normal forms

Immunocytochemistry procedure

After liquefying, the sperm was extracted from the ejaculated sample. First it was centrifugated at 1.200 rpm for 10 min at RT (Room Temperature) and then washed twice with 1xPBS (saline buffer) (7: Appendix).

To the final pellet was added 300 µl of a solution containing NCB (non-capacitating buffer) medium in 0.3% BSA.

NCB (Non-Capacitating Buffer) medium

The formulation of NCB medium (Table 4, see 7: Appendix) was done according to Dr. Christopher Barratt personal communication, that slightly differs from published data (Lishko *et al.*, 2009). The capacitation process is involved in losing the coating proteins that leads to a different organization of the plasma membrane (De, Jonje, 2006). Sperm capacitation needs elevation of intracellular calcium and bicarbonate (HCO_3) to activate adenylyl cyclase (AC) to produce cyclic-AMP, which in turn activates protein kinase A (PKA) to phosphorylate certain proteins (Breitbart, 2002). In contrast, in the NCB medium there is no HCO_3 and it also possess a lower concentration of BSA, to prevent cholesterol removal, and an increased concentration of Hepes to account the

reduction of HCO_3 (Dr. Christopher Barratt personal communication, Ferreira, 2010).

Table 4: Formulation of NCB (non-capacitating buffer) medium, NCB was buffered with Hepes (25mM) and adjusted to pH 7.4. 0.3% of BSA was added to the final solution (according to Dr. Christopher Barratt personal communication and Ferreira, 2010).

Components	Concentration (mM)	Amount (g/10 ml)	Volume (ml)
$CaCl_2$	1.8	0.027	1
KCl	5.4	0.040	1
$MgSO_4.7H_2O$	0.8	0.020	1
NaCl	116.4	0.680	1
NaH_2PO_4	1.0	0.016	1
D(+)-glucose	5.6	0.100	1
Sodium pyruvate	2.7	0.030	1
Sodium lactate	4.8	0.468	1

An aliquot of sperm cells (25µl) was placed onto a glass coverslip pre-coated with 100µg/ml of poly-L-ornithine, dried at RT, and then placed in a six well plate containing one coversplip per well. To each well was added 1ml of 4% paraformaldehyde in 1xPBS and it was left to stand for 10 min. Then, sperm cells were washed twice with 1ml 1xPBS for 10 min. The permeabilization of sperm cells was done with 1ml of 1:1 methanol/acetone (- 20°C) solution for 2 min and then washed twice with 1 ml of 1xPBS for 10 min. The cells were blocked out with 5% BSA in 1xPBS for 1 hour, and then incubated with primary antibody for 2 hours. After three washes with 1xPBS, the secondary antibody was added to the coversplis and left to stand for incubation for 2 hours. Finally, the cells were washed three times with 1xPBS and coversplis were mounted on microscope glass slides with one drop of anti-fading reagent containing DAPI for nucleid acid staining (Vectashield, Vector Laboratories). The images were acquired (1000x) using an epifluorescence microscope equipped with appropriated software (Olympus IX2-UCB).

2.2.1 Adjusting SARP-8C to the perfect dilution

To examine the possibility of using antibody SARP-8C, as a primary antibody, in immunocytochemistry, three different dilutions: 1:50, 1:100 and 1:250 were tested. In indirect immunocytochemistry it is necessary a secondary antibody (Texas Red was used). Texas-Red is a fluorochrome that is able to reveal the subcellular location of primary antibody. The secondary antibody was used at the dilution 1:500. Negative controls were performed without primary antibody and only with secondary antibody to ensure that no non-specific labelling or staining occurred (three dilutions were tested, 1:300, 1:500 and 1:750). All the antibodies used were diluted in 3% BSA in 1xPBS and were added subsequently, as follows (Figure 12).

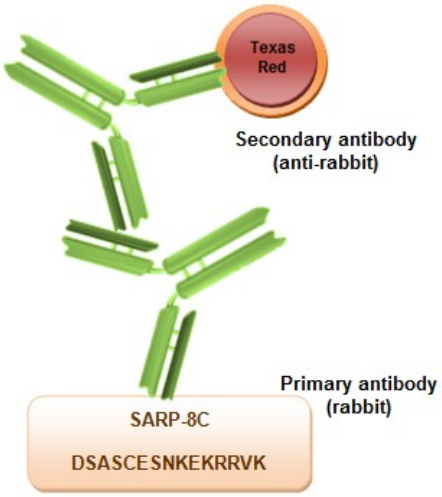

Figure 12: Immunocytochemistry procedure for subcellular localization of SARP2 within human spermatozoa. The primary and secondary antibodies used were added to the sperm sample subsequently. The amino acid sequence (DSASCENKEKRRVK) represented was the one used to make this antibody SARP-8C.

2.2.2 Evaluation of the different washing procedures: PBS and Percoll

To evaluate the different washing procedures, PBS and Percoll, the human sample used was analyzed according to WHO (2010) (see Human semen sample preparation). The difference between a simple washing procedure, with PBS, from one with Percoll reside in the way that sperm cells are retrieved from the ejaculated. Therefore, the human sperm sample was submitted to Percoll® (Sigma), which is a density gradient centrifugation that is used as an alternative washing procedure, besides PBS (simple washing, with saline buffer). This procedure was done according to Dravland and Mortimer (1985), Mortimer (2000), and Dr. Christopher Barrat personal communication (Figure 13).

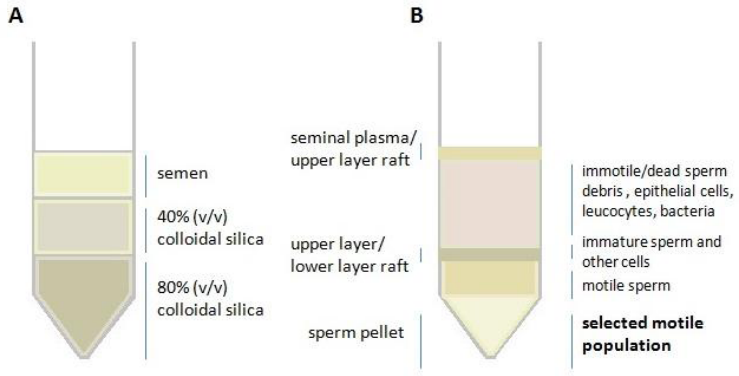

Figure 13: Sperm sample selective washing method using density gradient centrifugation with Percoll® 40%/80% buffered in NCB medium. A: Gradient obtained before centrifugation. B: Gradient obtained after centrifugation (adapted from Dr. Christopher Barratt personal communication and Ferreira, 2010).

This selective washing procedure consist firstly in layer the semen sample over 40%/80% of Percoll® gradients, buffered with NCB (non-capacitating buffer) and then centrifuge at 500g for 20 min at RT. After centrifugation a pellet of viable sperm was formed at the bottom of the tube, so the supernatants were discarded and the motile sperm population was selected (Figure 13). The sperm pellet was washed twice in 1ml of NCB, and the final pellet was resuspended in 300 µl of NCB.

The immunocytochemistry procedure was done in the exact same way as described before (see Immunocytochemistry procedure). Concurrently, with

the same sample a simple washing procedure, with PBS, was done in parallel, to get an overview of the two different washing procedures.

2.3 Results

2.3.1 Adjusting SARP-8C to the perfect dilution

The human semen sample was evaluated according to WHO 2010 (see Human semen sample preparation) (Table 5).

Table 5: Analysis of the sperm parameters evaluated according to WHO 2010.

Sperm parameters analysis			
Volume		ml	2
Motility	Progressive	%	30
	Non-progressive		28
	Immotile		42
Sperm concentration		sperm cells x 10^6/ml	77
Total sperm count		sperm cells x 10^6 per ejaculate	154
Morphology (%)		Normal	6
		Head defects	75
		Neck and middle piece defects	13
		Tail defects	4
		Cytoplasmatic droplets	2

The human semen sample analysed above (Table 5) can be classified as normal, since only the Progressive motility was compromised, being lower than the reference value according to WHO (2010) (see Table 3 for standard values). The motility was possibly deviated from the standard value as a result of the long period of time from the sampling and the sample reception.

According to these results, the antibody SARP-8C can be used in immunocytochemistry to obtain SARP2 subcellular localization (Figure 14).

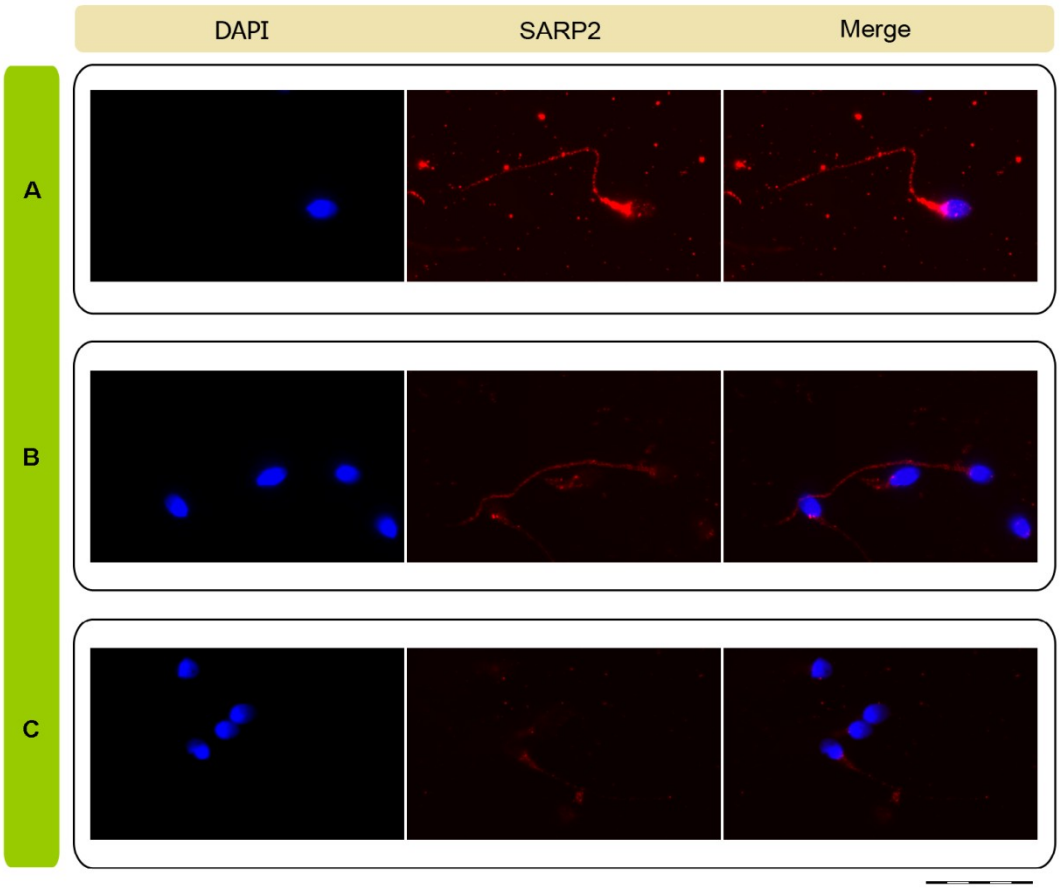

Figure 14: Subcelluar localization of SARP-8C within human spermatozoa conjugated with primary antibody SARP-8C and secondary antibody conjugated with Texas Red. A: Dilution 1:50. B: Dilution 1:100. C: Dilution 1:250 of SARP-8C. Scale bar = 20µm.

Apparentely in most of the morphologically normal spermatozoa SARP2 is located at the connecting piece and at the entire length of the tail (Figure 14). In contrast, no staining was observed in the equatorial region of the head, as it was previouslyobserved by Fardilha (2004).

Taking into account the previous results, the dilution of 1:100 for the primary antibody SARP2 was chosen, because the resultant background was lesser than in the others. Therefore, this dilution was used for all the following experiments afterwards.

2.3.2 Performance evaluation of different washing procedures: PBS and Percoll

The human semen sample was evaluated according to WHO 2010 (see Human semen sample preparation) (Table 6).

Table 6: Analysis of the sperm parameters evaluated according to WHO 2010 (* according to WHO, 1999).

Sperm analysis			
Volume		ml	5
Motility	Progressive	%	70
	Non-progressive		12
	Immotile		18
Sperm concentration		sperm cells x 10^6 /ml	30
Total sperm count		sperm cells x 10^6 per ejaculate	150
Morphology (%)*		Normal	18
		Head defects	26
		Neck and middle piece defects	7
		Tail defects	26
		Multiple defects	24

The human semen sample analysed above (Table 6) can be classified as normal, since all of the values were according WHO (2010) (see Table 3 for standard values).

The performance of the two different types of washing procedures was evaluated through the examination of several images, which were acquired to see the differences between them. Thus, as illustrated below (Figure 15) the differences between the two washing procedures were relevant.

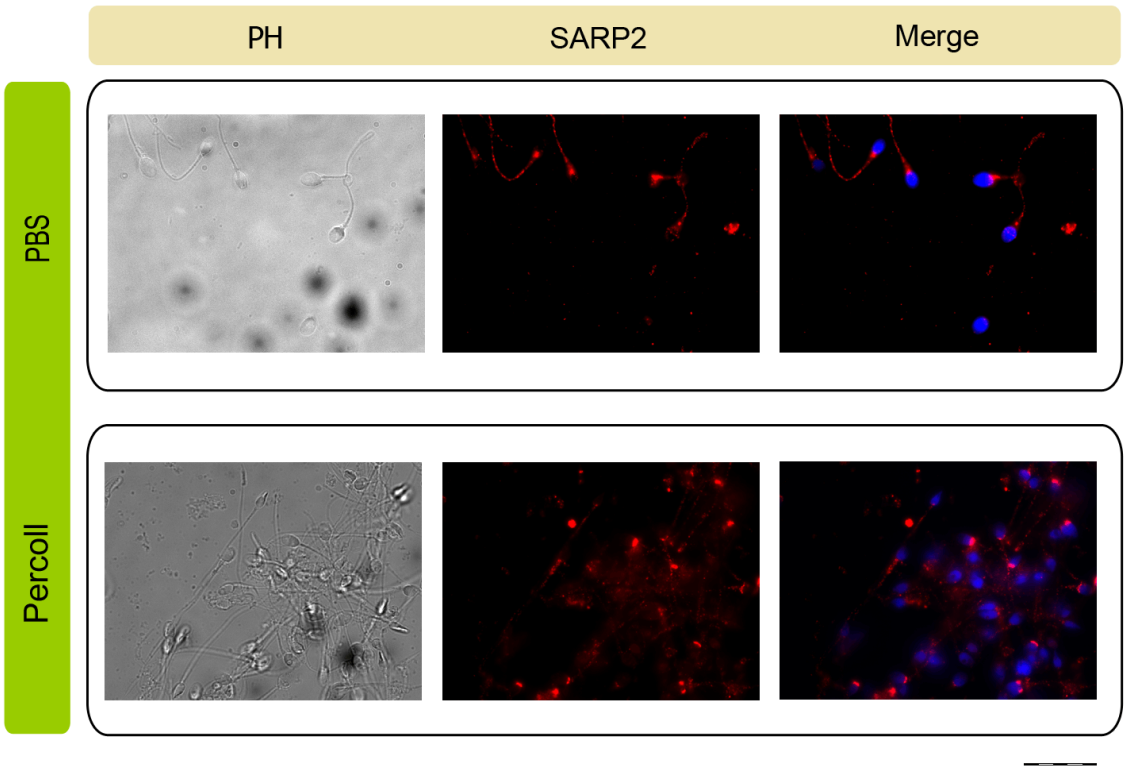

Figure 15: Immunofluorescence images, which represent the differences between the two different washing procedures, PBS and Percoll. PH: phase contrast. SARP2: with TRICT laser. Merge: composite image including DAPI fluorescence and SARP2 staining (1000x). Scale bar = 20µm

Regarding the last set of images (Figure 15), the most visible differences between the two procedures were the number of spermatozoa and the background. The selective washing (Percoll) had much more spermatozoa than the simple washing (PBS), which had less background and fewer spermatozoa. Taking into account the previous results, the simple washing (PBS) was the chosen procedure for the following experiments. No selection of a specific population occured in the PBS washing procedure, in contrast to Percoll (selection of motile spermatozoa). PBS was used as the standard procedure, since it mimic the evaluation of morphology according to WHO (2010). The possible changes in SARP2 subcellular localization were also checked in the two washing procedures, to confirm that no alterations due to the inherent procedure were observed (Figure 16).

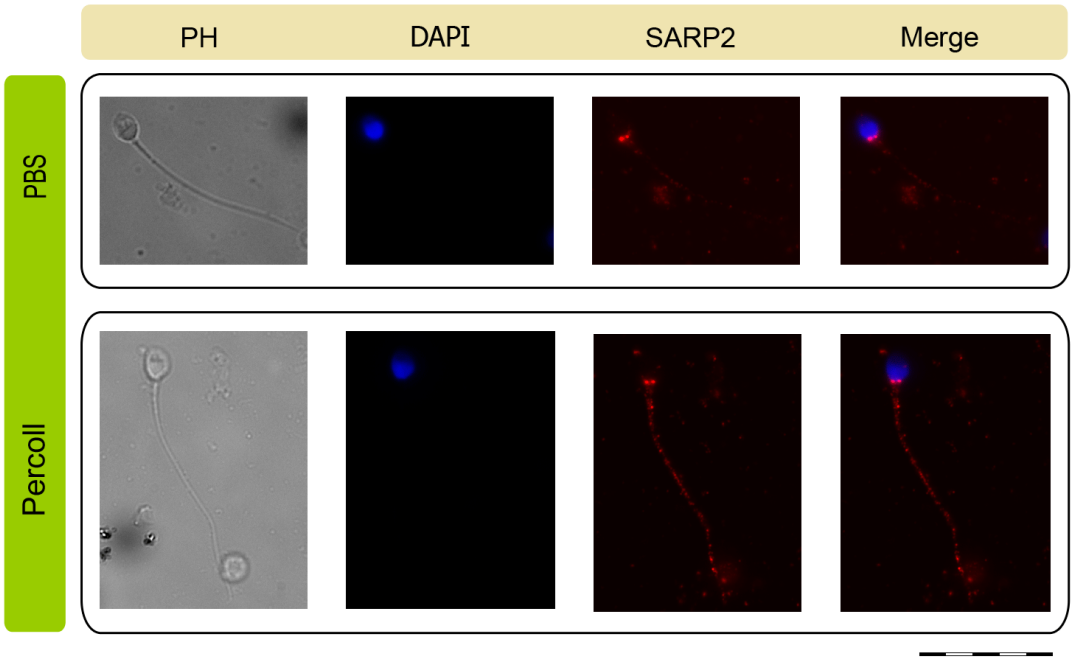

Figure 16: Subcellular localization of SARP2 within human spermatozoa conjugated with primary antibody SARP2 (dilution 1:100) and secondary antibody conjugated with Texas Red, for the two different washing procedures (1000x). Scale bar = 20µm.

The same subcellular localization of SARP2 was observed in the two different washing procedures. Although, the difficulty to find a spermatozoon isolated in the selective washing procedure (Percoll) was one of the reasons to abandon this procedure during the following experiments.

2.4 Discussion

Immunocytochemistry optimization for using the antibody SARP-8C was accomplished. Thus, the conditions optimized were the dilution 1:100 of the antibody, and the type of washing procedure for the human semen sample (PBS and Percoll®). The dilution 1:100 was the chosen one from three other dilutions (1:50, 1:100, 1:250), since little or no background was present and the spermatozoa were well stained, till the end of the tail. In the dilution 1:250, although almost no background was found but that is not the only condition to accept a dilution, since we still need to ensure that the spermatozoon is well stained. The evaluation of the two different washing procedures (PBS and Percoll®) revealed that the simple washing procedure was the most suitable to our purposes. The simple washing (PBS) procedure was chosen because it provides less background and spermatozoa *per* field, bringing more advantages for categorization and analyzis of the spermatozoa. Nevertheless, in this work it was important to have a final sperm preparation, which could be able to represent more accurately the initial semen sample, and with the selective washing (Percoll®) that was not achieved.

According to our results the subcellular localization of SARP2, within human spermatozoa was at the connecting piece and at the entire length of the tail. Nevertheless, previous studies of Fardilha (2004) revealed a slightly different subcellular localization of SARP2, in which, the equatorial region of the head was also stained. To note that the antibody used in the present work was different from the one used by Fardilha (2004), since the last one identified both SARP1 and SARP2 and here only SARP2 is identified. The immunoreactivity presented was valid, and consistent with all of thefollowing experiment.

3: Assessment of SARP2 expression pattern in human spermatozoa

3.1 Introduction

In previous studies with a different protein, I-2 (an inhibitor of PP1γ2), when the complex PP1γ2/PPP1R2 was investigated the co-localization was in the principal piece and middle piece of the spermatozoa. However, when spermatozoa with different morphologies (sperm defects) were analyzed for the same complex, PP1γ2/PPP1R2, different expression patterns of co-localization were revealed (Ferreira, 2010). This prompted further studies that are being conducted in order to use this complex as a molecular marker for the morphology analysis of sperm samples. SARP2 is related to sperm motility (Browne, *et al*., 2007; Fardilha, 2004) however here the suggestion was using the subcellular localization within spermatozoa to charachterize sperm defects. In fact, based in previous results (Ferreira, 2010), a similar approach (immunocytochemistry) was used for SARP2 to test if it could be a possible molecular marker for sperm defects. Also alterations in sperm motility may be caused by morphology defects. Furthermore, PP1γ2 function is related to sperm morphology (Chakrabarti, *et al*., 2007; Varmuza, *et al*., 1999) indicating that SARP2, being a PP1 regulator may also be involved in sperm morphology.

The counting was done in a total of 200 spermatozoa per replicate (400 spermatozoa), in more than five fields. In the present case six mounted coverslips were prepared for immunocytochemistry. Furthermore, the spermatozoa of each sperm samples of the four volunteers were categorized into a data table. This data table had two main categories, one comprising normal and abnormal staining of SARP2, and other the morphology analysis of each spermatozoon counted. The categories used for the staining category were the following: normal (A0) (connecting piece and tail) and abnormal (A1 to A14). The morphology analysis was done with the following categories: head defects, neck and middle piece defects, tail defects, multiple defects, and

normal, according to WHO (1999) all done in PH (phase contrast). In fact, the five morphology categories and the staining categories (A0-A15) were used to have only one correspondence to each of the spermatozoon.

The morphology parameter is highly subjective for very different reasons (Barratt, *et al*., 2011, WHO, 2010), however WHO suggested in its 5th edition (2010) to classify spermatozoa in just normal/abnormal ones, leaving the tallying of the location of abnormalities as something optional. Furthermore, after the statistical data validation the objective was having a much more simple way to categorize the spermatozoa in normal or ideal and abnormal, based on the SARP2 expression.

3.2 Material and Methods

3.2.1 Preparation of the volunteers samples

The four sperm samples of the four volunteers were first evaluated according to WHO 2010 parameters (see Human semen sample preparation) and then submitted to a simple washing procedure, with PBS followed by immunocytochemistry. In order to examine the expression pattern of SARP2 and its relationship to morphologic defects, 400 spermatozoa were categorized. Note that only the morphology parameter was evaluated according to WHO 1999, in which, multiple defects were inclued.

3.2.2 Data collection

The counting data were first collected having in mind the structure of the mammalian spermatozoon. The subdivisions of head, acrosomal, equatorial and post-acrosomal region and also the main division for our work the connecting piece, and the last division, the tail, in which the middle piece, principal piece and end piece are included (Figure 17).

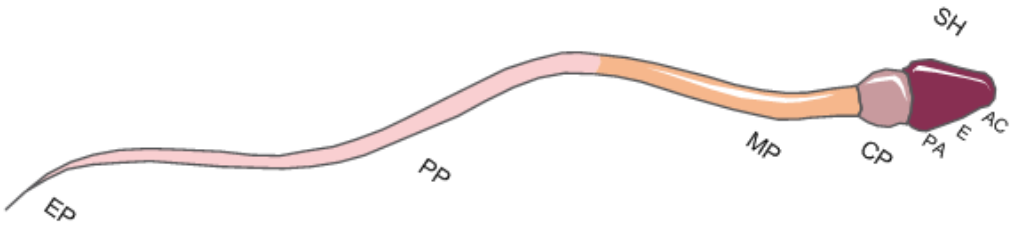

Figure 17: Structure of mammalian spermatozoon. A: Main divisons of the spermatozoon, sperm head (SH), connecting piece (CP), middle piece (MP), principal piece (PP) and end piece (EP). B: Subdivisions of the sperm head, acrosomal (AC), equatorial (E) and post-acrosomal (PA) region (adapted from De Jonge, *et al*., 2006).

The data was organized in a data table. One single category for staining and other for morphoglogy analysis was attributed to every single

spermatozoon counted. In order to classify the different categories of staining, a single division was performed, between normal and abnormal staining of SARP2. Therefore, several categories, like a normal category (A0), which represent the SARP2 staining (connecting piece and tail), and the last 14 categories related to an abnormal staining (Table 7) were established. The completed data table could be seen in the appendix (7: Appendix), in which, additional information regarding morphology analysis, was and recorded in Figure 27 (see 7: Appendix). The morphology analysis of each spermatozoon counted in this data table was assessed according to WHO (1999). Five categories of morphology (normal, head defects, neck and middle piece defects, tail defects and multiple defects) were used (Table 8).

Table 7: Category selection according to the main divisions of the spermatozoon (* Normal category, A1-A14 abnormal ones).

Selection of categories					
Categories	Acrosomal region	Equatorial region	Post-acrosomal	Connecting piece	Tail
A0*				x	x
A1	x	x		x	x
A2	x		x	x	x
A3	x			x	x
A4		x		x	x
A5		x	x	x	x
A6			x	x	x
A7	x				x
A8	x	x			x
A9	x		x		x
A10		x	x		x
A11		x			x
A12			x		x
A13					x
A14	x	x	x	x	x

Table 8: Codification of the five categories of sperm morphology, according to WHO (1999).

Morphology categories	
Categories	Description
B0	Normal
B1	Head defects
B2	Neck and middle piece defects
B3	Tail defects
B4	Multiple defects

3.3 Results

3.3.1 Volunteers semen sample analysis

The four volunteer human semen samples were evaluated according to WHO 2010 (see Human semen sample preparation) (Table 9).

Table 9: Volunteers analysis of sperm parameters according to WHO 2010. (* according to WHO 1999).

Sperm parameters sample analysis			Volunteer 1	Volunteer 2	Volunteer 3	Volunteer 4
Volume		ml	5	3	4	7
Motility	Progressive (PR)	%	70	71	25	26
	Non-progressive (NP)		12	5	31	26
	Immotile (IM)		18	24	44	48
Sperm concentration		sperm cells x 10^6 /ml	30	63	34	68
Total sperm count		sperm cells x 10^6 per ejaculate	150	189	136	476
Morphology (%)*		Normal	18	17	15	22
		Head defects	26	20	19	15
		Neck and middle piece defects	7	4	4	3
		Tail defects	26	35	41	37
		Multiple defects	24	25	20	24

The volunteers semen samples analysed above (Table 9) can be classified as normals, since only the Progressive motility was compromised (except on volunteer 1 and 2), being lower than the reference value according to WHO (2010) (see Table 3 for standard values). The motility was possibly deviated from the standard value as a result of the lag period of time between sampling and reception.

Table 10 represent the morphological caraterization of the semen sample of the four volunteers, coloured by hematoxylin-eosin method (according to WHO) and the same permorfed in a different time in the same samples by phase contrast analysis in fixed sperm cells. These two procedures were done to test if it was possible to correlate the morphological characterization by WHO (already validated) and by the methodology we aim to propose (PH).

Table 10: Volunteer´s semen sample analysis of the morphological defects using PH (phase contrast) and HE (hematoxylin-eosin) staining, according to the morphologic parameters of WHO (1999).

Sperm cell morphological categories	Number of sperm cells	
	HE	PH
B0	286	395
B1	319	178
B2	72	96
B3	552	532
B4	371	399

B0:Normal, B1:Head defects, B2:Neck and middle piece defects, B3:Tail defects, B4:Multiple defects

3.3.2 Data analysis

As illustrated in Figure 18, the two different approaches have similar results. Statistical analysis of the presented results will be performed in chapter four.

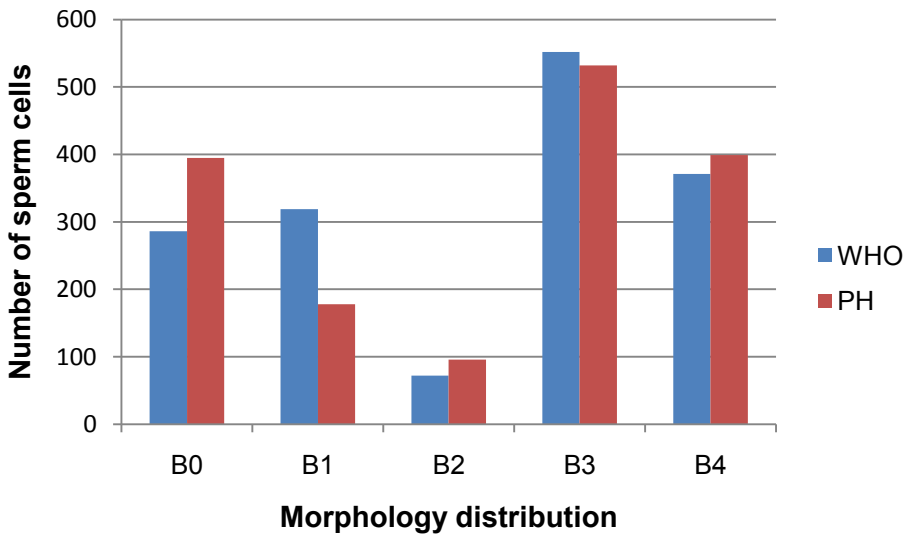

B0:Normal, B1:Head defects, B2:Neck and middle piece defects, B3:Tail defects, B4:Multiple defects

Figure 18: Comparison of volunteer's semen sample analysis of the morphological defects using PH (phase contrast) and WHO analysis.

Relatively to the final data table (see 7: Appendix), in which, we consider all of the categories presented before (Table 7 and Table 8) for each volunteer the relationship between SARP2 expression and morphology analysis was evaluated. The following tables and graphics represent each of the volunteer´s data analysis (Table 111, Figure 19, Table 12, Figure 20, Table 13, Figure 21, Table 14, and Figure 22).

Table 11: SARP2 expression pattern in sperm sample from volunteer 1 versus sperm morphology.

Volunteer 1		SARP2														
		Normal	Abnormal													
PH		A0	A1	A2	A3	A4	A5	A6	A7	A8	A9	A10	A11	A12	A13	A14
Normal	B0	48	0	0	2	0	0	0	0	0	3	0	0	41	5	63
Abnormal	B1	5	0	0	0	0	0	0	0	0	0	0	0	9	3	23
	B2	3	0	0	1	0	0	0	0	0	1	0	0	6	3	17
	B3	8	4	2	12	0	0	0	2	1	7	0	0	0	0	78
	B4	1	0	0	0	0	0	0	0	0	0	0	0	9	3	40

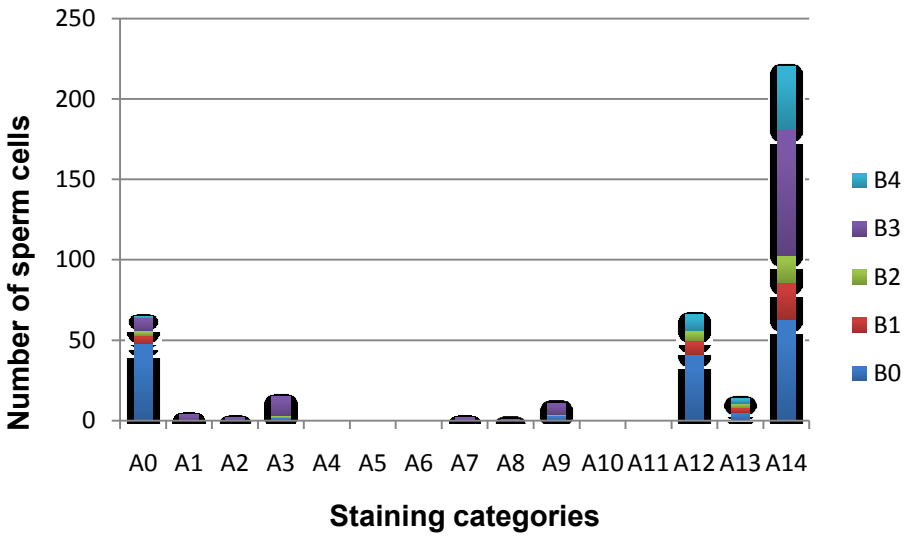

B0:Normal, B1:Head defects, B2:Neck and middle piece defects, B3:Tail defects, B4:Multiple defects

Figure 19: Volunteer´s 1 semen sample analysis of the relation of SARP2 expression pattern versus morphology.

According to Figure 19, three categories stood out from the rest: A14, which represents the staining of the entire spermatozoon, A12, which represents the staining of the post–acrosomal region of the spermatozoon and the tail and A0, which represents, the normal staining of SARP2. Besides these categories it was important to observe that only two of the three categories, A14 and A0, had all of the five categories of morphology represented (Table 11).

Table 12: SARP2 expression pattern in sperm sample from volunteer 2 versus sperm morphology.

Volunteer 2		SARP2														
		Normal	Abnormal													
PH		A0	A1	A2	A3	A4	A5	A6	A7	A8	A9	A10	A11	A12	A13	A14
Normal	B0	24	0	0	12	4	1	1	1	1	2	0	1	16	15	26
Abnormal	B1	6	0	0	6	0	0	1	1	0	2	0	0	6	5	10
	B2	6	0	0	1	0	0	0	1	1	1	0	0	7	7	12
	B3	37	0	0	1	2	1	4	0	0	0	1	0	64	22	1
	B4	13	2	0	9	1	0	4	1	0	4	1	0	15	17	23

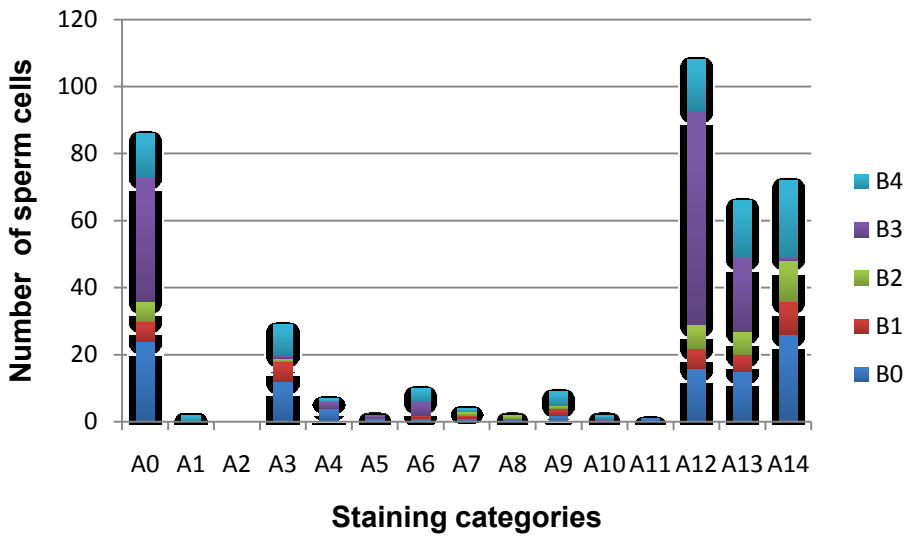

B0:Normal, B1:Head defects, B2:Neck and middle piece defects, B3:Tail defects, B4:Multiple defects

Figure 20: Volunteer´s 2 semen sample analysis of the relation of SARP2 expression pattern verus morphology.

Four categories that stood out in Figure 20: A12, which represents the staining of the post–acrosomal region of the spermatozoon and the tail, A0, which represents, the normal staining of SARP2, A14, which represents the staining of the entire spermatozoon, and A13, which represents the staining of the tail. Besides this type of distribution of the data, all of these four categories had all of the five categories of morphology represented (Table 12).

Table 13: SARP2 expression pattern in sperm sample from volunteer 3 versus sperm morphology.

Volunteer 3		SARP2														
		Normal	Abnormal													
PH		A0	A1	A2	A3	A4	A5	A6	A7	A8	A9	A10	A11	A12	A13	A14
Normal	B0	34	1	0	6	1	0	0	2	0	1	2	0	5	18	6
Abnormal	B1	19	0	0	8	3	0	0	3	0	2	0	0	6	16	8
	B2	4	0	0	1	0	0	0	0	0	1	0	0	0	3	2
	B3	54	3	0	6	2	0	1	5	0	1	1	0	9	46	10
	B4	36	1	0	10	1	0	0	7	0	2	2	0	9	33	9

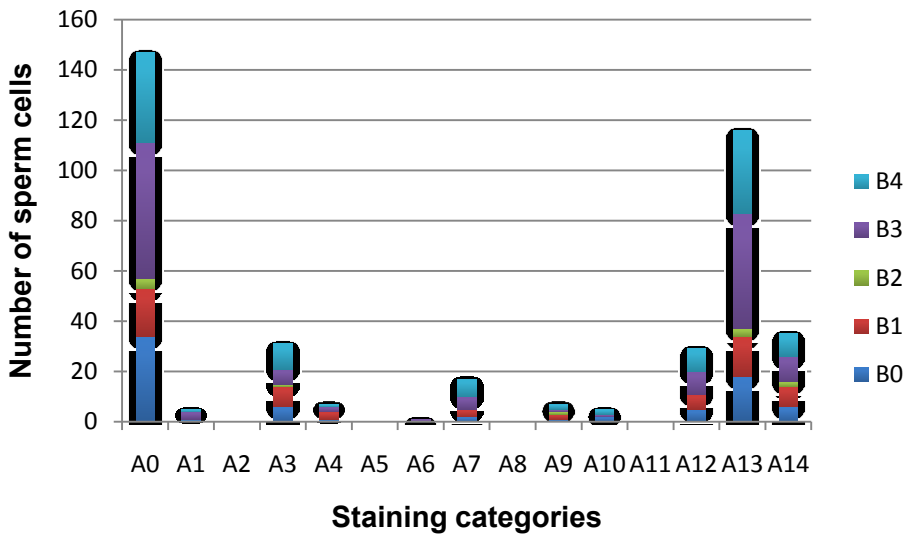

B0:Normal, B1:Head defects, B2:Neck and middle piece defects, B3:Tail defects, B4:Multiple defects

Figure 21: Volunteer´s 3 semen sample analysis of the relation of SARP2 expression pattern versus morphology.

Analyzing Figure 21 there were two categories that stood out from the rest; A0 category, which represents, the normal staining of SARP2 and A13, which represents the staining of the tail. Besides this type of distribution of the data, all of these two categories had all of the five categories of morphology represented (Table 13).

Table 14: SARP2 expression pattern in sperm sample from volunteer 4 versus sperm morphology.

Volunteer 4		SARP2														
		Normal	Abnormal													
PH		A0	A1	A2	A3	A4	A5	A6	A7	A8	A9	A10	A11	A12	A13	A14
Normal	B0	15	0	0	1	0	0	0	4	1	0	0	1	0	29	2
Abnormal	B1	7	1	0	1	1	0	0	1	0	0	0	2	0	22	1
	B2	0	0	0	1	0	0	0	2	0	0	0	1	0	14	0
	B3	34	2	0	10	5	0	0	5	2	0	1	8	6	61	13
	B4	25	0	0	4	2	0	0	9	1	1	1	3	13	78	9

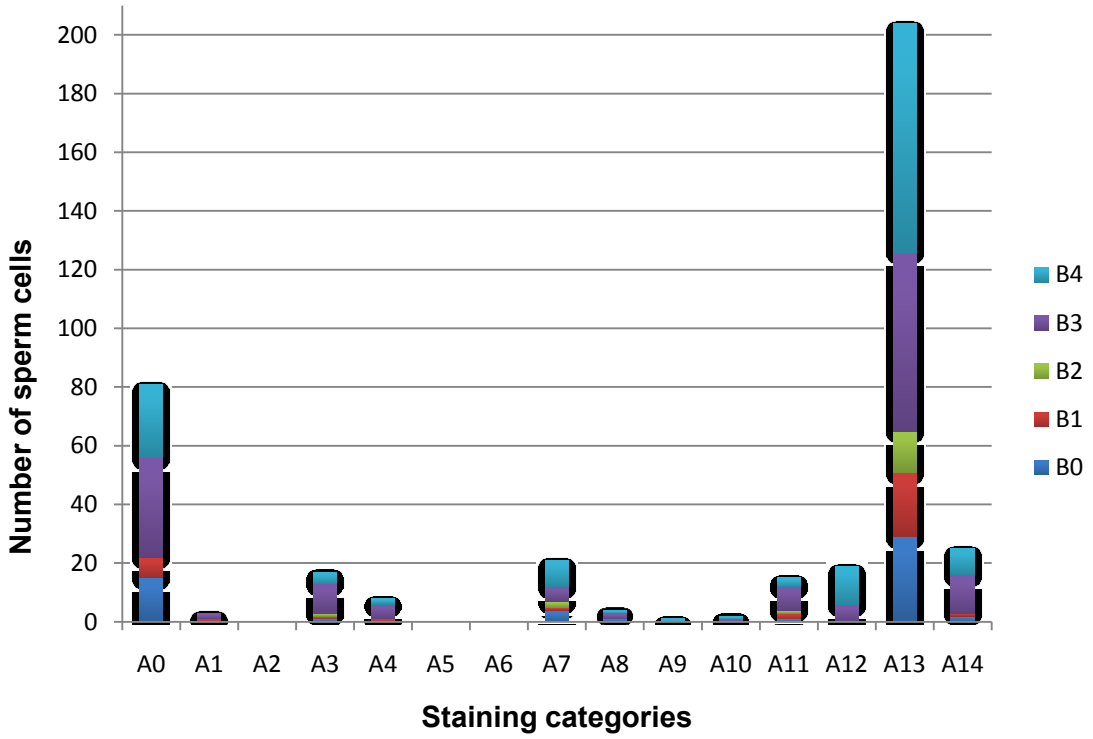

B0:Normal, B1:Head defects, B2:Neck and middle piece defects, B3:Tail defects, B4:Multiple defects

Figure 22: Volunteer´s 4 semen sample analysis of the relation of SARP2 expression pattern versus morphology.

Analyzing Figure 22 there were two categories that stood out from the rest; A0 category, which represents, the normal staining of SARP2 and A13, which represents the staining of the tail. Besides this type of distribution of the data, all of the five categories of morphology were represented, with the exception of the neck and middle piece defects that in A0 were absent (Table 14).

Regarding this type of analysis, in which the relationship between the morphology and the SARP2 staining was established, the same was applied to all of the data to get an overview of the entire sample (Table 15, Figure 23).

Table 15: SARP2 expression pattern in all of the volunteers versus sperm morphology.

Volunteers		SARP2														
		Normal	Abnormal													
PH		A0	A1	A2	A3	A4	A5	A6	A7	A8	A9	A10	A11	A12	A13	A14
Normal	B0	121	1	0	21	5	1	1	7	2	6	2	2	62	67	97
Abnormal	B1	37	1	0	15	4	0	1	5	0	4	0	2	21	46	42
	B2	13	0	0	4	0	0	0	3	1	3	0	1	13	27	31
	B3	133	9	2	29	9	1	5	12	3	8	3	8	79	129	102
	B4	75	3	0	23	4	0	4	17	1	7	4	3	46	131	81
Total		379	14	2	92	22	2	11	44	7	28	9	16	221	400	353

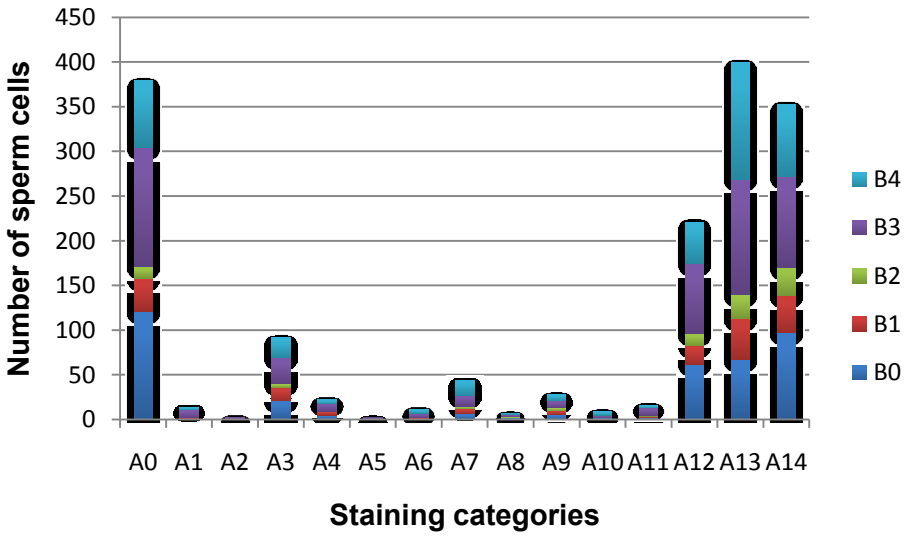

B0:Normal, B1:Head defects, B2:Neck and middle piece defects, B3:Tail defects, B4:Multiple defects

Figure 23: Volunteers semen sample analysis of the relation of SARP2 expression pattern versus morphology.

In all the samples there were at least three different expression pattern of SARP2 (A12, A13 e A14), besides the normal one (A0). At the normal staining of SARP2 all of the five categories of morphology analysis were represented (Table 15), although that did not happen for all of the other abnormal categories represented (Figure 23). Indeed, this was also consistent separately in the volunteer' data analysis. In a general overview we had four categories that stood out from the rest, A13, which represents the staining of the tail, A0, which represents the normal staining of SARP2, A14, in which the entire spermatozoon is stained and A12 which represents the staining of the post–

acrosomal region of the spermatozoon and the tail. The category A0 was the one that had the highest amount of normal (B0) sperm cells consistent with our initial assumption that SARP2 normal staining corresponded to A0. Thus, the preliminary results obtained lead us to propose that it might be considered as a possible mean of discrimination between normal and abnormal spermatozoa.

3.3.3 Sperm defects and SARP2 expression pattern

The relationship between SARP2 expression pattern and sperm morphological defects could be seen behind the counting data through the images acquired by the Olympus IX2-UCB microscope. The different sperm morphological defects analyzed, such as: head defects, neck and middle piece defects, tail defects and multiple defects were represented in the following set of images (Figure 24). Moreover, every set of images represent the several possibilities of subdivisions of morphological defects within a major morphologic defect, this classification was done according to WHO, 2010 (see Figure 27 in 7: Appendix). An important achievement was transposing the previous results reported in tables and graphics into images, which was the result of immunocytochemistry procedure applied to all of the volunteer's samples.

Analyzing the Figure 24, different scenarios emerged according to the different sperm defects. In spermatozoa with head defects, there were three main expression pattern of SARP2, whereas the most relevant were; A13, A14, A0 and A12 (Table 15), in a descending order. In the neck and middle piece defects, the most relevant were: A14, A13, A12 and A0 (Table 15). In tail defects, A0, A13, A14 and A12 (Table 15) were the most relevant. And at the spermatozoa with multiple defects, the most relevant were: A13, A14, A0 and A12 (Table 15). Therefore, the analysis of the data and images suggested that the expression pattern of SARP2 varies according to the sperm defects, but although it still showed that a big part of the spermatozoa are stained normally (A0).

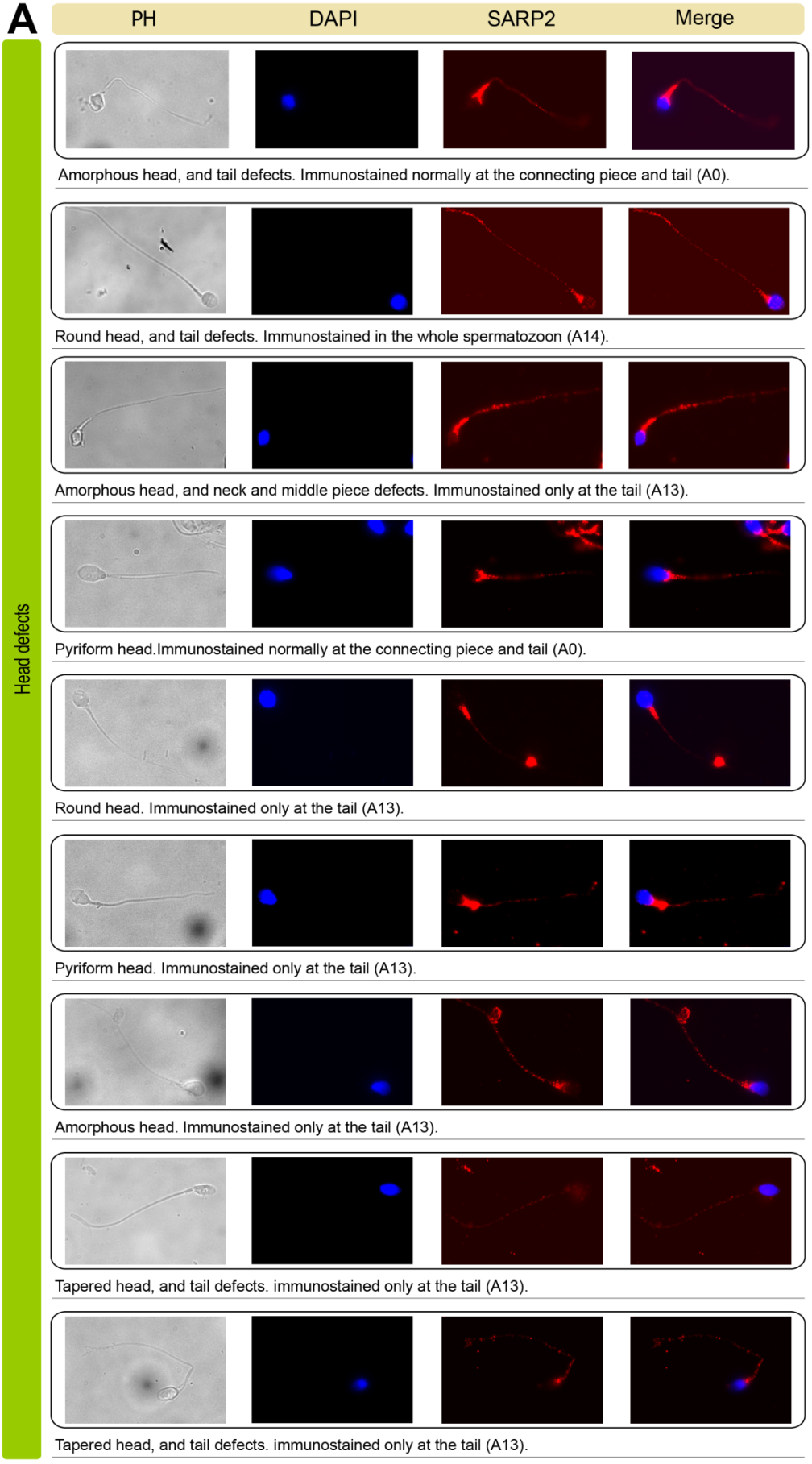
A
PH
DAPI
SARP2
Merge
Head defects
Amorphous head, and tail defects. Immunostained normally at the connecting piece and tail (A0).
Round head, and tail defects. Immunostained in the whole spermatozoon (A14).
Amorphous head, and neck and middle piece defects. Immunostained only at the tail (A13).
Pyriform head.Immunostained normally at the connecting piece and tail (A0).
Round head. Immunostained only at the tail (A13).
Pyriform head. Immunostained only at the tail (A13).
Amorphous head. Immunostained only at the tail (A13).
Tapered head, and tail defects. immunostained only at the tail (A13).
Tapered head, and tail defects. immunostained only at the tail (A13).

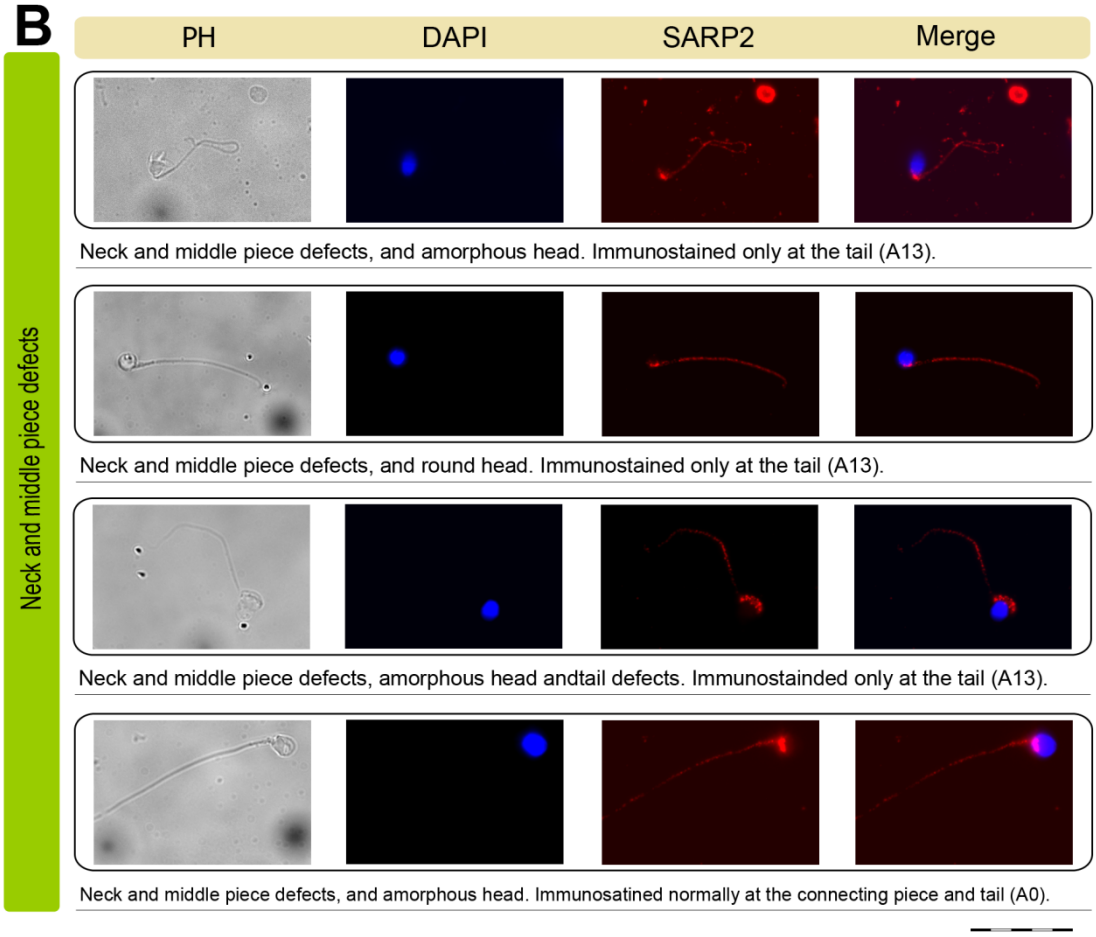
B
PH
DAPI
SARP2
Merge
Neck and middle piece defects
Neck and middle piece defects, and amorphous head. Immunostained only at the tail (A13).
Neck and middle piece defects, and round head. Immunostained only at the tail (A13).
Neck and middle piece defects, amorphous head andtail defects. Immunostainded only at the tail (A13).
Neck and middle piece defects, and amorphous head. Immunosatined normally at the connecting piece and tail (A0).

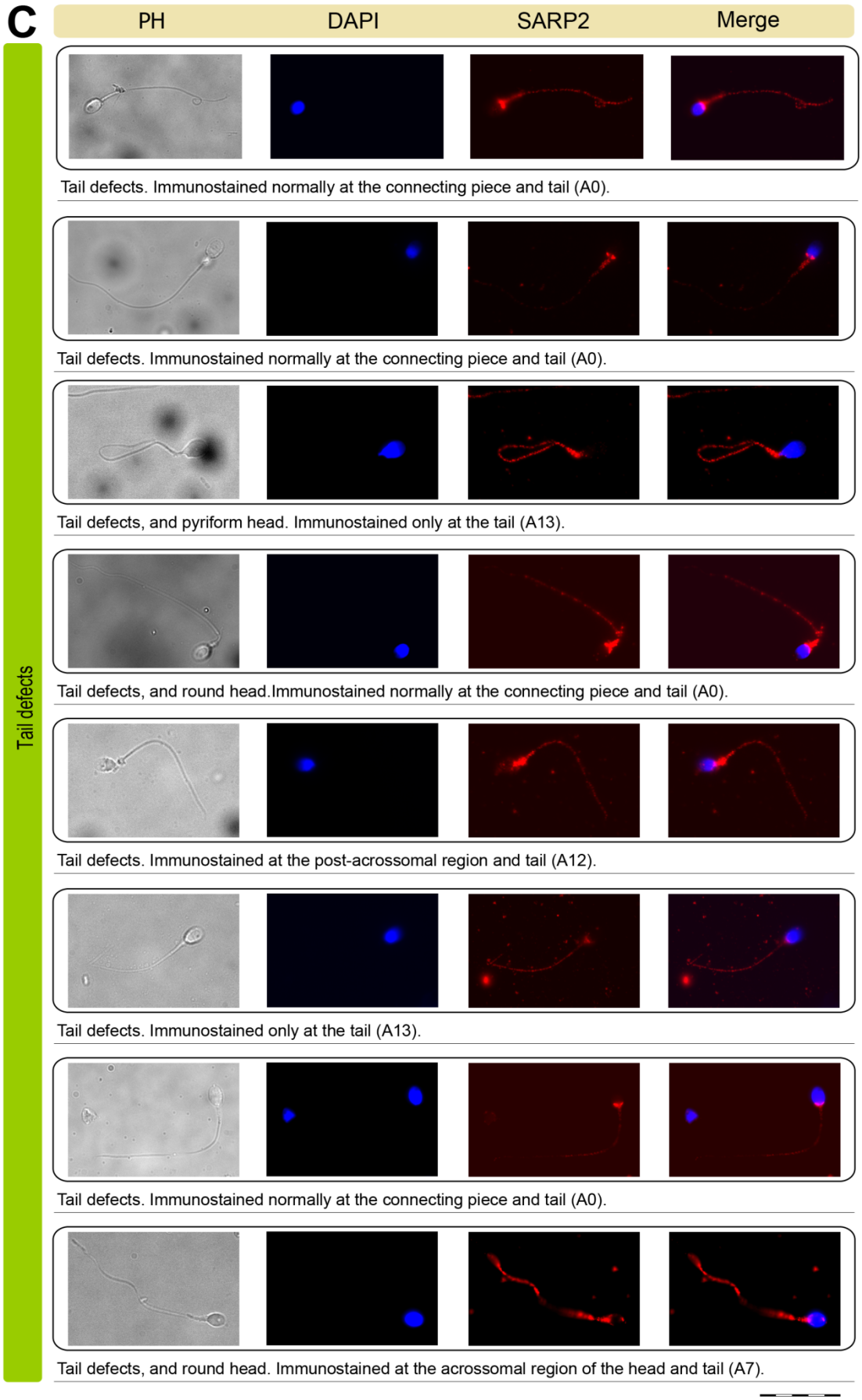
C
PH
DAPI
SARP2
Merge
Tail defects
Tail defects. Immunostained normally at the connecting piece and tail (A0).
Tail defects. Immunostained normally at the connecting piece and tail (A0).
Tail defects, and pyriform head. Immunostained only at the tail (A13).
Tail defects, and round head.Immunostained normally at the connecting piece and tail (A0).
Tail defects. Immunostained at the post-acrossomal region and tail (A12).
Tail defects. Immunostained only at the tail (A13).
Tail defects. Immunostained normally at the connecting piece and tail (A0).
Tail defects, and round head. Immunostained at the acrossomal region of the head and tail (A7).

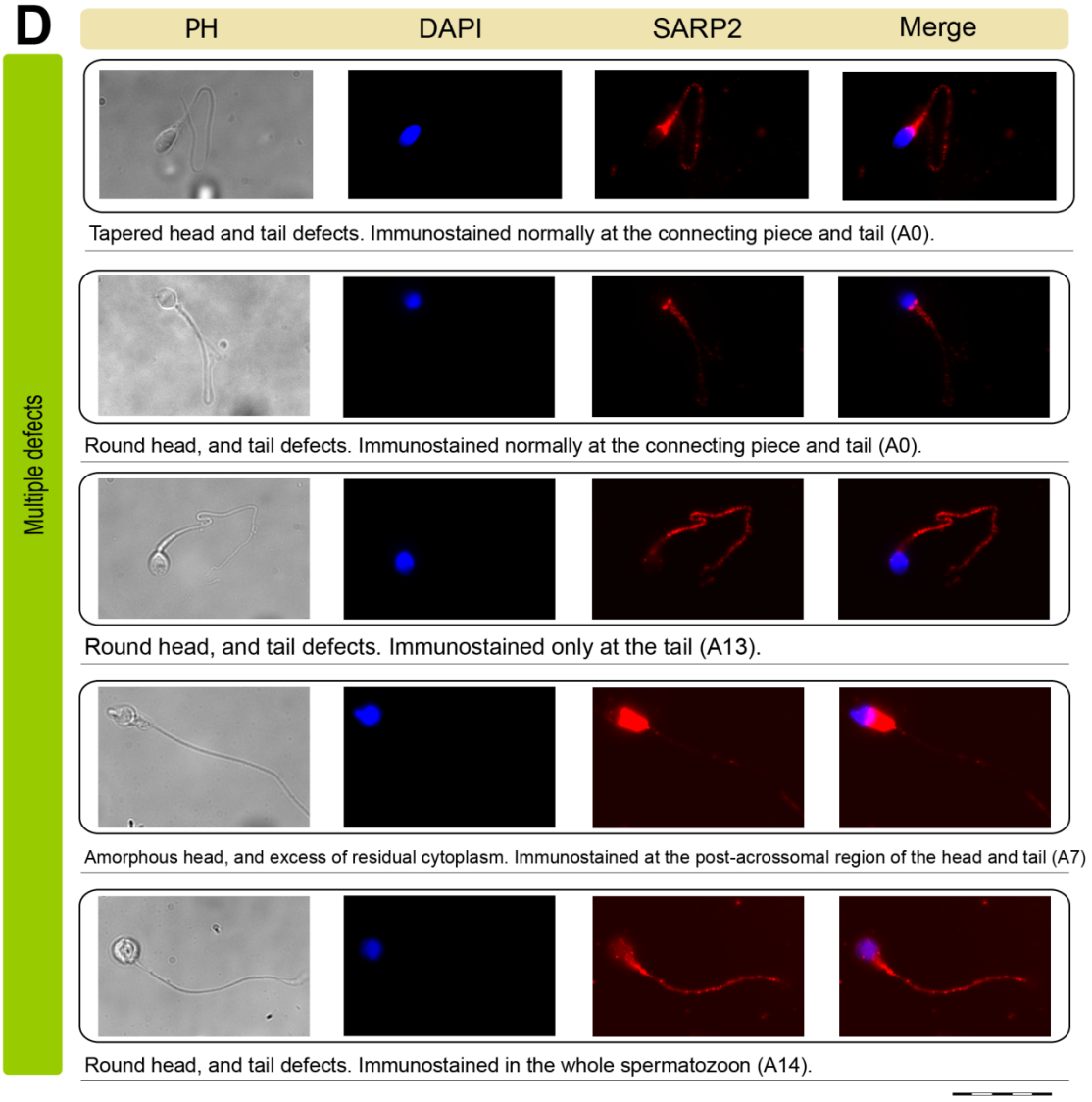

Figure 24: A: Head defects; B: Neck and middle piece defects; C: Tail defects; D: Multiple defects. Subcellular localization of SARP2 within human spermatozoa associated to all of the possible sperm defects. Primary antibody SARP2 (dilution1:100) and secondary antibody conjugated with Texas Red, images acquired with an epifluorescence microscope (Olympus IX2-UCB) with an appropriated software (1000x). Scale bar = 20µm.

3.4 Discussion

A study conducted at our laboratory by Ferreira (2010) revealed that the co-localization of the complex I-2/PP1γ2 was different in spermatozoa with morphological defects. Hence, like the studies that are being conducted in order to ascertain if this complex I-2/PP1γ2 could be used as a molecular marker for sperm morphology analysis, the same type of evaluation was proposed for SARP2. Therefore, the basis of the present thesis was to build of a data table, in which, 400 spermatozoa per each of the four volunteers was categorized and classified. The categorization was done in terms of the subcellular localization of SARP2 within each of the spermatozoon counted. Fourteen different categories (A1-A14) were found besides the normal one (A0), which incorporate the connecting piece and the tail characteristic of the SARP2 staining. These abnormal categories were obtained through the subdivisions of the spermatozoon in a preliminary analysis of the data.

In all of the volunteer samples at least three different abnormal expression patterns of SARP2 were observed when comparing with the normal expression of SARP2. In fact, at the A0 category all of the five categories of morphology (normal (B0), head defects (B1), neck and middle piece defects (B2), tail defects (B3) and multiple defects (B4)) were present in all of the volunteers. Nonetheless, that fact was not true for all of the abnormal (A1-A14) categories observed in each of the volunteer´s samples. In a global perspective there were four categories that stood out from the rest: A13, representing the staining at the tail; A0, representing the normal staining, A14; representing the staining of the entire spermatozoon; and A12, representing the staining of the post-acrosomal region and the tail of the spermatozoon. The relation between the expression pattern of SARP2 and the morphological analysis was also conducted, resulting in the same four categories referred before - A13, A0, A14 and A12, as the main ones. Though, the only thing that distinguished the different morphology categories analyzed (B0, B1, B2, B3, B4) was the order of importance of the four staining categories. First, the normal spermatozoa were characterized mainly by the A0 category, and then by A14, A13 and A12. The spermatozoa with head defects was charechterized by the following staining

categories, A14, A13, A0 and A12, the ones with neck and middle piece defects by, A14, A13, A12, and A0 category. Then the spermatozoa with tail defects were characterized mainly by, the A0, A13, A14 and A12, and the spermatozoa with multiple defects by, A13, A14, A0 and A12 category. Thus, we suggest that SARP2 expression pattern analysis can be a possible mean of discrimination between normal and abnormal spermatozoa, since we observed changes in the expression pattern according to the different morphologies.

4: Statistical validation of SARP2 as a molecular marker of sperm morphology

4.1 Introduction

The development of new technologies was supported by the overwhelming clinical need to identify infertile men without the requirement for a semen parameters assessment. The value of the traditional semen parameters assessment as a clinical tool in diagnosis and prognosis is still a polemic subject despite all of the progress made in this last edition of WHO (2010) (Barratt, *et al*., 2011). Consequently, new technology developments are emerging which promise to transform our diagnostic and treatment pathaways; e. g. the biomarkers discovery and home-testing of male fertility (Lefièvre, *et al*., 2007). The biomarkers discovery is being made through different techniques. Clinical proteomics by definition is an emerging field, in which, biomarkers are searched and profiles are generated, helping predicting, diagnosing and monitor human pathology (Varghese, *et al*., 2007). Although, there is a deficiency of markers of human sperm function at the molecular level, there are already several databases of sperm proteins (Barratt, *et al*., 2011, Oliva, *et al*., 2009). These databases, which “make up” the sperm, are just the beginning of a new era that already provides an important reference for further research (Oliva, *et al*., 2009). Several projects have identified putative biomarkers of sperm function, or at least are very close to that goal, like Pixton and co-workers in 2004 (Pixton, *et al*., 2004) and Barratt and co-workers in 2011 (Barratt, *et al*., 2011). Obviously, it is challenging to translate putative biomarkers from proteomic research into real-world diagnostic or prognostic applications. Besides this final challenge, all of the putative biomarkers need to get through a tough path of statistical validation, which evaluate the predictive power of that biomarker (Davis, *et al*., 2010, Hu, *et al*., 2008).

4.2 Material and Methods

The main objective was to ascertain if the morphology data obtained by two different methods (HE, according to WHO and PH) were comparable or not. Hence, with the data of the two different types of morphology analysis (HE and PH) the coefficient of Pearson correlation was calculated, and also graphically represented by a scatter plot. If no correlation is found between the two sets of data, the relation between PH and the SARP2 expression pattern can be assessed. To confirm if SARP2 expression was related with the morphology analysis, a contingency table or a two-by-two table was used. The contingency table allowed the evaluation of the procedures for the discrimination between normal and abnormal spermatozoa. Thus, to know the classification power of the two procedures the classification rate was calculated.

Statistcial analysis was carried out using the Statistical Package for the Social Sciences (SPSS) version 18 (2009).

4.3 Results

The morphology analysis (PH versus HE) was the only possibility to link SARP2 expression with the morphology analysis performed nowadays, done according to WHO. Therefore, the first objective of statistical analysis was to assess if the collected data of morphology analysis done by the two different procedures (HE versus PH) were correlated (Table 10). The following flowchart at Figure 25 shows all of the statistical analysis done in this chapter.

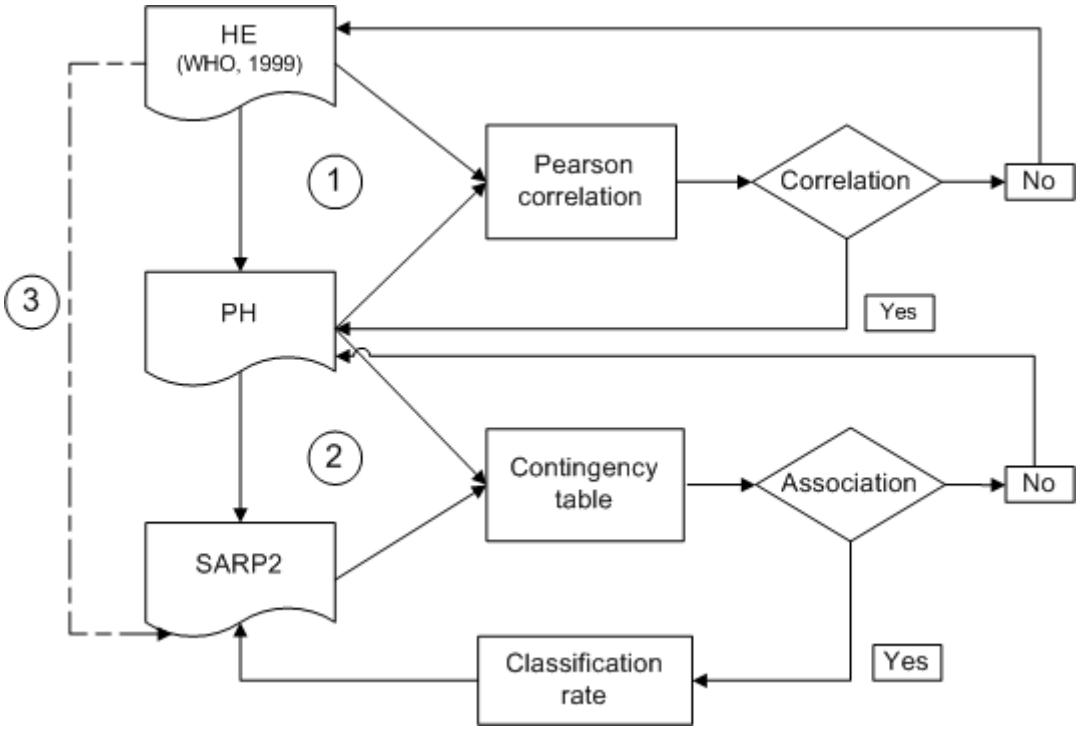

Figure 25: Flowchart of the statistical analysis. 1: HE versus PH analysis (Pearson correlation); 2: PH versus SARP2 analysis (Contingency table); 3: Relation of morphology current assessment and SARP2 expression analysis.

Regarding the analysis of the correlation expressed as the number 1 in the previous flowshart there was a positive correlation between the two variables. The coefficient of Pearson correlation was of r = 0.864 for an n = 5 and a p value of 0.059, with a significant level of 0.10 (Table 16). The data were graphically represented at a scatter plot (Figure 26) to get an overview of the relation between the two variables.

Table 16: Pearson correlation between the two different morphology analysis, HE and PH.

Correlation		HE	PH
HE (WHO, 1999)	Pearson Correlation	1	,864
	Sig. (2-tailed)		,059
	N	5	5
PH	Pearson Correlation	,864	1
	Sig. (2-tailed)	,059	
	N	5	5

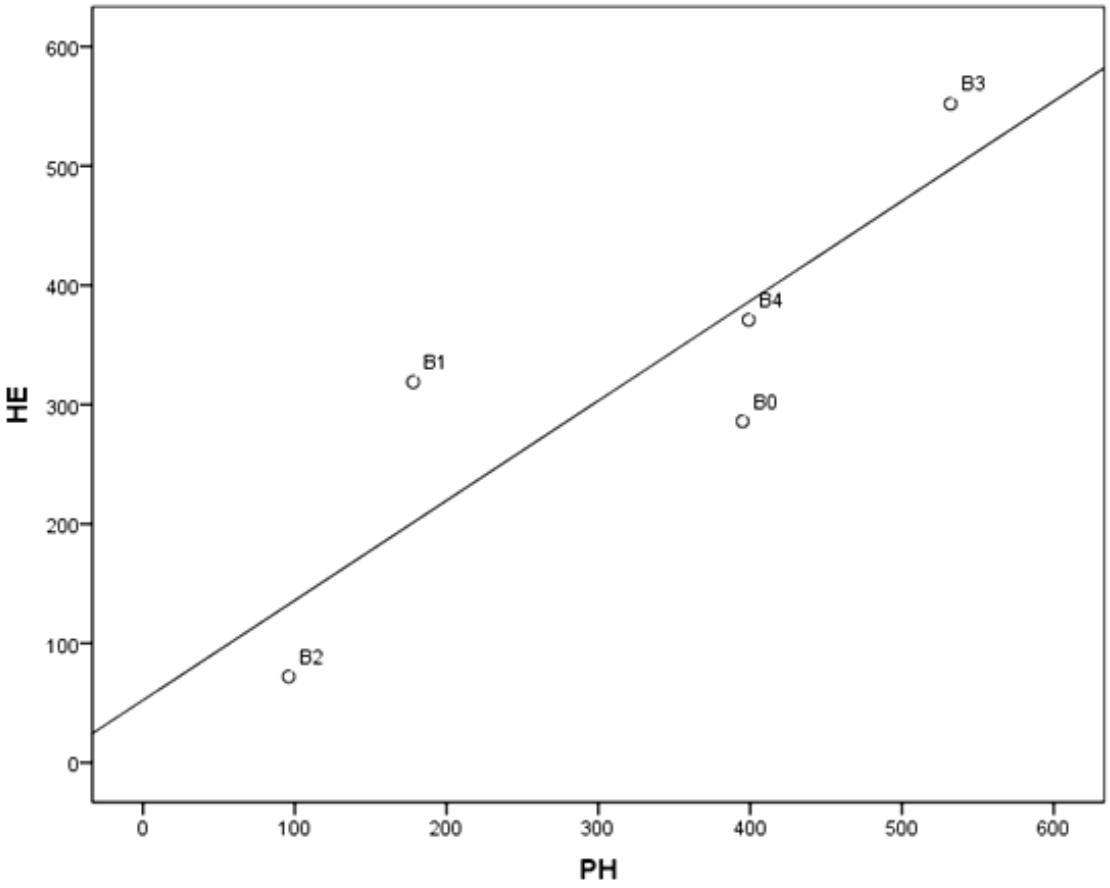

Figure 26: Scatter plot representation of the data from the two different morphology analysis.

A contingency table is essentially a display format used to analyse and record the relationship between two or more categorical variables (two-by-two tables). In our case, our variables were the morphology assessed by PH (phase contrast) and the SARP2 expression, both used to categorize the spermatozoa. Analyzing Table 17, for each of the two variables there were to two other variables, Normal and Abnormal. Those sub-categories (Normal and Abnormal) are connected by rows and columns, giving at the reunion the cells, in which each value is displaied. In each cell, there is the reunion of the two categorical variables, which are essentially the result of the counting data present in the datatable of the four volunteers (see 7: Appendix).

Table 17: Contingency table: morphology analysis (PH) in comparison with SARP2 expression, done with SPSS version 18.

Morphology (PH) * SARP2 staining

Count

		SARP2 staining		
		Abnormal	Normal	Total
PH	Abnormal	947	258	1205
	Normal	274	121	395
Total		1221	379	1600

The classification rate was calculated by the sum of the true positive and negative values, which are the cells with the same classification for the spermatozoa, in both of the different procedures, divided by the total number of observations, in percentage.

$$CR = \frac{947 + 121}{1600} \times 100 = 66,75\%$$

The classification rate was 66,75%, meaning that in 66,75% of the times a spermatozoon was classified equally by the two procedures of morphology analysis (SARP2 staining and PH). In 33,25% of the times the two procedures disagreed in the classification.

4.4 Discussion

Statistical validation is one of the phases that a putative molecular marker needs to get through to become accepted as biomarker. Although this was a preliminary study to assess if SARP2 was a molecular marker, biostatistical analysis was performed. Firstly, there was the necessity of finding something that could be the link between what exists now in terms of morphology analysis and a novel test with our protein of interest, SARP2. The simultaneous analysis by phase contrast of the morphology during the categorization of the expression of SARP2 was the way found. Therefore, the classifications for the spermatozoa found were two based on morphology, one according to WHO (1999) (HE) and other through PH (phase contrast), and one based on the SARP2 expression pattern. We concluded that the analysis performed by HE is correlated by the one done by PH (Table 16). SARP2 expression and PH classifications were then compared in a contingency table, in which the classification rate obtained was approximately 70% suggesting that the two procedures were not yet the most reliable to classify a spermatozoon in normal or abnormal. Meaning that in 30% of the cases a sperm cell is classified erroneously. The implications of this suggest that the SARP2 expression pattern analysis was not yet the most suitable procedure to classify a spermatozoon. More studies are being conducted to verify this hypothesis.

5: Discussion and perspectives

A custom-made antibody SARP-8C was raised especially to our laboratory to have an antibody capable of recognizing only the isoform 2 of SARP protein. Thus the use of this antibody for immunocytochemistry was successful, and the conditions of use optimizied. Indeed, a new subcellular localization of SARP2, within human spermatozoa, was discovered with the present study. It was identified in the connecting piece and in the entire length of the tail. In contrast, the previous results reported by Fardilha (2004) revealed a different localization, but it is important to remember that the antibody used was a different one, which was able to detect two different isoforms, SARP1 and SARP2. The samples of four volunteers were used for a normal characterization of the sample by a spermogram, according to WHO (2010). Morphological analysis (HE (WHO, 1999), PH) and expression pattern of SARP2 were studied. Besides the normal subcellular localization (A0) of SARP2 fourteen other types of expression of SARP2 within the human spermatozoa (A1-A14) were categorized. Essentiality, the categories A13, A0, A14 and A12 were the most representative. The association of the morphology analyis, assessed by five categories (B0=normal, B1=head defects, B2=neck and middle piece defects, B3=tail defects, B4=multiple categories) was also crossed with the expression pattern of SARP2, in which the four categories mentioned before stood out again. To ascertain if a putative molecular marker was present a statistical validation was performed.

Nowadays it is urgent to seek a new paradigm for the sperm analysis done currentely in the many clinics worldwide. The present study stablished enough settings for its further development. It provided enough knowledge and data to elaborate an optimized experimental plan in which, more volunteers are necessary in order to get a representative sample of the Portuguese population, or at least of the local population. Indeed, with this kind of approach the problems that were faced in terms of statistical analysis will no longer be a problem, leading to a much more reliable and complete statistical validation. Also, complementing this work with parallel screening for: DNA fragmentation,

membrane integrity, ROS levels determination, mytochondria function, would be important to assess if having a spermatozoon classified as normal (A0) is always synonymous of a normal spermatozoon. Furthermore, little is known about SARP2 functions, so investment in its study is important to understand its role in the human spermatozoon.

6: References

Barratt, C. L. R., Mansell, S., Beaton, C., Tardif, S., Oxenham, S. K. (2011). Review: Diagnostic tools in male infertility-the question of sperm dysfunction. *Asian Journalof Andrology*. **13**: 53-58.

Björndahl, L., Kirkman-Brown, J., Hart, G., Rattle, S., Barratt, C. L. R. (2006). Development of a novel home sperm test. *Human Reproduction*. **21**: 145-149.

Bollen, M. (2001). Review: Combinatorial control of protein phosphates-1. *Trends in Biochemical Sciences*. **26**: 426-431.

Bollen, M., Peti, W., Ragusa, M. J., Beullens, M. (2010). Review: The extended PP1 toolkit: designed to create specificity. *Trends in Biochemical Sciences.* **35**: 450-458.

Breitbart, H. (2002). Intracellular calcium regulation in sperm capacitation and acrosomal reaction. *Molecular and Cellular Endocrinology*. **187**: 139-144.

Browne, G. J., Fardilha, M., Oxenham, S. K., Wu, W., Helps, N. R., da Cruz e Silva, O. A. B., Cohen, P. T. W, da Cruz e Silva, E. F. (2007). SARP, a new alternatively spliced protein phosphatase 1 and DNA interacting protein. *Biochem. J*. **402**: 187-196.

Cebra-Thomas, J. A., Decker, C. L., Snyder, L. C., Pilder, S. H.,Silver, L. M. (1991). Allele- and haploid specific product generated by alternative splicing from a mouse t complex responder locus candidate. *Nature*. **349**: 239-241.

Ceulemans, H., Bollen, M. (2004). Functional diversity of protein phosphatase-1, a cellular economizer and reset button. *Physiological Reviews*. **84**: 1-39.

Ceulemans, H., Stalmans, W., Bollen, M. (2002). Regulatory-driven functional diversification of protein phosphatase-1 in eukaryotic evolution. *BioEssays*. **24**: 371-81.

Chakrabarti, R., Cheng, L., Puri, P., Soler, D., Vijayaraghavan, S. (2007a). Review: Protein phosphatase PP1γ2 in sperm morphogenesis and epididymal initiation of sperm motility. *Asian Journal of Andrology*. **9**: 445-452.

Chakrabarti, R., Kline, D., Lu, J., Orth, J., Pilder, S., Vijayaraghavan, S. (2007). Analysis of *Ppp1cc*-null mice suggests a role for PP1gamma2 in sperm morphogenesis. *Biology of Reproduction*. **76**: 992-1001.

Cheng, L., Pilder, S., Nairn, A. C.,Ramdas, S.,Vijayaraghavan, S. (2009). PP1γ2 and PPP1R11 are parts of a multimeric complex in developing testicular germ cells in which their steady state level are reciprocally related. *PLoS ONE*. **4**: e4861. doi:10.1371/journal.pone.0004861.

Cohen, P. (1992). Signal integration at the level of protein kinases, protein phosphatases and their substrates. *Trends in Bichemical Sciences*. **17**: 408-413.

Cohen, P. T. (2002). Protein phosphatase 1-targeted in many directions. *Journal of Cell Science.* **115:** 241-256.

da Cruz e Silva, E. F., Fox, C. A., Quimet, C. C., Gustafson, E., Watson, S. J., Greengard, P. (1995). Differential expression of protein phosphatase 1 isoforms in mammalian brain. *The Journal of Neuroscience*. **15**: 3375-3389.

Davis, V. W., Bathe, O. F., Schiller, D. E., Slupsky, C. M., Sawyer, M. B. (2010). Review: Metabolomics and surgical oncology: potential role for small molecule biomarkers. *Journal of Surgical Oncology*. **21831**: 1-9.

De Jonge, C., Barrat, C. 2006. *The sperm cell: production, maturation, fertilization, regeneration*. 1st edition. Cambridge University Press. UK. pp 1-169.

Deepinder, F., Chowdary, H. T., Agarwal, A. (2007). Review: Role of metabolomic analysis of biomarkers in the management of male infertility. *Expert Rev. Mol. Diagn.* **7**: 351-358.

Dravland, J. E., Mortimer, D. (1985). A simple discontinuous Percoll gradient procedure for washing human spermatozoa. *IRCS Med Sci.* **13**:16–17.

Egloff, M. P., Johnson, D. F., Moorhead, G., Cohen, P. T., Cohen, P., Barford, D. (1997) Structural basis for the recognition of regulatory subunits by the catalytic subunit of protein phosphatase 1. *The EMBO Journal.* **16**: 1876-1887.

Embi, N, Rylatt, D. B, Cohen, P. (1980) Glycogen synthase kinase-3 from rabbit skeletal muscle. Separation from cyclic-AMP-dependent protein kinase and phosphorylase kinase. *European Journal Biochemistry.***107**: 519–527.

Fardilha, M. (2004). *Characterization of the PP1 interactome from human testis*. Doctoral thesis in Biology. University of Aveiro. Aveiro. 247 pp.

Fardilha, M., Esteves, S. L. C., Korrodi-Gregório, L., Pelech, S., da Cruz e Silva, O., A., da Cruz e Silva, E. (2011). Review: Protein phosphatase 1 complexes modulate sperm motility and present novel targets for male infertility. *Molecular Human Reproduction*. Jan 20. [Epub ahead of print].

Fardilha, M., Esteves, S. L. C., Korrodi-Gregório, L., Vintém, A. P., Domingues, S. C., Rebelo, S., Morrice, N., Choen, P. T. W, da Cruz e Silva, O. A., da Cruz e Silva, E. F. (2011a). Identification of the human testis protein phosphatase 1 interactome. *Biochem Pharmacology*. doi:10.1016/j.bcp.2011.02.018.

Fardilha, M., Esteves, S. L., Korrodi, L. M. G., da Cruz e Silva, O. A., da Cruz e Silva, E. F. (2010). The physiological relevance of protein phosphatase 1 and its interacting proteins to health and disease. *Current Medicinal Chemistry*. **17**: 3996-4017.

Ferreira, M., A. S., (2010). *I-2, a novel putative PP1 inhibitor in human sperm*. Master thesis in Biology. University of Aveiro. Aveiro. 90 pp.

Gardino, A. K., Smerdon, S. J., Yaffe, M. B. (2006). Structural determinants of 14-3-3 binding specificities and regulation of subcellular localization of 14-3-3-ligand complexes: a comparison of the X-ray crystal structures of all human 14-3-3 isoforms. *Seminars in Cancer Biology*. **16**: 173-182.

Giffon, T., Lepourcelet, M., Pichon, L., Jezequel, P., Bouric, P., Carn, G., Pontarotti, P., Gall, J. Y., David, V. (1996). Cloning of a human homologue of the mouse Tctex-5 gene within the MHC class I region. *Immunogenetics*. **44**:331-339.

Han, Y., B., Feng, H., L., Cheung, C. K., Lam, P. M., Wang, C. C., Haines, C. J. (2007a) Expression of a novel T-*complex testis expressed 5* (*Tctex5*) in mouse testis, epididymis, and spermatozoa. *Molecular Reproduction*. **74**:1132-1140.

Han, Y., Haines, C. J. (2007). Review and Hypothesis: Role(s) of the serine/threonine protein phosphatase 1 on mammalian sperm motility. *Archives of Andrology: Journal of Reproductive Systems*. **53**: 1-9.

Hendrickx, A., Beullens, M., Ceulemans, H., Abt, T. D., Eynde, A. V., Nicolaescu, E., Lesage, B., Bollen, M. (2009). Docking motif-guided mapping of the interactome of protein phosphatase-1. *Chemistry & Biology*. **16**: 365-371.

Honkanen, R. E., Golden, T. (2002). Regulators of serine/threonine protein phosphatases at the dawn of a clinical era? *Current Medical Chemistry*. **9**: 1967-1987.

Hu, S., Arellano, M., Boontheung, P, Wang, J., Zhou, H., Jiang, J., Elashoff, D., Wei, R., Loo, J. A., Wong, D. T. (2008). Salivary proteomics for oral cancer biomarker discovery. *Clin Cancer Res 2008*. **14**: 6246-6252.

Huang, Z., Khatra, B., Bollen, M., Carr, D. W., Vijayaraghavan, S. (2002). Sperm PP1γ2 is regulated by a homologue of the yeast protein phosphatase binding protein sds22. *Biology of Reproduction*. **67**: 1936-1942.

Huang, Z., Myers, K., Khatra, B., Vijayaraghavan, S. (2004a). Protein 14-3-3ζ binds to protein phosphatase PP1γ2 in bovine epididymal spermatozoa. *Biology of Reproduction*. **71**: 177-184.

Huang, Z., Vijayaraghavan, S. (2004). Increased phosphorylation of a distinct subcellular pool of protein phosphatase, PP1γ2, during epididymal sperm maturation. *Biology of Reproduction*. **70**: 439-447.

Hui, L., Lu, J., Han, Y., Pilder, S. H. (2006). The mouse *t* complex gene *Tsga2*, encoding polypeptides located in the sperm tail and anterior acrosome, maps to a locus associated with sperm motility and sperm-egg interaction abnormalities. *Biology of Reproduction*. **74**: 633-643.

Ingebritsen, T. S., Cohen, P. (1983). Protein phosphatases: properties and roles in cellular regulation. *Science*. **221**: 331-338.

Küpker, W., Diedrich, K., Edwards, R. G. (1998). Principles of mammalian fertilization. *European Society for Human Reproduction & Embryology*. **13**: 20-32.

Lefièvre, L., Bedu-Addo, K., Conner, S. J., Machado-Oliveira, G. S. M., Chen, Y., Kirkman-Brown, J. C., Afnan, M. A., Publicover, S. J., Ford, W. C. L, Barratt, C. L.R. (2007). Review: Counting sperm does not add up any more: time for a new equation? *Reproduction.* **133**: 675-684.

Lesage, B., Beullens, M., Pedelini, L., Garcia-Gimeno, M. A., Waelkens, E., Sanz, P., Bollen, M. (2007). A complex of catalytically inactive protein phosphatase-1 sandwiched between Sds22 and inhibitor-3. *Biochemistry*. **46**: 8909-8919.

Lishko, P. V., Botchkina, I. L., Fedorenko, A., Kirichok, Y. (2009). Acid extrusion from human spermatozoa is mediated by flagellar voltage-gated proton channel. *Cell*. **140**: 327-337.

Meiselbach, H., Sticht, H., Enz, R. (2006). Structural analysis of the protein phosphatase 1 docking motif: molecular description of binding specificities identifies interacting proteins. *Chemistry & Biology*. **13**: 49-59.

Mishra, S., Somanath, P. R., Huang, Z., Vijayaraghavan, S. (2003). Binding and inactivation of the germ cell-specific protein phosphatase PP1γ2 by sds22 during epididymal sperm maturation. *Biology of Reproduction*. **69**: 1572-1579.

Mortimer, D. (2000). Sperm preparation methods. *Journal of Andrology*. **21**: 357-365.

Oliva, R., de Mateo, S., Estanyol, J. M. (2009). Review: Sperm cell proteomics. *Proteomics 2009*. **9**: 1004-1017.

Pilder, S. H., Hammer, M. F., Silver, L. M. (1991). A novel mouse chromosome 17 hybrid sterility locus: implications for the origin of *t* haplotypes. *Genetics*. **129**: 237-246.

Pilder, S. H., Lu, J., Han, Y., Hui, L., Samant, S. A., Olugbemiga, O. O., Meyers, K. W., Cheng, L., Vijayaraghavan, S. (2007). The molecular basis of "curlicue":

a sperm motility abnormality linked to the sterility of *t* haplotype homozygous male mice. *Soc Reprod Fertil Suppl*. **63**:123-133.

Pilder, S. H., Olds-Clarke, P., Phillips, D. M., Silver, L. M. (1993). Hybrid sterility-6: a mouse t complex locus controlling sperm flagellar assembly and movement. *Dev Biol*. **159**: 631-642.

Pixton, K. L., Deeks, E. D., Flesch, F. M., Moseley, F. L. C., Björndahl, L., Ashton, P. R., Barratt, C. L. R. (2004). Sperm proteome mapping of a patient who experienced failed fertilization at IVF reveals altered expression of at least 20 proteins compared with fertile donors: Case report. *Human Reproduction*. **19**: 1438-1447.

Puri, P., Snow, A., Kline, D., Vijayaraghavan, S. (2008). Identification of 14-3-3 Binding proteins in mouse testis by tandem affinity tag purification. *The FASEB Journal.* **22**: 1205.2.

Smith, G. D., Wolf, D. P., Trautman, K. C., da Cruz e Silva, E. F., Greengard, P., Vijayaraghavan, S. (1996). Primate sperm contain phosphatase 1, a biochemical mediator of motility. *Biology of Reproduction*. **54**: 719-727.

Smith, G. D., Wolf, D. P., Trautman, K. C., Vijayaraghavan, S. (1999). Motility potential of macaque epididymal sperm: The role of protein phosphatase and glycogen synthase kinase-3 activities. *Journal of Andrology*. **20**: 47-53.

Somanath, P. R., Jack, S. L., Vijayaraghavan, S. (2004) Changes in sperm glycogen synthase kinase-3 serine phosphorylation and activity accompany motility initiation and stimulation. *Journal of Andrology*. **25**: 605-617.

Sun, S., Wong, E. W., Li, M. W., Lee, W. M., Cheng, C. Y. (2009). 14-3-3 and its binding partners are regulators of protein-protein interactions during spermatogenesis. *J Endocrinol*. **202**: 327-336.

Terrak, M., Kerff, F., Langsetmo, K., Tao, T., Dominguez, R. (2004). Structural basis of protein phosphatase 1 regulation. *Nature*. **429**: 780-784.

Varghese, A. C., Golberg, E., Bhattacharyya, A. K., Agarwal, A. (2007). Emerging technologies for the molecular study of infertility, and potential clinical applications. *Reproductive BioMedicine Online*. **15**: 451-456.

Varmuza, S., Jurisicova, A., Okano, K., Hudson, J., Boekelheide, K., Shipp, E. B. (1999) Spermiogenesis is impaired in mice bearing a targeted mutation in the protein phosphatase 1cgamma gene. *Developmental Biology.* **205**: 98-110.

Vijayaraghavan, S., Mohan, J., Gray, H., Khatra, B., Carr, D. W. 2000. A role for phosphorylation of glycogen synthase kinase-3α in bovine sperm motility regulation. *Biology of Reproduction*. **62**: 1647-1654.

Vijayaraghavan, S., Stephens, D. T., Trautman, K., Smith, G. D., Khatra, B., da Cruz e Silva, E. F., Greengard, P. (1996). Sperm motility development in the epididymis is associated with decreased glycogen synthase kinase-3 and protein phosphatase 1 activity. *Biology of Reproduction*. **54**: 709-718.

Virshup, D. M., Shenolikar, S. (2009). Review: From promiscuity to precision: protein phosphatases get a makeover. *Molecular Cell*. **33**: 537-545.

Wakula, P., Beullens, M., Ceulemans, H., Stalmans, W., Bollen, M. (2003). Degeneracy and function of the ubiquitous RVXF motif that mediates binding to protein phosphatse-1. *The Journal of Biological Chemistry.* **278**: 18817-18823.

Wang, R., Sperry, A. O. (2008). Research article: Identification of a novel leucine-rich repeat protein and candidate PP1 regulatory subunit expressed in developing spermatids. *BMC Cell Biology*. **9**: 9 doi:10.1186/1471-2121-9-9.

WHO (World Health Organization). 1999. *Collection and examination of human semen and sperm-cervical mucus interaction*. Chapter 2. Cambridge University Press. pp 4-30.

WHO (World Health Organization). 2010. *WHO Laboratory manual for the examination and processing of human semen*. 5th edition. WHO Press. Switzerland. pp 1-286.

Zhang, J., Zhang, L., Zhao, S., Lee, E.,Y. (1998). Identification and characterization of the human HCG V gene product as a novel inhibitor of protein phosphatase-1. *Biochemistry*. **37**: 16728-16734.

Zhao, S., Lee, E. Y. C. (1997). A protein phosphatase-1-binding motif identified by panning of a random peptide display library. *The Journal of Biological Chemistry*. **45**: 28368-28372.

7: Appendix

Immunocytochemistry solutions

1xPBS

For a final volume of 500 ml, dissolve one pack of BupH Modified Dulbecco´s Phosphatase Buffered Saline Pack (Pearce) in deionized H_2O. Final composition,

8 mM Sodium Phosphate

2 mM Potassium Phosphate

40 mM NaCl

10 mM KCl

Sterilize by filtering a 0.2 µm filter and store at 4 °C

10x 1 mg/ml Poly-L-ornithine solution

To a final volume of 100ml, dissolved in ionized H_2O 100 mg of poly-L-ornithine

4% Paraformaldehyde

For a final volume of 100 ml, add 4 g of paraformaldehyde to 25 ml of deionized H_2O. Dissolve by heating the mixture at 58 °C while stirring. Add 1-2 drops of 1 M NaOH to clarify the solution and filter (0.2 µm filter). Add 50 ml of 2x PBS and adjust the volume to 100 ml with deionized H_2O.

1x PBS 3% BSA Buffer

For a final volume of 10 ml, add 0.3 g of BSA to 10 ml of 1x PBS and dissolve.

NCB stock solutions

10x $CaCl_2$

For a final volume of 10 ml, add 0.027 g of $CaCl_2$ to deionized H_2O. Dissolve and filter (0.2 µm filter) the solution.

10x KCl

For a final volume of 10 ml, add 0.04 g of KCl to deionized H_2O.

10x $MgSO_4.7H_2O$

For a final volume of 10 ml, add 0.02 g of $MgSO_4.7H_2O$ to deionized H_2O.

10x NaCl

For a final volume of 10 ml, add 0.680g of NaCl to deionized H_2O.

10x $NaHPO_4$

For a final volume of 10 ml, add 0.016g of $NaHPO_4$ to deionized H_2O.

10x D(+)-glucose

For a final volume of 10 ml, add 0.1g of D(+)-glucose to deionized H_2O.

10x Na pyruvate

For a final volume of 10 ml, add 0.03 g of Na pyruvate to deionized H_2O.

10x Na lactate

For a final volume of 10ml, add 0.468 g of Na lactate to deionized H_2O.

10x Hepes

For a final volume of 10 ml, add 0.0595 g of Hepes to deionized H_2O.

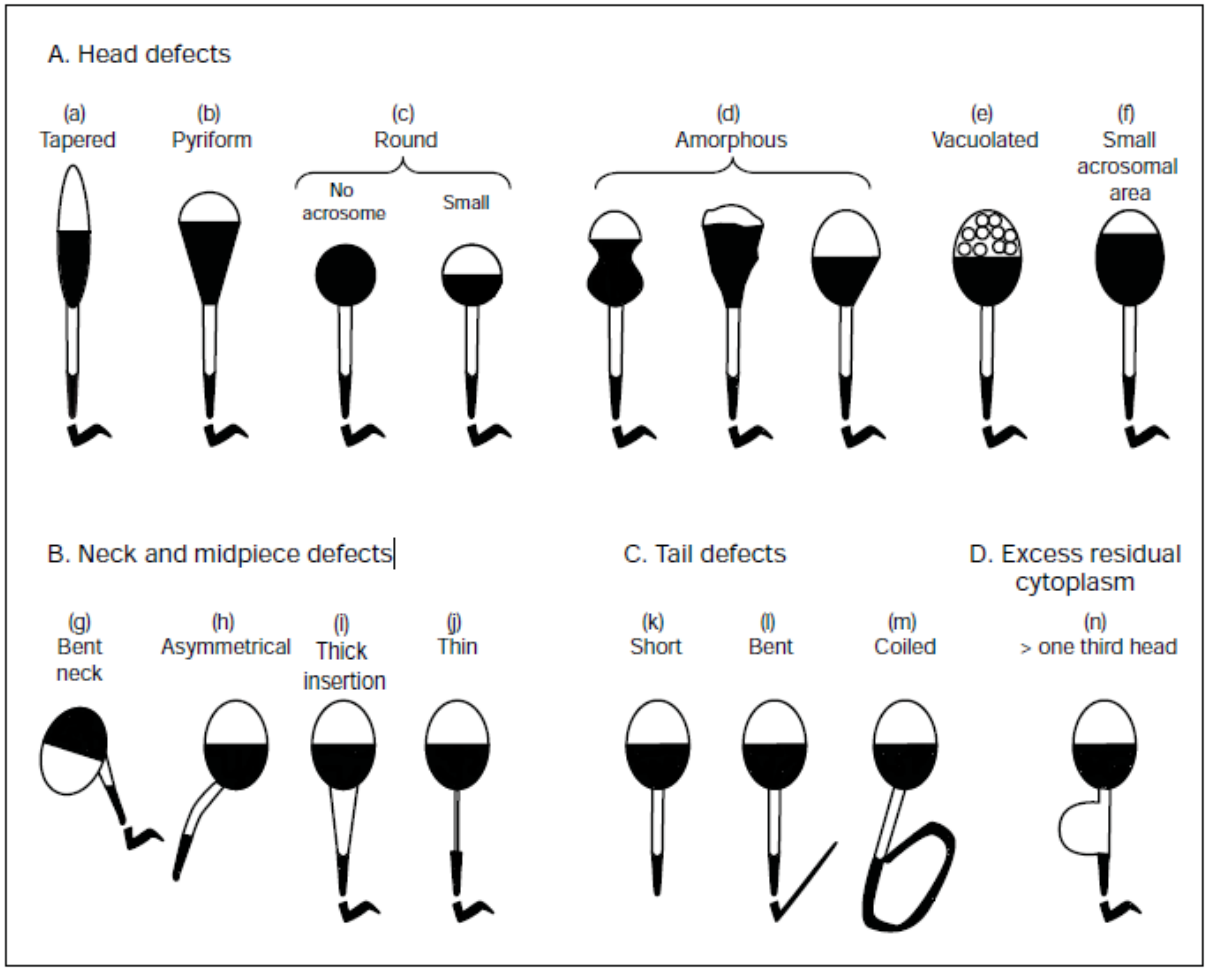

Figure 27: Schematic drawings of some abnormal forms of human spermatozoa (adapted from WHO, 2010

Data table (N=1600) of all volunteers, and morphology analysis

n	Staining	PH	Additional information
1	A14	B4	head defects (round)+ neck and middle piece defects
2	A14	B3	tail defects
3	A14	B1	head defects(pyriform)
4	A0	B0	normal
5	A14	B0	normal
6	A14	B3	tail defects
7	A14	B3	tail defects
8	A14	B4	head defects (round)+ tail defects
9	A14	B3	tail defects
10	A14	B3	tail defects
11	A0	B0	normal
12	A12	B0	normal
13	A14	B3	tail defects
14	A14	B2	neck and middle piece defects(thick insertion)
15	A14	B0	normal
16	A12	B2	neck and middle piece defects
17	A14	B3	tail defects
18	A14	B2	neck and middle piece defects(thick insertion)
19	A14	B3	tail defects
20	A13	B2	neck and middle piece defects(thick insertion)
21	A14	B3	tail defects
22	A14	B4	head defects (round)+ tail defects
23	A0	B0	normal

24	A14	B3	tail defects
25	A14	B2	neck and middle piece defects
26	A12	B4	head defects (tapered)+neck and middle piece defects
27	A14	B0	normal
28	A14	B2	neck and middle piece defects
29	A14	B4	head defects (amorphous)+tail defects
30	A14	B0	normal
31	A14	B3	tail defects
32	A14	B0	normal
33	A14	B3	tail defects
34	A14	B4	head defects (round)+ tail defects
35	A14	B3	tail defects
36	A14	B4	head defects (round)+ tail defects
37	A0	B0	normal
38	A14	B0	normal
39	A0	B0	normal
40	A14	B1	head defects(pyriform)
41	A0	B0	normal
42	A0	B0	normal
43	A14	B0	normal
44	A14	B3	tail defects
45	A14	B4	head defects (amorphous)+tail defects
46	A14	B4	head defects (round)+tail defects
47	A14	B3	tail defects
48	A14	B2	neck and middle piece defects
49	A14	B4	head defects(tapered)+neck and middle piece defects

50	A14	B0	normal
51	A14	B3	tail defects
52	A14	B3	tail defects
53	A12	B0	normal
54	A14	B0	normal
55	A12	B4	head defects(amorphous)+tail defects
56	A14	B3	tail defects
57	A0	B0	normal
58	A0	B0	normal
59	A0	B4	neck and middle piece defects+tail defects
60	A12	B2	neck and middle piece defects
61	A12	B4	head defects (tapered)+neck and middle piece defects+tail defects
62	A12	B0	normal
63	A0	B0	normal
64	A14	B4	neck and middle piece defects+tail defects
65	A14	B0	normal
66	A0	B0	normal
67	A0	B1	head defects(tapered)
68	A12	B1	head defects(tapered)
69	A14	B3	tail defects
70	A12	B0	normal
71	A14	B0	normal
72	A14	B4	head defects(round)+tail defects
73	A14	B4	head defects(round)+neck and middle piece defects
74	A13	B4	head defects (round)+neck and middle piece defects
75	A14	B3	tail defects

76	A14	B0	normal
77	A14	B3	tail defects
78	A14	B3	tail defects
79	A14	B1	head defects(tapered)
80	A14	B4	head defects (tapered)+tail defects
81	A14	B3	tail defects
82	A12	B4	head defects(round)+tail defects
83	A14	B3	tail defects
84	A14	B0	normal
85	A14	B0	normal
86	A12	B0	normal
87	A14	B3	tail defects
88	A14	B4	head defects(amorphous)+tail defects
89	A14	B2	neck and middle piece defects
90	A14	B0	normal
91	A12	B2	neck and middle piece defects
92	A14	B0	normal
93	A14	B3	tail defects
94	A0	B0	normal
95	A14	B3	tail defects
96	A14	B4	head defects (amorphous)+tail defects
97	A14	B3	tail defects
98	A14	B3	tail defects
99	A14	B3	tail defects
100	A0	B1	head defects(amorphous)
101	A14	B3	tail defects

102	A14	B3	tail defects
103	A14	B3	tail defects
104	A14	B3	tail defects
105	A12	B0	normal
106	A14	B2	neck and middle piece defects
107	A14	B3	tail defects
108	A14	B4	head defects(tapered)+neck and middle piece defects(thick insertion)
109	A12	B4	neck and middle piece defects(thick insertion)+tail defects
110	A14	B4	head defects (round)+neck and middle piece defects+tail defects
111	A14	B4	head defects (round)+tail defects
112	A14	B3	tail defects
113	A14	B3	tail defects
114	A14	B3	tail defects
115	A12	B0	normal
116	A14	B2	neck and middle piece defects
117	A14	B0	normal
118	A0	B0	normal
119	A14	B2	neck and middle piece defects
120	A12	B0	normal
121	A0	B1	head defects(round)
122	A14	B3	tail defects
123	A12	B0	normal
124	A0	B0	normal
125	A14	B1	head defects(amorphous)
126	A14	B4	head defects+neck and middle piece defects
127	A0	B0	normal

128	A0	B0	normal
129	A14	B0	normal
130	A14	B1	head defects(round)
131	A12	B0	normal
132	A13	B1	head defects(round)
133	A0	B0	normal
134	A14	B3	tail defects
135	A14	B4	head defects(round)+neck and middle piece defects(thick insertion)
136	A14	B3	tail defects
137	A14	B0	normal
138	A14	B0	normal
139	A0	B0	normal
140	A14	B3	tail defects
141	A14	B4	head defects(round)+neck and middle piece defects
142	A12	B0	normal
143	A12	B0	normal
144	A0	B0	normal
145	A14	B0	normal
146	A14	B4	head defects(round)+neck and middle piece defects+tail defects
147	A12	B4	head defects(tapered)+neck and middle piece defects(thick insertion)+tail defects
148	A14	B4	head defects(round)+neck and middle piece defects
149	A14	B3	tail defects
150	A9	B2	neck and middle piece defects
151	A14	B0	normal
152	A14	B0	normal
153	A0	B0	normal

154	A14	B2	neck and middle piece defects
155	A3	B2	neck and middle piece defects
156	A14	B0	normal
157	A12	B1	head defects(round)
158	A14	B0	normal
159	A14	B3	tail defects
160	A14	B0	normal
161	A14	B3	tail defects
162	A14	B4	neck and middle piece defects(thick insertion)+tail defects
163	A14	B0	normal
164	A14	B2	neck and middle piece defects
165	A14	B0	normal
166	A12	B0	normal
167	A14	B3	tail defects
168	A0	B0	normal
169	A0	B0	normal
170	A14	B3	tail defects
171	A14	B4	head defects(round)+tail defcts
172	A14	B1	head defects(tapered)
173	A12	B0	normal
174	A12	B1	head defects(round)
175	A14	B3	tail defects
176	A14	B1	head defects(round)
177	A0	B0	normal
178	A13	B1	head defects(tapered)
179	A14	B0	normal

180	A12	B0	normal
181	A14	B1	head defects(round)
182	A12	B0	normal
183	A14	B3	tail defects
184	A12	B0	normal
185	A14	B3	tail defects
186	A14	B2	neck and middle piece defects
187	A14	B3	tail defects
188	A12	B0	normal
189	A14	B0	normal
190	A14	B3	tail defects
191	A0	B0	normal
192	A12	B0	normal
193	A14	B2	neck and middle piece defects
194	A14	B4	head defects(round)+neck and middle piece defects
195	A14	B4	head defects(tapered)+tail defects
196	A14	B0	normal
197	A14	B3	tail defects
198	A0	B0	normal
199	A0	B0	normal
200	A14	B3	tail defects
201	A0	B0	normal
202	A13	B4	neck and middle piece defects(thick insertion)+tail defects
203	A14	B4	head defects(round)+tail defects
204	A12	B1	head defects(round)
205	A0	B0	normal

206	A12	B0	normal
207	A14	B3	tail defects
208	A14	B3	tail defects
209	A0	B2	neck and middle piece defects
210	A14	B1	head defects(round)
211	A14	B0	normal
212	A3	B0	normal
213	A14	B3	tail defects
214	A0	B0	normal
215	A14	B3	tail defects
216	A12	B0	normal
217	A14	B1	head defects(round)
218	A12	B0	normal
219	A12	B0	normal
220	A0	B0	normal
221	A14	B3	tail defects
222	A14	B3	tail defects
223	A14	B3	tail defects
224	A14	B0	normal
225	A14	B3	tail defects
226	A14	B0	normal
227	A14	B3	tail defects
228	A14	B3	tail defects
229	A12	B2	neck and middle piece defects
230	A0	B0	normal
231	A14	B4	head defects(round)+tail defects

232	A14	B3	tail defects
233	A14	B3	tail defects
234	A14	B1	head defects(round)
235	A12	B4	head defects(round)+tail defects
236	A14	B0	normal
237	A14	B0	normal
238	A0	B0	normal
239	A14	B1	head defects(tapered)
240	A0	B0	normal
241	A14	B3	tail defects
242	A12	B0	normal
243	A14	B0	normal
244	A14	B3	tail defects
245	A14	B0	normal
246	A14	B0	normal
247	A12	B0	normal
248	A14	B0	normal
249	A12	B0	normal
250	A14	B1	head defects(round)
251	A12	B1	head defects(amorphous)
252	A14	B3	tail defects
253	A14	B1	head defects(round)
254	A14	B0	normal
255	A0	B0	normal
256	A9	B0	normal
257	A14	B3	tail defects

258	A14	B0	normal
259	A14	B2	neck and middle piece defects
260	A14	B3	tail defects
261	A12	B2	neck and middle piece defects(thick insertion)
262	A13	B2	neck and middle piece defects
263	A14	B3	tail defects
264	A14	B3	tail defects
265	A14	B0	normal
266	A12	B0	normal
267	A14	B4	head defects(tapered)+tail defects
268	A14	B0	normal
269	A14	B3	tail defects
270	A12	B0	normal
271	A14	B3	tail defects
272	A14	B3	tail defects
273	A13	B0	normal
274	A14	B3	tail defects
275	A14	B4	head defects(round)+tail defects
276	A12	B0	normal
277	A12	B0	normal
278	A14	B4	head defects(round)+tail defects
279	A14	B0	normal
280	A14	B0	normal
281	A0	B0	normal
282	A9	B0	normal
283	A12	B0	normal

284	A0	B1	head defects(round)
285	A12	B0	normal
286	A13	B0	normal
287	A14	B3	tail defects
288	A3	B3	tail defects
289	A3	B3	tail defects
290	A12	B0	normal
291	A2	B3	tail defects
292	A3	B3	tail defects
293	A3	B0	normal
294	A3	B3	tail defects
295	A14	B4	head defects(round)+tail defects
296	A12	B1	head defects(round)
297	A13	B0	normal
298	A0	B0	normal
299	A3	B3	tail defects
300	A3	B3	tail defects
301	A14	B0	normal
302	A0	B0	normal
303	A3	B3	tail defects
304	A14	B0	normal
305	A0	B0	normal
306	A14	B0	normal
307	A3	B3	tail defects
308	A14	B2	neck and middle piece defects
309	A0	B0	normal

310	A14	B0	normal
311	A0	B0	normal
312	A14	B1	head defects(round)
313	A1	B3	tail defects
314	A12	B0	normal
315	A14	B1	head defects(round)
316	A14	B4	head defects(round)+tail defects
317	A3	B3	tail defects
318	A12	B4	head defects(tapered)+tail defects
319	A12	B4	head defects(amorphous)+excess residual cytoplasm
320	A1	B3	tail defects
321	A0	B0	normal
322	A14	B1	head defects(round)
323	A14	B4	head defects(round)+neck and middle piece defects
324	A14	B0	normal
325	A3	B3	tail defects
326	A12	B1	head defects(tapered)
327	A13	B0	normal
328	A2	B3	tail defects
329	A3	B3	tail defects
330	A0	B1	head defects(tapered)
331	A0	B0	normal
332	A0	B0	normal
333	A1	B3	tail defects
334	A0	B0	normal
335	A12	B0	normal

336	A1	B3	tail defects
337	A14	B1	head defects(round)
338	A3	B3	tail defects
339	A7	B3	tail defects
340	A14	B1	head defects(amorphous)
341	A14	B0	normal
342	A14	B1	head defects(round)
343	A14	B2	neck and middle piece defects
344	A13	B2	neck and middle piece defects
345	A9	B3	tail defects
346	A14	B0	normal
347	A0	B2	neck and middle piece defects
348	A9	B3	tail defects
349	A14	B0	normal
350	A12	B0	normal
351	A14	B0	normal
352	A9	B3	tail defects
353	A14	B0	normal
354	A9	B3	tail defects
355	A14	B0	normal
356	A9	B0	normal
357	A7	B3	tail defects
358	A0	B0	normal
359	A12	B0	normal
360	A12	B2	neck and middle piece defects
361	A9	B3	tail defects

362	A14	B0	normal
363	A12	B0	normal
364	A13	B4	head defects(round)+neck and middle piece defects
365	A14	B0	normal
366	A13	B1	head defects(round)
367	A14	B0	normal
368	A12	B0	normal
369	A14	B4	head defects(tapered)+tail defects
370	A0	B2	neck and middle piece defects
371	A14	B1	head defects(tapered)
372	A9	B3	tail defects
373	A9	B3	tail defects
374	A0	B0	normal
375	A0	B0	normal
376	A8	B3	tail defects
377	A14	B0	normal
378	A0	B3	tail defects
379	A0	B3	tail defects
380	A14	B0	normal
381	A0	B3	tail defects
382	A12	B4	head defects(round)+tail defects
383	A13	B0	normal
384	A0	B3	tail defects
385	A14	B4	head defects(round)+neck and middle piece defects
386	A12	B1	head defects(tapered)
387	A14	B1	head defects(round)

388	A0	B0	normal
389	A12	B1	head defects(round)
390	A0	B3	tail defects
391	A14	B1	head defects(tapered)
392	A0	B3	tail defects
393	A14	B2	neck and middle piece defects
394	A12	B0	normal
395	A14	B4	head defects(round)+tail defects
396	A14	B0	normal
397	A14	B4	head defects(round)+tail defects
398	A0	B3	tail defects
399	A0	B3	tail defects
400	A12	B0	normal
401	A14	B4	head defects(tapered)+neck and middle piece defects
402	A13	B2	neck and middle piece defects
403	A0	B3	tail defects
404	A12	B4	head defects(amoprphous)+neck and middle piece defects+tail defets
405	A13	B1	head defects(round)
406	A8	B2	neck and middle piece defects
407	A13	B0	normal
408	A14	B4	head defects(tapered)+ neck and middle piece defects+tail defects
409	A13	B0	normal
410	A14	B0	normal
411	A9	B1	head defects(round)
412	A14	B0	normal
413	A12	B2	neck and middle piece defects

414	A12	B4	head defects(tapered)+tail defects
415	A12	B4	head defects(amoprphous)+neck and middle piece defects
416	A14	B2	neck and middle piece defects
417	A14	B1	head defects(pyriform)
418	A14	B1	head defects(round)
419	A12	B0	normal
420	A14	B0	normal
421	A14	B0	normal
422	A0	B3	tail defects
423	A0	B3	tail defects
424	A0	B4	head defects(amorphous)+tail defects
425	A9	B0	normal
426	A0	B3	tail defects
427	A14	B2	neck and middle piece defects
428	A12	B1	head defects(pyriform)
429	A0	B3	tail defects
430	A14	B2	neck and middle piece defects
431	A0	B4	head defects(amorphous)+tail defects
432	A3	B3	tail defects
433	A13	B3	tail defects
434	A9	B2	neck and middle piece defects
435	A13	B0	normal
436	A3	B0	normal
437	A14	B0	normal
438	A0	B0	normal
439	A12	B2	neck and middle piece defects

440	A12	B4	head defects(round)+neck and middle piece defects
441	A14	B4	head defects(amorphous)+tail defects
442	A9	B1	head defects(amorphous)
443	A13	B2	neck and middle piece defects
444	A13	B1	head defects(round)
445	A14	B3	tail defects
446	A0	B3	tail defects
447	A14	B0	normal
448	A0	B2	neck and middle piece defects
449	A12	B0	normal
450	A0	B0	normal
451	A13	B2	neck and middle piece defects
452	A3	B4	neck and middle piece defects+tail defects
453	A0	B3	tail defects
454	A14	B2	neck and middle piece defects
455	A0	B3	tail defects
456	A3	B0	normal
457	A14	B0	normal
458	A14	B2	neck and middle piece defects
459	A12	B0	normal
460	A14	B0	normal
461	A0	B3	tail defects
462	A0	B3	tail defects
463	A14	B0	normal
464	A14	B2	neck and middle piece defects
465	A14	B0	normal

466	A14	B2	neck and middle piece defects
467	A0	B3	tail defects
468	A3	B1	head defects(round)
469	A0	B0	normal
470	A14	B0	normal
471	A0	B3	tail defects
472	A14	B4	head defects(round)+tail defects
473	A4	B0	normal
474	A0	B0	normal
475	A3	B0	normal
476	A4	B4	head defects(tapered)+tail defects
477	A0	B3	tail defects
478	A0	B4	head defects(round)+tail defects
479	A0	B0	normal
480	A12	B0	normal
481	A0	B3	tail defects
482	A14	B0	normal
483	A0	B3	tail defects
484	A14	B4	head defects(round)+neck and middle piece defects
485	A0	B3	tail defects
486	A0	B3	tail defects
487	A13	B0	normal
488	A13	B0	normal
489	A0	B3	tail defects
490	A0	B3	tail defects
491	A0	B3	tail defects

492	A13	B1	head defects(tapered)
493	A0	B1	head defects(round)
494	A4	B3	tail defects
495	A12	B0	normal
496	A3	B0	normal
497	A0	B1	head defects(round)
498	A0	B0	normal
499	A3	B4	neck and middle piece defects+tail defects
500	A14	B0	normal
501	A0	B3	tail defects
502	A0	B4	head defects(amorphous)+tail defects
503	A0	B3	tail defects
504	A13	B0	normal
505	A6	B4	neck and middle piece defects+tail defects
506	A0	B1	head defects(round)
507	A14	B0	normal
508	A12	B0	normal
509	A0	B3	tail defects
510	A0	B0	normal
511	A0	B3	tail defects
512	A0	B3	tail defects
513	A13	B4	head defects(round)+neck and middle piece defects+tail defects
514	A14	B0	normal
515	A8	B0	normal
516	A0	B3	tail defects
517	A14	B4	head defects(amorphous)+tail defects

518	A14	B4	head defects(round)+tail defects
519	A0	B2	neck and middle piece defects
520	A0	B3	tail defects
521	A12	B0	normal
522	A0	B3	tail defects
523	A3	B4	neck and middle piece defects+tail defects
524	A0	B4	head defects(round)+tail defects
525	A14	B2	neck and middle piece defects
526	A12	B1	head defects(round)
527	A9	B4	head defects(round)+tail defects
528	A0	B3	tail defects
529	A12	B4	neck and middle piece defects+tail defects
530	A3	B0	normal
531	A6	B3	tail defects
532	A12	B1	head defects(round)
533	A14	B4	head defects(round)+tail defects
534	A0	B3	tail defects
535	A14	B0	normal
536	A14	B4	head defects(pyriform)+tail defects
537	A14	B0	normal
538	A7	B2	neck and middle piece defects
539	A13	B4	head defects(amorphous)+tail defects
540	A0	B3	tail defects
541	A14	B4	head defects(amorphous)+tail defects
542	A13	B2	neck and middle piece defects
543	A4	B0	normal

544	A12	B4	head defects(round)+tail defects
545	A13	B4	head defects(round)+tail defects
546	A4	B3	tail defects
547	A7	B1	head defects(tapered)
548	A12	B0	normal
549	A14	B1	head defects(round)
550	A6	B4	neck and middle piece defects+tail defects
551	A14	B0	normal
552	A0	B2	neck and middle piece defects
553	A0	B3	tail defects
554	A0	B3	tail defects
555	A9	B0	normal
556	A0	B0	normal
557	A6	B3	tail defects
558	A0	B0	normal
559	A14	B2	neck and middle piece defects
560	A6	B3	tail defects
561	A3	B0	normal
562	A0	B1	head defects(round)
563	A3	B0	normal
564	A7	B4	head defects(round)+neck and middle piece defects+tail defects
565	A12	B0	normal
566	A5	B3	tail defects
567	A14	B4	head defects(round)+tail defects
568	A14	B4	head defects(amorphous)+tail defects
569	A0	B4	head defects(tapered)+tail defects

570	A14	B0	normal
571	A0	B3	tail defects
572	A13	B4	head defects(amorphous)+tail defects
573	A6	B3	tail defects
574	A0	B4	head defects(tapered)+tail defects
575	A14	B0	normal
576	A0	B3	tail defects
577	A13	B4	neck and middle piece defects+tail defects
578	A13	B4	head defects(tapered)+tail defects
579	A3	B0	normal
580	A13	B0	normal
581	A0	B3	tail defects
582	A0	B3	tail defects
583	A12	B3	tail defects
584	A12	B3	tail defects
585	A1	B4	head defects(round)+tail defects
586	A13	B0	normal
587	A0	B4	head defects(round)+neck and middle piece defects
588	A12	B2	neck and middle piece defects
589	A9	B4	head defects(amorphous)+tail defects
590	A12	B3	tail defects
591	A12	B3	tail defects
592	A13	B4	neck and middle piece defects+tail defects
593	A13	B3	tail defects
594	A0	B0	normal
595	A12	B2	neck and middle piece defects

596	A12	B3	tail defects
597	A12	B3	tail defects
598	A13	B4	head defects(amorphous)+tail defects
599	A14	B1	head defects(tapered)
600	A14	B4	head defects(round)+tail defects
601	A12	B3	tail defects
602	A13	B0	normal
603	A12	B3	tail defects
604	A12	B4	head defects(round)+tail defects
605	A0	B0	normal
606	A12	B3	tail defects
607	A0	B0	normal
608	A1	B4	neck and middle piece defects+tail defects
609	A14	B1	head defects(round)
610	A14	B1	head defects(tapered)
611	A0	B0	normal
612	A12	B3	tail defects
613	A13	B0	normal
614	A12	B3	tail defects
615	A12	B3	tail defects
616	A3	B1	head defects(tapered)
617	A12	B3	tail defects
618	A12	B3	tail defects
619	A3	B0	normal
620	A12	B3	tail defects
621	A14	B4	head defects(tapered)+middle piece defects

622	A14	B4	head defects(round)+tail defects
623	A12	B4	head defects(amorphous)+neck and middle piece defects+tail defects
624	A12	B3	tail defects
625	A3	B4	head defects(tapered)+tail defects
626	A12	B3	tail defects
627	A12	B3	tail defects
628	A12	B3	tail defects
629	A12	B3	tail defects
630	A14	B2	neck and middle piece defects
631	A12	B2	neck and middle piece defects
632	A0	B2	neck and middle piece defects
633	A0	B1	head defects(tapered)
634	A13	B2	neck and middle piece defects
635	A12	B4	head defects(round)+neck and middle piece
636	A9	B4	neck and middle piece defects+tail defects
637	A3	B0	normal
638	A14	B0	normal
639	A12	B3	tail defects
640	A14	B0	normal
641	A12	B3	tail defects
642	A13	B4	head defects(round)+neck and middle piece
643	A3	B4	head defects(round)+tail defects
644	A3	B1	head defects(round)
645	A13	B0	normal
646	A12	B3	tail defects
647	A0	B0	normal

648	A14	B4	head defects(amorphous)+neck and middle piece defects+tail defects
649	A12	B4	head defects(round)+neck and middle piece
650	A12	B4	head defects(round)+tail defects
651	A12	B3	tail defects
652	A0	B0	normal
653	A0	B0	normal
654	A12	B3	tail defects
655	A12	B3	tail defects
656	A12	B3	tail defects
657	A13	B1	head defects(round)
658	A7	B0	normal
659	A11	B0	normal
660	A13	B4	head defects(tapered)+tail defects
661	A12	B3	tail defects
662	A13	B4	head defects(round)+tail defects
663	A12	B3	tail defects
664	A13	B3	tail defects
665	A12	B3	tail defects
666	A12	B0	normal
667	A14	B1	head defects(amorphous)
668	A12	B3	tail defects
669	A12	B3	tail defects
670	A3	B1	head defects(round)
671	A12	B3	tail defects
672	A0	B2	neck and middle piece defects
673	A12	B3	tail defects

674	A12	B0	normal
675	A3	B1	head defects(round)
676	A0	B4	head defects(round)+tail defects
677	A12	B3	tail defects
678	A13	B0	normal
679	A4	B0	normal
680	A12	B3	tail defects
681	A12	B3	tail defects
682	A12	B4	head defects(round)+tail defects
683	A12	B3	tail defects
684	A12	B3	tail defects
685	A13	B4	neck and middle piece defects+tail defects
686	A12	B0	normal
687	A0	B0	normal
688	A13	B0	normal
689	A12	B3	tail defects
690	A14	B0	normal
691	A12	B3	tail defects
692	A4	B0	normal
693	A12	B3	tail defects
694	A12	B3	tail defects
695	A12	B3	tail defects
696	A3	B4	head defects(tapered)+tail defects
697	A13	B3	tail defects
698	A14	B4	head defects(round)+neck and middle piece defects
699	A12	B0	normal

700	A13	B3	tail defects
701	A12	B2	neck and middle piece defects
702	A0	B4	head defects(round)+tail defects
703	A14	B4	head defects(amorphous)+tail defects
704	A14	B4	head defects(round)+tail defects
705	A12	B1	head defects(tapered)
706	A12	B3	tail defects
707	A13	B3	tail defects
708	A0	B4	neck and middle piece defects+tail defects
709	A13	B4	head defects(tapered)+neck and middle piece defects
710	A13	B4	head defects(round)+tail defects
711	A0	B0	normal
712	A0	B0	normal
713	A13	B3	tail defects
714	A13	B3	tail defects
715	A12	B3	tail defects
716	A0	B0	normal
717	A12	B4	head defects(tapered)+tail defects
718	A0	B1	head defects(round)
719	A12	B2	neck and middle piece defects
720	A14	B4	head defects(round)+neck and middle piece defects
721	A0	B2	neck and middle piece defects
722	A14	B4	head defects(round)+neck and middle piece defects
723	A12	B1	head defects(round)
724	A5	B0	normal
725	A12	B3	tail defects

726	A12	B3	tail defects
727	A0	B0	normal
728	A3	B0	normal
729	A13	B3	tail defects
730	A13	B2	neck and middle piece defects
731	A6	B4	head defects(round)+tail defects
732	A12	B3	tail defects
733	A13	B3	tail defects
734	A12	B0	normal
735	A6	B0	normal
736	A12	B3	tail defects
737	A12	B3	tail defects
738	A13	B4	neck and middle piece defects+tail defects
739	A13	B3	tail defects
740	A6	B4	head defects(round)+neck and middle piece defects+tail defects
741	A12	B0	normal
742	A10	B4	head defects(pyriform)+tail defects
743	A13	B3	tail defects
744	A12	B3	tail defects
745	A12	B3	tail defects
746	A10	B3	tail defects
747	A14	B4	head defects(round)+neck and middle piece defects
748	A12	B3	tail defects
749	A14	B2	neck and middle piece defects
750	A12	B3	tail defects
751	A14	B2	neck and middle piece defects

752	A13	B0	normal
753	A12	B1	head defects(pyriform)
754	A13	B3	tail defects
755	A13	B3	tail defects
756	A12	B0	normal
757	A12	B3	tail defects
758	A14	B1	head defects(pyriform)
759	A0	B0	normal
760	A12	B3	tail defects
761	A13	B3	tail defects
762	A13	B1	head defects(amorphous)
763	A14	B1	head defects(amorphous)
764	A3	B4	head defects(amorphous)+tail defects
765	A13	B3	tail defects
766	A13	B3	tail defects
767	A3	B0	normal
768	A13	B4	head defects(pyriform)+tail defects
769	A0	B0	normal
770	A13	B4	head defects(tapered)+tail defects
771	A14	B0	normal
772	A12	B3	tail defects
773	A13	B0	normal
774	A12	B3	tail defects
775	A13	B2	neck and middle piece defects
776	A13	B3	tail defects
777	A3	B4	head defects(amorphous)+neck and middle piece defects

778	A14	B0	normal
779	A13	B3	tail defects
780	A3	B1	head defects(round)
781	A12	B3	tail defects
782	A12	B4	neck and middle piece defects+tail defects
783	A6	B1	head defects(amorphous)
784	A12	B3	tail defects
785	A0	B4	head defects(round)+tail defects
786	A12	B4	head defects(tapered)+neck and middle piece defects+tail defects
787	A12	B3	tail defects
788	A14	B4	head defects(amorphous)+neck and middle piece defects
789	A13	B3	tail defects
790	A0	B0	normal
791	A3	B2	neck and middle piece defects
792	A12	B3	tail defects
793	A13	B3	tail defects
794	A3	B4	head defects(tapered)+tail defects
795	A12	B3	tail defects
796	A13	B3	tail defects
797	A14	B0	normal
798	A0	B4	head defects(tapered)+tail defects
799	A9	B4	head defects(round)+tail defects
800	A14	B1	head defects(round)
801	A0	B4	head defects(tapered)+tail defects
802	A0	B3	tail defects
803	A13	B3	tail defects

804	A13	B3	tail defects
805	A13	B4	head defects(tapered)+tail defects
806	A12	B1	head defects(tapered)
807	A0	B1	head defects(round)
808	A12	B3	tail defects
809	A12	B4	head defects(tapered)+tail defects
810	A0	B0	normal
811	A0	B2	neck and middle piece defects
812	A13	B0	normal
813	A0	B4	head defects(amorphous)+tail defects
814	A0	B4	head defects(round)+tail defects
815	A12	B0	normal
816	A10	B0	normal
817	A13	B0	normal
818	A7	B1	head defects(round)
819	A4	B1	head defects(amorphous)
820	A12	B3	tail defects
821	A3	B1	head defects(tapered)
822	A0	B3	tail defects
823	A3	B2	neck and middle piece defects
824	A10	B0	normal
825	A10	B4	neck and middle piece defects+tail defects
826	A0	B4	head defects(round)+tail defects
827	A13	B0	normal
828	A0	B0	normal
829	A0	B0	normal

830	A12	B1	head defects(round)
831	A13	B4	head defects(tapered)+tail defects
832	A0	B1	head defects(amorphous)
833	A6	B3	tail defects
834	A0	B3	tail defects
835	A0	B0	normal
836	A0	B0	normal
837	A13	B4	head defects(round)+tail defects
838	A13	B3	tail defects
839	A0	B1	head defects(round)
840	A0	B0	normal
841	A13	B3	tail defects
842	A12	B3	tail defects
843	A0	B1	head defects(tapered)
844	A4	B0	normal
845	A13	B4	head defects(amorphous)+tail defects
846	A14	B3	tail defects
847	A0	B2	neck and middle piece defects
848	A4	B4	head defects(round)+neck and middle piece defects
849	A3	B1	head defects(amorphous)
850	A3	B0	normal
851	A13	B0	normal
852	A3	B0	normal
853	A14	B2	neck and middle piece defects
854	A3	B1	head defects(round)
855	A7	B3	tail defects

856	A14	B1	head defects(round)
857	A3	B3	tail defects
858	A13	B0	normal
859	A4	B1	head defects(round)
860	A7	B3	tail defects
861	A14	B3	tail defects
862	A13	B4	head defects(amorphous)+tail defects
863	A13	B3	tail defects
864	A0	B3	tail defects
865	A3	B4	head defects(amorphous)+tail defects
866	A0	B0	normal
867	A13	B4	head defects(round)+neck and middle piece defects+tail defects
868	A0	B3	tail defects
869	A14	B3	tail defects
870	A12	B1	head defects(amorphous)
871	A13	B1	head defects(tapered)
872	A0	B4	head defects(amorphous)+necka and middle piece defects+tail defects
873	A0	B3	tail defects
874	A7	B4	head defects(tapered)+tail defects
875	A3	B4	head defects(round)+tail defects
876	A14	B3	tail defects
877	A0	B1	head defects(round)
878	A3	B1	head defects(amorphous)
879	A13	B1	head defects(amorphous)
880	A3	B0	normal
881	A0	B3	tail defects

882	A0	B0	normal
883	A0	B4	head defects(round)+tail defects
884	A13	B1	head defects(tapered)
885	A12	B4	head defects(round)+neck and middle piece defefct+tail defects
886	A9	B3	tail defects
887	A7	B3	tail defects
888	A0	B0	normal
889	A13	B3	tail defects
890	A3	B3	tail defects
891	A0	B1	head defects(round)
892	A13	B3	tail defects
893	A13	B4	head defects(round)+tail defects
894	A14	B0	normal
895	A0	B0	normal
896	A14	B4	head defects(amorphous)+tail defects
897	A0	B3	tail defects
898	A0	B0	normal
899	A0	B0	normal
900	A0	B3	tail defects
901	A13	B1	head defects(amorphous)
902	A0	B0	normal
903	A0	B3	tail defects
904	A0	B3	tail defects
905	A14	B0	normal
906	A13	B3	tail defects
907	A13	B4	head defects(pyriform)+tail defects

908	A0	B3	tail defects
909	A13	B2	neck and middle piece defects
910	A3	B0	normal
911	A13	B4	neck and middle piece defects+tail defects
912	A14	B2	neck and middle piece defects
913	A0	B1	head defects(tapered)
914	A0	B1	head defects(amorphous)
915	A7	B3	tail defects
916	A3	B0	normal
917	A13	B3	tail defects
918	A13	B3	tail defects
919	A4	B1	head defects(amorphous)
920	A13	B1	head defects(round)
921	A13	B3	tail defects
922	A0	B4	head defects(round)+tail defects
923	A0	B3	tail defects
924	A12	B4	head defects(tapered)+tail defects
925	A0	B4	head defects(round)+tail defects
926	A7	B4	head defects(amorphous)+tail defects
927	A14	B3	tail defects
928	A0	B3	tail defects
929	A0	B3	tail defects
930	A13	B2	neck and middle piece defects
931	A13	B3	tail defects
932	A0	B2	neck and middle piece defects
933	A14	B0	normal

934	A0	B3	tail defects
935	A0	B4	head defects(amorphous)+tail defects
936	A0	B3	tail defects
937	A12	B4	head defects(round)+tail defects
938	A3	B4	head defects(amorphous)+tail defects
939	A13	B3	tail defects
940	A0	B0	normal
941	A13	B3	tail defects
942	A0	B0	normal
943	A0	B3	tail defects
944	A0	B0	normal
945	A13	B4	head defects(pyriform)+tail defects
946	A13	B4	head defects(pyriform)+tail defects
947	A13	B3	tail defects
948	A0	B4	head defects(round)+tail defects
949	A0	B3	tail defects
950	A0	B0	normal
951	A0	B3	tail defects
952	A0	B3	tail defects
953	A0	B0	normal
954	A0	B0	normal
955	A13	B1	head defects(amorphous)
956	A0	B0	normal
957	A0	B3	tail defects
958	A0	B3	tail defects
959	A13	B1	head defects(round)

960	A0	B0	normal
961	A0	B3	tail defects
962	A0	B3	tail defects
963	A0	B1	head defects(pyriform)
964	A7	B4	head defects(tapered)+tail defects
965	A0	B4	neck and middle piece defects+tail defects
966	A0	B4	head defects(round)+tail defects
967	A3	B1	head defects(round)
968	A14	B4	head defects(pyriform)+tail defects
969	A3	B3	tail defects
970	A13	B4	head defects(amorphous)+tail defects
971	A12	B3	tail defects
972	A3	B3	tail defects
973	A13	B1	head defects(round)
974	A0	B1	head defects(tapered)
975	A14	B1	head defects(amorphous)
976	A0	B3	tail defects
977	A13	B3	tail defects
978	A9	B1	head defects(pyriform)
979	A0	B3	tail defects
980	A0	B3	tail defects
981	A0	B0	normal
982	A0	B2	neck and middle piece defects
983	A14	B0	normal
984	A12	B3	tail defects
985	A3	B4	head defects(round)+tail defects

986	A0	B4	head defects(tapered)+tail defects
987	A0	B0	normal
988	A13	B3	tail defects
989	A14	B4	head defects(pyriform)+neck and middle piece defects
990	A7	B4	head defects(round)+tail defects
991	A9	B4	head defects(round)+tail defects
992	A9	B4	head defects(tapered)+tail defects
993	A7	B0	normal
994	A0	B4	head defects(amorphous)+tail defects
995	A0	B3	tail defects
996	A12	B0	normal
997	A12	B3	tail defects
998	A14	B4	head defects(round)+tail defects
999	A0	B1	head defects(round)
1000	A0	B1	head defects(tapered)
1001	A12	B1	head defects(amorphous)
1002	A0	B1	head defects(round)
1003	A0	B4	head defects(round)+tail defects
1004	A13	B0	normal
1005	A13	B0	normal
1006	A12	B3	tail defects
1007	A13	B0	normal
1008	A13	B0	normal
1009	A0	B0	normal
1010	A0	B3	tail defects
1011	A0	B3	tail defects

1012	A13	B2	neck and middle piece defects
1013	A13	B0	normal
1014	A3	B0	normal
1015	A1	B3	tail defects
1016	A14	B3	tail defects
1017	A13	B3	tail defects
1018	A13	B0	normal
1019	A0	B3	tail defects
1020	A0	B4	head defects(round)+tail defects
1021	A0	B3	tail defects
1022	A0	B1	head defects(amorphous)
1023	A0	B0	normal
1024	A13	B3	tail defects
1025	A13	B0	normal
1026	A0	B4	head defects(round)+tail defects
1027	A0	B0	normal
1028	A4	B3	tail defects
1029	A13	B0	normal
1030	A0	B3	tail defects
1031	A0	B3	tail defects
1032	A13	B3	tail defects
1033	A0	B3	tail defects
1034	A14	B4	head defects(round)+tail defects
1035	A0	B3	tail defects
1036	A13	B3	tail defects
1037	A3	B4	head defects(round)+tail defects

1038	A13	B3	tail defects
1039	A14	B1	head defects(round)
1040	A0	B3	tail defects
1041	A14	B3	tail defects
1042	A0	B4	head defects(round)+tail defects
1043	A13	B3	tail defects
1044	A14	B0	normal
1045	A3	B3	tail defects
1046	A0	B3	tail defects
1047	A1	B3	tail defects
1048	A10	B3	tail defects
1049	A10	B4	head defects(pyriform)+tail defects
1050	A0	B0	normal
1051	A13	B4	head defects(tapered)+tail defects
1052	A0	B4	head defects(round)+tail defects
1053	A3	B1	head defects(round)
1054	A12	B3	tail defects
1055	A13	B3	tail defects
1056	A13	B0	normal
1057	A14	B4	head defects(round)+tail defects
1058	A0	B0	normal
1059	A13	B0	normal
1060	A12	B1	head defects(amorphous)
1061	A7	B4	head defects(pyriform)+neck and middle piece defects
1062	A0	B3	tail defects
1063	A14	B4	head defects(round)+tail defects

1064	A13	B1	head defects(round)
1065	A0	B1	head defects(round)
1066	A13	B4	head defects(amorphou)+neck and middle piece defects+tail defects
1067	A14	B1	head defects(round)
1068	A7	B3	tail defects
1069	A13	B3	tail defects
1070	A13	B0	normal
1071	A0	B0	normal
1072	A0	B3	tail defects
1073	A13	B4	head defects(round)+tail defects
1074	A13	B3	tail defects
1075	A14	B1	head defects(round)
1076	A13	B4	head defects(amorphous)+tail defects
1077	A0	B3	tail defects
1078	A13	B3	tail defects
1079	A13	B4	head defects(round)+tail defects
1080	A13	B1	head defects(round)
1081	A0	B3	tail defects
1082	A14	B4	head defects(amorphous)+tail defects
1083	A0	B3	tail defects
1084	A0	B3	tail defects
1085	A13	B4	head defects(round)+tail defects
1086	A13	B3	tail defects
1087	A0	B1	head defects(round)
1088	A0	B4	head defects(round)+tail defects
1089	A13	B1	head defects(amorphous)

1090	A13	B3	tail defects
1091	A13	B3	tail defects
1092	A0	B4	head defects(round)+tail defects
1093	A13	B3	tail defects
1094	A0	B4	head defects(round)+tail defects
1095	A0	B4	head defects(tapered)+tail defects
1096	A0	B3	tail defects
1097	A7	B1	head defects(amorphous)
1098	A13	B3	tail defects
1099	A13	B3	tail defects
1100	A13	B4	head defects(amorphous)+tail defects
1101	A0	B4	head defects(round)+tail defects
1102	A13	B3	tail defects
1103	A13	B4	head defects(pyriform)+tail defects
1104	A0	B3	tail defects
1105	A13	B3	tail defects
1106	A12	B3	tail defects
1107	A9	B2	neck and middle piece defects
1108	A3	B4	head defects(round)+tail defects
1109	A13	B3	tail defects
1110	A12	B4	head defects(pyriform)+tail defects
1111	A0	B4	head defects(amorphous)+tail defects
1112	A0	B3	tail defects
1113	A13	B3	tail defects
1114	A13	B4	head defects(pyriform)+tail defects
1115	A7	B1	head defects(round)

1116	A3	B4	head defects(amorphous)+tail defects
1117	A13	B1	head defects(amorphous)
1118	A0	B0	normal
1119	A3	B1	head defects(tapered)
1120	A12	B4	head defects(pyriform)+tail defects
1121	A0	B4	head defects(amorphous)+tail defects
1122	A0	B0	normal
1123	A14	B0	normal
1124	A13	B1	head defects(round)
1125	A0	B3	tail defects
1126	A12	B4	head defects(tapered)+tail defects
1127	A13	B3	tail defects
1128	A0	B0	normal
1129	A0	B4	head defects(round)+tail defects
1130	A14	B1	head defects(round)
1131	A13	B4	neck and middle piece defects+tail defects
1132	A0	B3	tail defects
1133	A0	B1	head defects(round)
1134	A14	B1	head defects(round)
1135	A13	B0	normal
1136	A0	B3	tail defects
1137	A0	B0	normal
1138	A0	B3	tail defects
1139	A13	B3	tail defects
1140	A0	B1	head defects(tapered)
1141	A13	B4	head defects(round)+neck and middle piece defects

1142	A13	B1	head defects(pyriform)
1143	A0	B4	head defects(tapered)+tail defects
1144	A13	B3	tail defects
1145	A0	B4	head defects(tapered)+tail defects
1146	A13	B0	normal
1147	A13	B3	tail defects
1148	A0	B4	head defects(tapered)+tail defects
1149	A9	B1	head defects(tapered)
1150	A12	B4	head defects(tapered)+tail defects
1151	A0	B0	normal
1152	A3	B4	head defects(tapered)+tail defects
1153	A13	B3	tail defects
1154	A12	B0	normal
1155	A3	B1	head defects(pyriform)
1156	A12	B4	neck and middle piece defects+tail defects
1157	A0	B4	head defects(round)+tail defects
1158	A12	B1	head defects(amorphous)
1159	A0	B3	tail defects
1160	A12	B0	normal
1161	A13	B1	head defects(amorphous)
1162	A13	B3	tail defects
1163	A9	B0	normal
1164	A13	B4	head defects(amorphous)+tail defects
1165	A0	B1	head defects(tapered)
1166	A13	B4	head defects(amorphous)+tail defects
1167	A13	B4	neck and middle piece defects+tail defects

1168	A0	B3	tail defects
1169	A1	B3	tail defects
1170	A4	B3	tail defects
1171	A0	B4	head defects(round)+tail defects
1172	A14	B4	head defects(round)+tail defects
1173	A14	B3	tail defects
1174	A14	B3	tail defects
1175	A7	B0	normal
1176	A1	B0	normal
1177	A14	B1	head defects(pyriform)
1178	A0	B4	head defects(round)+tail defects
1179	A0	B4	head defects(amorphous)+neck and middle piece defects+tail defects
1180	A13	B4	head defects(tapered)+tail defects
1181	A13	B4	head defects(round)+tail defects
1182	A13	B1	head defects(tapered)
1183	A13	B4	head defects(amorphous)+neck and middle piece defects
1184	A13	B3	tail defects
1185	A3	B4	head defects(tapered)+tail defects
1186	A1	B4	head defects(round)+tail defects
1187	A12	B0	normal
1188	A14	B3	tail defects
1189	A13	B4	head defects(round)+tail defects
1190	A13	B4	head defects(amorphous)+neck and middle piece defects+tail defects
1191	A13	B4	head defects(tapered)+tail defects
1192	A0	B4	head defects(round)+tail defects
1193	A13	B3	tail defects

1194	A0	B4	head defects(round)+tail defects
1195	A13	B4	head defects(pyriform)+neck and middle piece defects
1196	A3	B4	head defects(round)+neck and middle piece defects
1197	A3	B3	tail defects
1198	A7	B4	head defects(amorphous)+tail defects
1199	A13	B3	tail defects
1200	A7	B4	head defects(amorphous)+tail defects
1201	A13	B3	tail defects
1202	A13	B1	head defects(pyriform)
1203	A13	B3	tail defects
1204	A13	B3	tail defects
1205	A13	B4	neck and middle piece defects+tail defects
1206	A0	B3	tail defects
1207	A13	B0	normal
1208	A13	B1	head defects(tapered)
1209	A13	B0	normal
1210	A14	B3	tail defects
1211	A0	B4	head defects(pyriform)+tail defects
1212	A0	B0	normal
1213	A0	B0	normal
1214	A11	B0	normal
1215	A13	B0	normal
1216	A13	B3	tail defects
1217	A13	B0	normal
1218	A0	B0	normal
1219	A13	B4	head defects(pyriform)+neck and middle piece defects

1220	A13	B4	head defects(amorphous)+tail defects
1221	A11	B3	tail defects
1222	A13	B4	head defects(pyriform)+tail defects
1223	A0	B3	tail defects
1224	A0	B4	head defects(round)+tail defects
1225	A13	B0	normal
1226	A0	B0	normal
1227	A13	B2	neck and middle piece defects
1228	A12	B3	tail defects
1229	A3	B3	tail defects
1230	A13	B3	tail defects
1231	A0	B3	tail defects
1232	A0	B3	tail defects
1233	A7	B3	tail defects
1234	A0	B4	head defects(round)+tail defects
1235	A13	B3	tail defects
1236	A13	B3	tail defects
1237	A0	B3	tail defects
1238	A0	B3	tail defects
1239	A7	B3	tail defects
1240	A13	B3	tail defects
1241	A14	B3	tail defects
1242	A12	B4	head defects(round)+neck and middle piece defects+tail defects
1243	A3	B4	head defects(amorphous)+tail defects
1244	A13	B0	normal
1245	A13	B3	tail defects

1246	A13	B3	tail defects
1247	A12	B3	tail defects
1248	A1	B3	tail defects
1249	A0	B0	normal
1250	A13	B0	normal
1251	A13	B3	tail defects
1252	A13	B3	tail defects
1253	A7	B3	tail defects
1254	A13	B1	head defects(tapered)
1255	A3	B3	tail defects
1256	A13	B3	tail defects
1257	A14	B0	normal
1258	A14	B3	tail defects
1259	A13	B3	tail defects
1260	A7	B4	head defects(tapered)+tail defects
1261	A14	B3	tail defects
1262	A13	B4	head defects(tapered)+tail defects
1263	A13	B3	tail defects
1264	A13	B0	normal
1265	A13	B1	head defects(round)
1266	A13	B4	head defects(round)+tail defects
1267	A13	B4	head defects(pyriform)+neck and middle piece defects
1268	A13	B3	tail defects
1269	A0	B3	tail defects
1270	A13	B3	tail defects
1271	A13	B3	tail defects

1272	A13	B2	neck and middle piece defects
1273	A13	B0	normal
1274	A13	B4	head defects(pyriform)+neck and middle piece defects+tail defects
1275	A14	B4	head defects(amorphous)+tail defects
1276	A0	B3	tail defects
1277	A13	B4	head defects(round)+tail defects
1278	A0	B4	head defects(tapered)+tail defects
1279	A13	B3	tail defects
1280	A0	B3	tail defects
1281	A13	B3	tail defects
1282	A12	B3	tail defects
1283	A13	B3	tail defects
1284	A13	B3	tail defects
1285	A13	B0	normal
1286	A11	B3	tail defects
1287	A11	B3	tail defects
1288	A13	B4	head defects(pyriform)+tail defects
1289	A13	B4	head defects(pyriform)+tail defects
1290	A13	B4	head defects(pyriform)+tail defects
1291	A0	B1	head defects(amorphous)
1292	A7	B0	normal
1293	A0	B3	tail defects
1294	A0	B4	head defects(amorphous)+tail defects
1295	A13	B0	normal
1296	A4	B3	tail defects
1297	A13	B4	head defects(round)+tail defects

1298	A7	B0	normal
1299	A13	B2	neck and middle piece defects
1300	A0	B4	head defects(amorphous)+neck and middle piece defects+tail defects
1301	A13	B3	tail defects
1302	A13	B3	tail defects
1303	A13	B4	head defects(round)+tail defects
1304	A13	B2	neck and middle piece defects
1305	A0	B4	head defects(round)+tail defects
1306	A13	B1	head defects(pyriform)
1307	A13	B3	tail defects
1308	A0	B1	head defects(amorphous)
1309	A3	B2	neck and middle piece defects
1310	A7	B4	head defects(tapered)+tail defects
1311	A13	B4	neck and middle piece defects+tail defects
1312	A0	B4	head defects(round)+neck and middle piece defects
1313	A0	B4	head defects(round)+tail defects
1314	A12	B4	head defects(tapered)+tail defects
1315	A0	B1	head defects(round)
1316	A13	B1	head defects(tapered)
1317	A7	B3	tail defects
1318	A14	B3	tail defects
1319	A13	B2	neck and middle piece defects
1320	A0	B4	head defects(round)+tail defects
1321	A0	B4	head defects(round)+tail defects
1322	A3	B0	normal
1323	A13	B4	head defects(tapered)+neck and middle piece defects+tail defects

1324	A13	B4	head defects(amorphous)+tail defects
1325	A13	B4	head defects(tapered)+tail defects
1326	A12	B4	head defects(tapered)+tail defects
1327	A13	B4	head defects(tapered)+tail defects
1328	A0	B4	head defects(amorphous)+tail defects
1329	A13	B4	head defects(tapered)+tail defects
1330	A13	B4	head defects(round)+tail defects
1331	A0	B0	normal
1332	A13	B4	head defects(round)+tail defects
1333	A0	B3	tail defects
1334	A13	B4	head defects(tapered)+tail defects
1335	A0	B0	normal
1336	A13	B4	head defects(tapered)+tail defects
1337	A12	B4	head defects(tapered)+tail defects
1338	A13	B1	head defects(tapered)
1339	A3	B3	tail defects
1340	A0	B4	head defects(amorphous)+tail defects
1341	A13	B3	tail defects
1342	A0	B4	head defects(amorphous)+tail defects
1343	A13	B4	head defects(round)+tail defects
1344	A13	B1	head defects(pyriform)
1345	A12	B4	neck and middle piece defects+tail defects
1346	A13	B3	tail defects
1347	A0	B3	tail defects
1348	A13	B3	tail defects
1349	A13	B4	head defects(amorphous)+tail defects

1350	A7	B3	tail defects
1351	A11	B4	head defects(tapered)+tail defects
1352	A11	B3	tail defects
1353	A12	B4	head defects(tapered)+tail defects
1354	A12	B4	head defects(round)+tail defects
1355	A13	B3	tail defects
1356	A13	B3	tail defects
1357	A13	B3	tail defects
1358	A13	B2	neck and middle piece defects
1359	A13	B1	head defects(amorphous)
1360	A14	B0	normal
1361	A0	B1	head defects(pyriform)
1362	A0	B4	head defects(round)+tail defects
1363	A7	B4	head defects(round)+tail defects
1364	A3	B3	tail defects
1365	A12	B4	neck and middle piece defects+tail defects
1366	A3	B3	tail defects
1367	A13	B1	head defects(round)
1368	A13	B4	head defects(tapered)+tail defects
1369	A0	B3	tail defects
1370	A0	B4	neck and middle piece defects+tail defects
1371	A13	B4	head defects(amorphous)+tail defects
1372	A4	B4	head defects(round)+tail defects
1373	A0	B0	normal
1374	A0	B3	tail defects
1375	A13	B4	head defects(pyriform)+tail defects

1376	A13	B4	head defects(round)+tail defects
1377	A0	B0	normal
1378	A13	B0	normal
1379	A14	B3	tail defects
1380	A13	B4	head defects(amorphous)+tail defects
1381	A3	B4	head defects(round)+tail defects
1382	A12	B4	head defects(round)+neck and middle piece defects+tail defects
1383	A12	B3	tail defects
1384	A14	B4	head defects(round)+tail defects
1385	A4	B4	head defects(tapered)+tail defects
1386	A0	B3	tail defects
1387	A8	B3	tail defects
1388	A13	B4	head defects(amorphous)+tail defects
1389	A13	B4	head defects(tapered)+tail defects
1390	A3	B1	head defects(round)
1391	A14	B4	head defects(tapered)+tail defects
1392	A11	B4	neck and middle piece defects+tail defects
1393	A13	B0	normal
1394	A14	B4	head defects(round)+tail defects
1395	A4	B3	tail defects
1396	A11	B1	head defects(amorphous)
1397	A13	B3	tail defects
1398	A0	B4	head defects(tapered)+tail defects
1399	A13	B3	tail defects
1400	A0	B3	tail defects
1401	A0	B3	tail defects

1402	A13	B3	tail defects
1403	A13	B0	normal
1404	A13	B4	head defects(tapered)+neck and middle piece defects
1405	A13	B4	head defects(tapered)+neck and middle piece defects
1406	A3	B4	head defects(round)+tail defects
1407	A13	B4	head defects(round)+tail defects
1408	A11	B4	head defects(tapered)+tail defects
1409	A13	B3	tail defects
1410	A3	B3	tail defects
1411	A14	B4	head defects(round)+tail defects
1412	A13	B4	head defects(round)+neck and middle piece defects
1413	A13	B3	tail defects
1414	A4	B3	tail defects
1415	A13	B4	head defects(amorphous)+tail defects
1416	A13	B3	tail defects
1417	A13	B3	tail defects
1418	A13	B3	tail defects
1419	A13	B4	head defects(tapered)+tail defects
1420	A0	B4	head defects(round)+tail defects
1421	A11	B3	tail defects
1422	A0	B4	head defects(tapered)+tail defects
1423	A12	B4	neck and middle piece defects+tail defects
1424	A0	B0	normal
1425	A13	B4	head defects(round)+tail defects
1426	A13	B3	tail defects
1427	A14	B4	head defects(pyriform)+tail defects

1428	A13	B4	head defects(round)+tail defects
1429	A13	B3	tail defects
1430	A14	B3	tail defects
1431	A9	B4	head defects(round)+tail defects
1432	A13	B1	head defects(tapered)
1433	A13	B4	head defects(round)+tail defects
1434	A13	B2	neck and middle piece defects
1435	A13	B3	tail defects
1436	A13	B0	normal
1437	A13	B4	head defects(pyriform)+tail defects
1438	A14	B3	tail defects
1439	A14	B3	tail defects
1440	A0	B3	tail defects
1441	A13	B4	head defects(round)+tail defects
1442	A13	B0	normal
1443	A13	B4	head defects(round)+tail defects
1444	A13	B0	normal
1445	A13	B1	head defects(tapered)
1446	A12	B4	head defects(pyriform)+tail defects
1447	A13	B3	tail defects
1448	A12	B3	tail defects
1449	A3	B3	tail defects
1450	A13	B3	tail defects
1451	A11	B3	tail defects
1452	A7	B1	head defects(pyriform)
1453	A0	B3	tail defects

1454	A0	B3	tail defects
1455	A0	B3	tail defects
1456	A0	B3	tail defects
1457	A13	B4	head defects(tapered)+tail defects
1458	A13	B1	head defects(round)
1459	A13	B3	tail defects
1460	A13	B4	head defects(tapered)+neck and middle piece defects+tail defects
1461	A13	B0	normal
1462	A0	B3	tail defects
1463	A13	B2	neck and middle piece defects
1464	A13	B4	head defects(tapered)+tail defects
1465	A0	B4	head defects(tapered)+tail defects
1466	A13	B0	normal
1467	A13	B3	tail defects
1468	A7	B0	normal
1469	A14	B3	tail defects
1470	A13	B3	tail defects
1471	A13	B0	normal
1472	A0	B4	head defects(amorphous)+tail defects
1473	A13	B2	neck and middle piece defects
1474	A7	B2	neck and middle piece defects
1475	A13	B2	neck and middle piece defects
1476	A13	B3	tail defects
1477	A7	B2	neck and middle piece defects
1478	A14	B4	head defects(round)+tail defects
1479	A0	B3	tail defects

1480	A13	B1	head defects(tapered)
1481	A7	B0	normal
1482	A13	B4	head defects(amorphous)+tail defects
1483	A14	B3	tail defects
1484	A12	B4	head defects(tapered)+tail defects
1485	A13	B4	head defects(tapered)+tail defects
1486	A12	B4	head defects(round)+tail defects
1487	A13	B0	normal
1488	A13	B3	tail defects
1489	A13	B4	head defects(tapered)+tail defects
1490	A14	B4	head defects(round)+tail defects
1491	A13	B3	tail defects
1492	A0	B0	normal
1493	A13	B4	head defects(tapered)+tail defects
1494	A0	B3	tail defects
1495	A0	B3	tail defects
1496	A0	B3	tail defects
1497	A0	B0	normal
1498	A13	B4	head defects(amorphous)+tail defects
1499	A13	B4	head defects(pyriform)+neck and middle piece defects+tail defects
1500	A13	B4	head defects(tapered)+tail defects
1501	A10	B4	head defects(tapered)+tail defects
1502	A0	B1	head defects(amorphous)
1503	A13	B4	head defects(pyriform)+neck and middle piece defects
1504	A3	B3	tail defects
1505	A0	B3	tail defects

1506	A8	B3	tail defects
1507	A1	B3	tail defects
1508	A13	B0	normal
1509	A0	B0	normal
1510	A3	B3	tail defects
1511	A13	B3	tail defects
1512	A13	B2	neck and middle piece defects
1513	A0	B4	head defects(amorphous)+tail defects
1514	A13	B3	tail defects
1515	A13	B2	neck and middle piece defects
1516	A13	B4	head defects(round)+tail defects
1517	A13	B4	head defects(amorphous)+tail defects
1518	A11	B3	tail defects
1519	A4	B1	head defects(pyriform)
1520	A0	B3	tail defects
1521	A13	B4	head defects(tapered)+neck and middle piece defects
1522	A13	B4	head defects(round)+neck and middle piece defects+tail defects
1523	A14	B3	tail defects
1524	A13	B4	head defects(tapered)+tail defects
1525	A13	B4	head defects(round)+tail defects
1526	A13	B4	head defects(amorphous)+neck and middle piece defects
1527	A14	B4	head defects(tapered)+tail defects
1528	A1	B1	head defects(round)
1529	A7	B4	head defects(tapered)+tail defects
1530	A8	B4	head defects(round)+tail defects
1531	A13	B4	head defects(round)+tail defects

1532	A7	B4	head defects(round)+tail defects
1533	A13	B4	head defects(tapered)+neck and middle piece defects
1534	A10	B3	tail defects
1535	A11	B3	tail defects
1536	A13	B4	head defects(tapered)+tail defects
1537	A13	B4	head defects(tapered)+tail defects
1538	A13	B0	normal
1539	A0	B3	tail defects
1540	A13	B4	head defects(round)+tail defects
1541	A11	B1	head defects(tapered)
1542	A13	B3	tail defects
1543	A13	B3	tail defects
1544	A13	B1	head defects(pyriform)
1545	A13	B2	neck and middle piece defects
1546	A13	B1	head defects(tapered)
1547	A13	B0	normal
1548	A13	B1	head defects(round)
1549	A13	B4	head defects(tapered)+tail defects
1550	A13	B1	head defects(pyriform)
1551	A13	B4	head defects(amorphous)+tail defects
1552	A13	B1	head defects(round)
1553	A7	B4	head defects(tapered)+tail defects
1554	A13	B4	head defects(tapered)+neck and middle piece defects
1555	A8	B0	normal
1556	A0	B1	head defects(round)
1557	A7	B4	head defects(tapered)+tail defects

1558	A11	B2	neck and middle piece defects
1559	A13	B0	normal
1560	A7	B4	head defects(tapered)+neck and middle piece defects+tail defects
1561	A4	B3	tail defects
1562	A13	B4	neck and middle piece defects+tail defects
1563	A0	B4	head defects(round)+tail defects
1564	A14	B1	head defects(round)
1565	A0	B3	tail defects
1566	A13	B1	head defects(round)
1567	A0	B4	head defects(round)+tail defects
1568	A0	B3	tail defects
1569	A13	B3	tail defects
1570	A3	B4	head defects(tapered)+tail defects
1571	A0	B3	tail defects
1572	A0	B0	normal
1573	A13	B4	head defects(tapered)+neck and middle piece defects
1574	A4	B3	tail defects
1575	A0	B0	normal
1576	A13	B4	head defects(pyriform)+tail defects
1577	A13	B3	tail defects
1578	A13	B1	head defects(round)
1579	A13	B4	head defects(tapered)+tail defects
1580	A13	B4	head defects(amorphous)+tail defects
1581	A13	B3	tail defects
1582	A0	B3	tail defects
1583	A13	B3	tail defects

1584	A13	B4	head defects(tapered)+tail defects
1585	A13	B0	normal
1586	A13	B0	normal
1587	A13	B4	head defects(amorphous)+tail defects
1588	A12	B3	tail defects
1589	A7	B4	head defects(tapered)+tail defects
1590	A13	B3	tail defects
1591	A14	B3	tail defects
1592	A13	B1	head defects(round)
1593	A13	B3	tail defects
1594	A0	B1	head defects(round)
1595	A13	B2	neck and middle piece defects
1596	A3	B3	tail defects
1597	A0	B4	head defects(round)+tail defects
1598	A13	B0	normal
1599	A13	B3	tail defects
1600	A13	B0	normal